Copper Zinc Sulphide - a novel material in photovoltaics: material characterization and device fabrication

Thesis submitted to

Cochin University of Science and Technology

in partial fulfilment of the requirements for the award of the degree of

DOCTOR OF PHILOSOPHY

by

Sreejith M. S.

(Reg.No: 4633)

Department of Physics
Cochin University of Science and Technology
Kochi - 682022, Kerala, India

March 2019

Copper Zinc Sulphide - a novel material in photovoltaics: material characterization and device fabrication

Ph. D. Thesis in Photovoltaics

Author
Sreejith M. S.
Department of Physics
Cochin University of Science and Technology
Kochi - 682022, Kerala, India
sreejith.sankaran@gmail.com

Research Supervisor
Dr. K. P. Vijayakumar
Emeritus Scientist
Department of Physics
Cochin University of Science and Technology
Kochi - 682022, Kerala, India
vijayakumar.kandathil@gmail.com

CERTIFICATE

Certified that the work presented in this thesis entitled **"Copper Zinc Sulphide - a novel material in photovoltaics: material characterization and device fabrication"** submitted by Mr. Sreejith M. S. is an authentic record of research work carried out by him under my supervision at the Department of Physics in partial fulfilment of the requirements for the award of degree of Doctor of Philosophy of Cochin University of Science and Technology and the work embodied in this thesis has not been included in any other thesis submitted for the award of any other degree. All the relevant corrections and modifications suggested by the audience during the pre-synopsis seminar and recommendations by doctoral committee of the candidate have been incorporated in the thesis.

Kochi
15 March, 2019

Dr. K. P. Vijayakumar
(Supervising Guide)

DECLARATION

I hereby declare that the work presented in this thesis entitled **" Copper Zinc Sulphide - a novel material in photovoltaics: material characterization and device fabrication"** is based on the original research work done by me under the guidance of Dr. K. P. Vijayakumar, Emeritus scientist, Department of Physics, Cochin University of Science and Technology, Kochi, 682022, India, and no part has been included in any other thesis submitted previously for the award of any degree.

Kochi
15 March, 2019

Sreejith M. S.

Acknowledgements

First and foremost I would like to express my heartfelt gratitude to my supervising guide, Dr. K. P. Vijayakumar for his supervision, guidance and advice given throughout my research work. This thesis would not have been possible deprived of the help, support and patience of my guide, who gave me ample freedom to do my work. I am so thankful to Dr. C. Sudha Kartha for her advice and moral support. I am extremely grateful to Dr. M. Jathavedan and Dr. K. Rajeev Kumar for their valuable suggestions and guidance given throughout this work.

I am thankful to the present and former, Heads of Physics Department for all the facilities extended to me in carrying out this work. I would like to express my sincere thanks to all the faculty members and office staffs of Physics Department for giving support and help whenever needed. I acknowledge MNRE, BHEL, UGC-BSR and Cochin University of Science and Technology for providing financial assistance. I would like to say a big thank you to my family and friends, I couldn't have done it without you all.

Sreejith M. S.

Preface

Solar energy is a never ending source of energy. World needs energy and energy consumption is increasing day by day. When we see statistics of electricity production from different energy sources most of the countries depend on oil, natural gases and renewable energy sources. Among different renewable energy sources, hydro power, wind and solar energy sources dominate nowadays. In solar energy harvesting, either we can utilize heat of solar radiation(solar thermal power units) or depend on direct conversion of light energy to electrical energy. Second one is called "photovoltaics" and most of the energy conversion from solar radiation is taking place through photovoltaics. The device that can perform energy conversion is called "solar cell". In markets, crystalline silicon solar cells have monopoly of contributing to most of the energy needs. Presently people are thinking about new semiconductor materials capable to replace silicon solar cells mainly because of the difficulty in disposal as well as high cost of production. Among such materials, CIGS and CZTS are well known and established candidates for thin film fabrication.

This thesis particularly describes about new and novel material "Copper Zinc Sulphide(CZS)". All the elements in this compound semiconductor material are earth abundant, nontoxic and cheap. In this work, we also try to develop solar cells using CuZnS. The methods we adopted

for the fabrication are "chemical spray pyrolysis (CSP)" and "chemical bath deposition (CBD)" which are popular non vacuum techniques for thin film fabrication.

Chapter 1 describes importance of solar energy source among different renewable energy sources and how much it can contribute globally to the electricity production. It describes in details the possibilities of solar energy and how can we extract and utilize it. Then a detailed description is given on the present status of different solar cell materials and how much efficiencies have been reached in 2018. Following this, we have given description of different thin film solar materials which are available in market and their contribution to power production. Finally we explain how we developed this new material CuZnS as an absorber layer in solar cells, followed by a short review on CuZnS.

Chapter 2 deals with fabrication of CuZnS material using CBD technique. Material has double band gap, which is clearly explained. Then it describes about structural and compositional analysis using XRD and XPS; these studies proved that the material exists like a mixture of CuS and ZnS. Raman analysis confirms picture of the material as an alloy (mixture of two different phases) which is described in detail. Photoluminescence studies of the material showed dominance of CuS and ZnS related emissions according to the concentration of elements in it. In the following sections, electrical properties using Hall measurements are explained; this showed that the material properties can easily be tuned by varying the concentration of elements in the material. In final section, properties of solar cell devices fabricated using CuZnS materials are well described.

Chapter 3 explains about the deposition of CuZnS material using CSP

(keeping the concentration of Zn constant and varying that of Cu) technique and their characterizations. From XRD, Raman and XPS analysis, we could confirm the alloy nature of the material and existence of two independent phases viz., CuS and ZnS, which is well explained in first section. In the section dealing with studies on electrical properties using Hall measurement setup, the conductivity type conversion from n to p is clearly explained which is a promising result. In final sections the characterizations are extended to samples prepared at different temperatures and from this we came to the conclusion that material prepared at the temperature of 350^0C is quite good. Material shows good mobility and minimum roughness at this particular temperature and hence we decided to choose this particular temperature for device fabrication.

Chapter 4 describes the junction fabrication using CuZnS with different buffer layers. In first section, details of devices fabricated using CuZnS with CdS are given. The studies reveal the possibilities of CuZnS material acting as good absorber layer in solar cells as they show good open circuit voltage and considerable short circuit current values. In the next section, detailed description of devices fabricated using CuZnS and ZnS is given. Unfortunately devices with ZnS do not show any light activity and hence we were forced to shift from ZnS to other buffer layers like Indium sulphide which is explained in the next section. Indium sulphide seems to be a good candidate for CuZnS for cell fabrication as they show good open circuit voltage (above 400 mV) and short circuit current which is included in final section.

Chapter 5 presents the deposition of CuZnS having different concentrations of Zn, keeping concentration of Cu constant. In the following sections, properties of deposited samples are well explained. We could see that even though CuZnS material exists like mixture of CuS and ZnS

phases, the presence of Zn seems very necessary for the formation of CuS crystalline phase, which is explained with the help of Raman and XRD analysis. Final section contains major observations from XPS analysis of cells fabricated using CuZnS samples. We could see that, in addition to CuZnS and Indium sulphide phases, Copper Indium Sulfide (CIS) phase is also formed in the devices which enhanced the performance of the cell and hence the efficiency of devices. This is well explained in the final section.

Chapter 6 summarizes the major conclusions obtained from this PhD work, and discusses some potential areas for future works.

List of Publications

Research articles

1. **Sreejith M S**, Deepu D R, C Sudha Kartha, Rajeevkumar K and K P Vijayakumar, *Tuning the properties of sprayed CuZnS films for fabrication of solar cell*, Applied Physics Letters 105, 202107 (2014)

2. **Sreejith M S**, Deepu D R, C Sudha Kartha, Rajeevkumar K and K P Vijayakumar, *Improvement of sprayed CuZnS/In2S3 solar cell efficiency by making multiple band gap nature more prominent*, Journal of Renewable and Sustainable Energy 8, 023502 (2016)

3. Aswathy G, Rajesh C S, **Sreejith M S**, K P Vijayakumar and C Sudha Kartha, *Designing photovoltaic concentrators using holographic lens recorded in nickel ion doped photopolymer material*, Solar Energy 163, 77 (2018)

4. Jubimol J, **Sreejith M S**, C Sudha Kartha, K P Vijayakumar and Godfrey Louis, *Analysis of spray pyrolysed copper zinc sulfide thin films using photoluminescence*, Journal of Luminescence 203, 440 (2018)

Conference Proceedings

1. **Sreejith M S**, Deepu D R, C Sudha Kartha and K P Vijayakumar, *Tuning of properties of sprayed CuZnS films*, AIP Conference Proceedings 1591, 1741, DAE punjab, India (2014)

2. **Sreejith M S**, Deepu D R, C Sudha Kartha and K P Vijayakumar, *Sprayed ZnO as effective window layer for CIS/CdS solar cell*, AIP Conference Proceedings 1576, 67, OMTAT Cochin, India (2014)

3. Santhosh M V, **Sreejith M S**, C Sudha Kartha and K P Vijayakumar, *Improvement in properties of window layer of sprayed CuInS2/In2S3 solar cell by optimization of tin doping*, AIP Conference Proceedings 1576, 76, OMTAT Cochin, India (2014)

4. **Sreejith M S**, Sari P S, C Sudha Kartha and K P Vijayakumar, *Deposition and Characterization Of CuZnS thin films Using Chemical bath deposition technique*, IC EEE Cochin, India (2015)

5. Jubimol J, **Sreejith M S**, C Sudha Kartha, K P Vijayakumar and Godfrey Louis, *Photoluminescence studies on CuZnS thin films synthesized through CBD*, ICONMAT Cochin, India (2019)

Contents

Chapter 1

An introduction to renewable energy and importance of CuZnS in photovoltaics

1.1 Introduction

When we see statistical review of world energy 2018[1], it is clear that energy consumption is increasing at the rate of 2% to 2.5% per year in last 30 years. Period of two decades (from 1985 to 2005) shows most challenging growth in energy consumption which is about 2.4% . Interestingly China and India are consuming more energy on comparison with other countries. Energy consumption of India is almost constant in last 30 years while China's statistics is like, increasing in the first 25 years and then a small decrease in growth in final years. All other countries have almost same growth statistics during these years. It simply says that energy consumption of the whole world is increasing year by year, which leads to more intense search for energy for future. Demand of energy(and

much more dangerous than this, the pollution created by the extensive usage)definitely forces all countries to other energy sources or in other words, in addition or as a substitution to all the conventional energy sources, renewable energy sources are becoming inevitable in future.

In the world statistics of energy, rate of consumption and production are proportional in the case of oil[2], gas, nuclear, hydroelectric power and renewable energies. However in the case of coal, production considerably decreased due to less consumption. Presently the most important and popular energy sources are renewable energy sources. Energy consumption from different energy sources during 1965 to 2016 is showing different consumption values. In case of oil, in first 3 decades, consumption is increasing at about 10% and then decreasing to 20% of the initial value; still oil consumption remains maximum. Second source is coal[3, 4] which at the beginning was about 40% of the total consumption then it decreased to 30%, remaining more or less stable at the same value. Gas consumption was only about 15% at the beginning then it subsequently increased to 30% in last 50 years.

In the world picture, hydroelectric power consumption is only about 6% and it maintains the status without any variation in the value for last 50 years[5]. Nuclear is one of the prominent energy source when Europe is concerned. A very huge hike was observed between 1980 and 2010 in nuclear energy consumption, but after that improvement is comparatively low[6]. Finally in case of renewable energy sources, very clear growth is observed after 2005 and it is going on increasing.

When we see the global energy potential and consumption of renewable energies, sun has 1,73,000 TW capacity. From tidal energy sources, 0.3 TW energy is being produced. Geothermal energy source(0.3 - 2 TW) is bit higher than wave energy source(0.2-2 TW). Hydroelectric power has capacity of about 3-4 TW and Biomass fuels has around 2-6 TW. Wind has a huge capability of about 25-70 TW[7]. At the same time when we see the statistics of non renewable energy sources, coal has huge reserve of 900 TW-yr. In case of Uranium it is about 90-300 TW-yr. When we consider oil and natural gas sources, these have 240TW-yr and 215 TW-yr respectively. Total energy consumption of the world is about power of 18 TW- yr which means that our needs can easily be solved with renewable energy sources.

Next we can see economical statistics of different renewable energy sources. There is a term " EROEI ", which is " Energy Return Over Energy Invested " that is actually the ratio between "energy returned and energy invested"[8]. If the ratio is 1:1, we get equal amount of money in return after the investment. Economists say the ratio should be at least 3:1 i.e. the gain should be at least three times larger. In case of coal the EROEI, 80:1 i.e. 80 times money is returned with coal. Hydroelectric power has the highest EROEI which is 100:1[9, 10]. Even for small scale power production using wave and tidal energy sources, we have 15:1 EROEI.

Solar energy sources can be classified as "active" and "passive" solar energy techniques. Passive solar thermal techniques are very effective

though their economic gain is very low (about 2:1); with good insulating systems, one can utilize even direct solar heat through windows. In the case of active solar energy techniques (like photovoltaics)one can get EROEI of about 6.8:1 which will increase in next 5 to 10 years. Even in the case of geothermal power sources EROEI is high (about 9:1) and can be utilized with more concentration. Only disadvantage is high emission of greenhouse gases like CO_2. Wind energy is very useful if it is properly used; wind power systems have economic gain of about 18:1 which is high when compared to other power sources. Along with all these, some countries very cleverly use hydrogen for energy; however for large scale production, this has to be done only after taking proper precautions due to security issues.

In India, world's largest solar power plant was installed by 2016 in the place "Kamuthi" near Madurai in Tamil Nadu; this is maintained by Adani Group. 3250 acres of land was allotted for that. This huge power plant can deliver 648 MW which means that it meets energy needs of 300,000 homes. In 2013, a massive project was completed in California which is capable to deliver 579 MW. In biomass catagory, fuel wood has gain of 25:1 which is economically viable. Especially in mountain areas and forest areas wood fuel is more dependable for energy. But main problem with charcoal and wood is deforestation and excess amount of CO_2 release[11]. Presently world mainly depends on fossil fuels like coal, petrolium for energies(almost 67%). Approximately 11% of energy is from nuclear power sources and remaining 22% from renewable energy sources. Countries like UAE, Saudi Arabia, Oman, Botswana, Libya,

Jordan etc are totally depending on fossil fuels for energy commitments. 90% of their energy needs are being fulfilled by fossil fuels, due to availability of high oil reserve and naturally the most convenient option would be fossil fuel sources for energy generation. But there are some countries which completely depend on renewable energies; these are Ethiopia, Nepal, Albania, Tajkistan, Zambia, Namibia, Mozambique, Iceland, Norway etc. Iceland gets most of its energy from geothermal energy sources. All other countries are depending on hydroelectric power plants.

France is the country which depends on nuclear energy to fulfill at least 74% of energy needs[12, 13]. When we see picture of Europe, most of the countries like Sweden, Finland, Slovakia, France, Switzerland, Hungary etc depend on nuclear power plants. However US remains dependent on fossil fuels for about 70% of whole energy needs. Nuclear energy comes around 20% only and renewable around 10%.

1.2 Renewable energy

China is the country which produces 25% of their whole electricity through solar power technologies[14]. Then comes Japan and Germany producing 14% and 13% respectively. United states, Italy and UK are below 10%, while India produces just 2% of the whole power, which is equal to approximately 9000 MW. Mainly photovoltaic solar panels are contributing to energy production and in parallel, solar concentrators also produce large quantity of thermal energy[15, 16]. Very recently(2008 to 2013) China has become the most emerging country in photovoltaics. In every year they improve their solar energy production capacity by

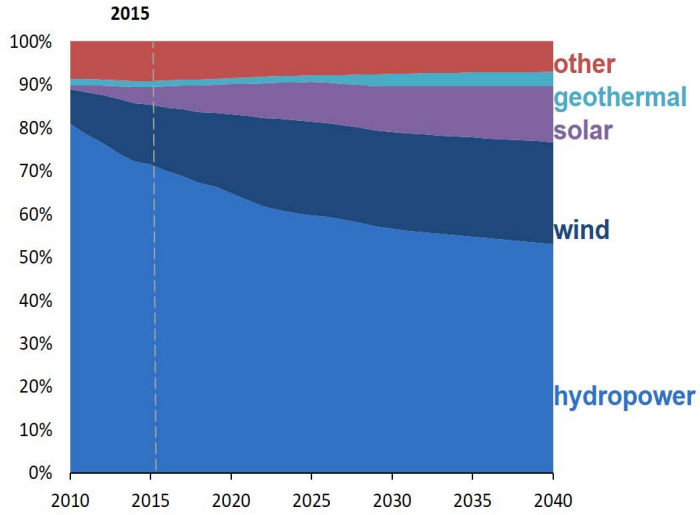

Figure 1.1: Statistics of electricity production from different renewable energy sources

13% during last 5 years. Mainly the increase in growth started from 2015 and they concentrate on polycrystalline silicon production. Japan is the second in photovoltaic energy production. They produce 4% to 5% of their power through solar technologies and 14% power through renewable energy sources. Germany is the country which has installed capacity, around 40000 MW. By the year 2030, they are planning to have 50% of power production through solar photovoltaics and by 2050 it is expected to be 80%.

1.3 Energy production using renewable energy sources and the statistics

When we see the statistics of world energy production between 2010 and 2040, among different renewable energy sources, hydroelectric power source dominates. Almost 80% of contribution in 2010 was from hydroelectric power sources. Then 10% of contribution was from wind energy sources and in 2015 the contribution improved to 15%. During 2010, photovoltaics was not at all an attractive source; but its improvement is very clear from statistics and percentage of contribution from this source in 2040 seems to be very promising[17]. Obviously geothermal and other energy sources do contribute to energy production and the statistics shows that these are constant in percentage when years proceeds. However in the case of hydroelectric power sources, growth is coming down from 2010 to 2040[18].

1.4 Photovoltaics and different Thin film solar cell materials

Photovoltaics involves direct conversion of light into electrical energy and the device that does the work is called "solar cell". First solar cell was invented in BELL laboratories in 1954 having efficiency about 6% and material was silicon. Main persons behind the device were Gerald Pearson, Daryl Chapin and Calvin Fuller. Light sensitive materials can absorb light and they are able to generate electron-hole pairs. Crystalline Silicon was used for the solar cells; this type of cells became very popular

and are also known as 'First Generation Solar Cells'. After silicon era, there came a new generation called "Thin film solar cells". Third generation is organic solar cells and recently the fourth generation has evolved which is solar cells using bio/defect assisted semiconductors/nano materials.

Most common materials are single crystalline silicon[19] and GaAs[20, 21, 22]. These two are mainly controlling photovoltaic market on earth and in space respectively. Other materials of course in thin film solar cells are CdTe (which has Zinc blend structure)[23] , Copper Indium Selinide(CIS)[24, 25]and Copper Indium Gallium Selinide(CIGS)[26] and finally CZTS[27]with the speciallity that its elements are cheap, earth abundant and non toxic.

On searching for record efficiencies of single junction thin film PV technologies, one can see that there are many materials exhibiting high efficiencies. CuS/CdS is the candidate born along with Silicon cells in 1953, exhibiting an efficiency of 10%. Similarly $CuInS_2$/CdS cells had efficiency of around 11% efficiency while kesterite material CZTSSe had efficiency around 12.6% whose structure is similar to CZTS[28]. GaAs is the most efficient material among thin film solar cells and has efficiency around 28%. Amorphous Si cells have efficiency about 13.4%, which is very commonly used for indoor applications[29, 30].

Perovskites are one of the recently developed materials; but unfortunately it has strong stability issues which are yet to be solved[31]. Likewise $CuInSe_2$ also has good potential and cell based on this material

had efficiency of 15.4%. Most promising thin film materials in the markets are CIGS(which is developed from $CuInSe_2$) and CdTe which are having band gaps of around 1.15 eV and 1.4 eV; in the case of efficiencies also they have 22.9% and 22.1% respectively in lab scale.

Crystalline silicon solar cells have good advantage of having large grain size along with high mobility(for electrons the mobility is around 1400 cm^2/VS). Mainly two kind of silicon solar cells are there; one is crystalline and other one is amorphous. Crystalline silicon solar cells have efficiency of about 26% in lab and amorphous silicon has 14%. Crystalline Silicon has the monopoly of solar cell in markets because of fast and stable technology development and/or back up due to intense research development. However Silicon has many disadvantages like high cost of production, difficulty in processing as well as purification of semiconductor silicon etc. As we know silicon is a poor absorber which has indirect band gap and needs more thickness to attain expected absorbance (about 200 nm). Moreover disposal of expired solar cell modules will be the major problem for environmental scientists in the near future.

As stated earlier, thin film solar cells are the second generation solar cells. Comparing to crystalline silicon solar cells, thin film solar cells need less material requirement. A variety of processing methods applicable for thin film solar cell production. Again weight of solar cell is very less comparing to silicon cells as thickness in this case is just few hundred nano meters instead of microns. In defense, nowadays thin film are very widely used for the exclusion of heavy batteries. Variety of thin films

are suitable for solar cell production. In thin films, more than single semiconductor materials, compound semiconductors are preferred. Such materials can easily be doped so as to modify material properties or according to the needs even band gap can be changed. Comparing to silicon cells; efficiencies are low but enough can be produced employing economically viable techniques for commercial uses. Cost of production of thin film solar cells are very low on comparing to silicon solar cells, much more than that, re-usability of materials is possible here through rather simple chemical methods. This prevents accumulation of dead solar cells as waste.

Thin film solar cells are having many advantages over commercial silicon wafer panels. Low cost of production per watt, different options for deposition, and requirement of less quantity of the material are a few. Simultaneously power consumption for fabrication is much less. All these result in reduction of production cost considerably. Thin film cells can be folded provided these are deposited over any flexible materials. Apart from Si thin film solar cells, CIGS and CdTe solar cells are very much established in technology and hence commercially implemented.

National Renewable Energy Laboratory(NREL) has tabulated best cell efficiency(Fig.2)values on lab scale[20]. The most efficient solar cells are multijunction solar cells which have efficiencies of 45% where different solar cells are arranged to get array of cells, for absorbing different wavelengths. They are coming under the division of "concentrated solar cells"(4 or more junction) where light is concentrated to a particular

portion of solar cell using high power mirrors/lenses.

Then another highly efficient material is GaAs(single crystal) which has reached an efficiency around 29%. Single crystal silicon is there at 27% efficiency and below is heterostructure silicon at 28%. Multi crystalline silicon cells reached 23% of efficiency in lab scale. Among single junction thin film solar cells, CIGS is most efficient. CIGS has reached efficiency of 25% in 2017. CdTe based cell is also equally good in efficiency but due to some toxicity issue some countries avoid Cd and Te based solar cells. Amorphous silicon cells are very established in markets due to their good efficiency and flexibility. They have efficiency about 14% in lab scale. The next generation of solar cells are based on organic polymer materials and some blended organic metal materials like Perovskites. Dye sensitized solar cells(DSC) came in 1990s and efficiency of DSC is presently around 13% in lab scale. Unlike other thin film materials, CZTS is an upcoming and non toxic, novel material in solar cell field. CZTS cell has an efficiency of about 12% in lab scale. But in case of CIGS, Indium and Gallium are very expensive and in CZTS, we are replacing these with Zinc and Tin, which are earth abundant and cheap. Like CZTS there are other options from CIGS; one is Copper Tin Sulphide(CTS) and the other one is Copper Zinc Sulphide(CZS). CTS is promising material in photovoltaics, and researches are going on with an intention that it is to be developed as a good absorber layer in solar cells.

In Copper Zinc Sulphide, we are avoiding Tin due to its corrosive

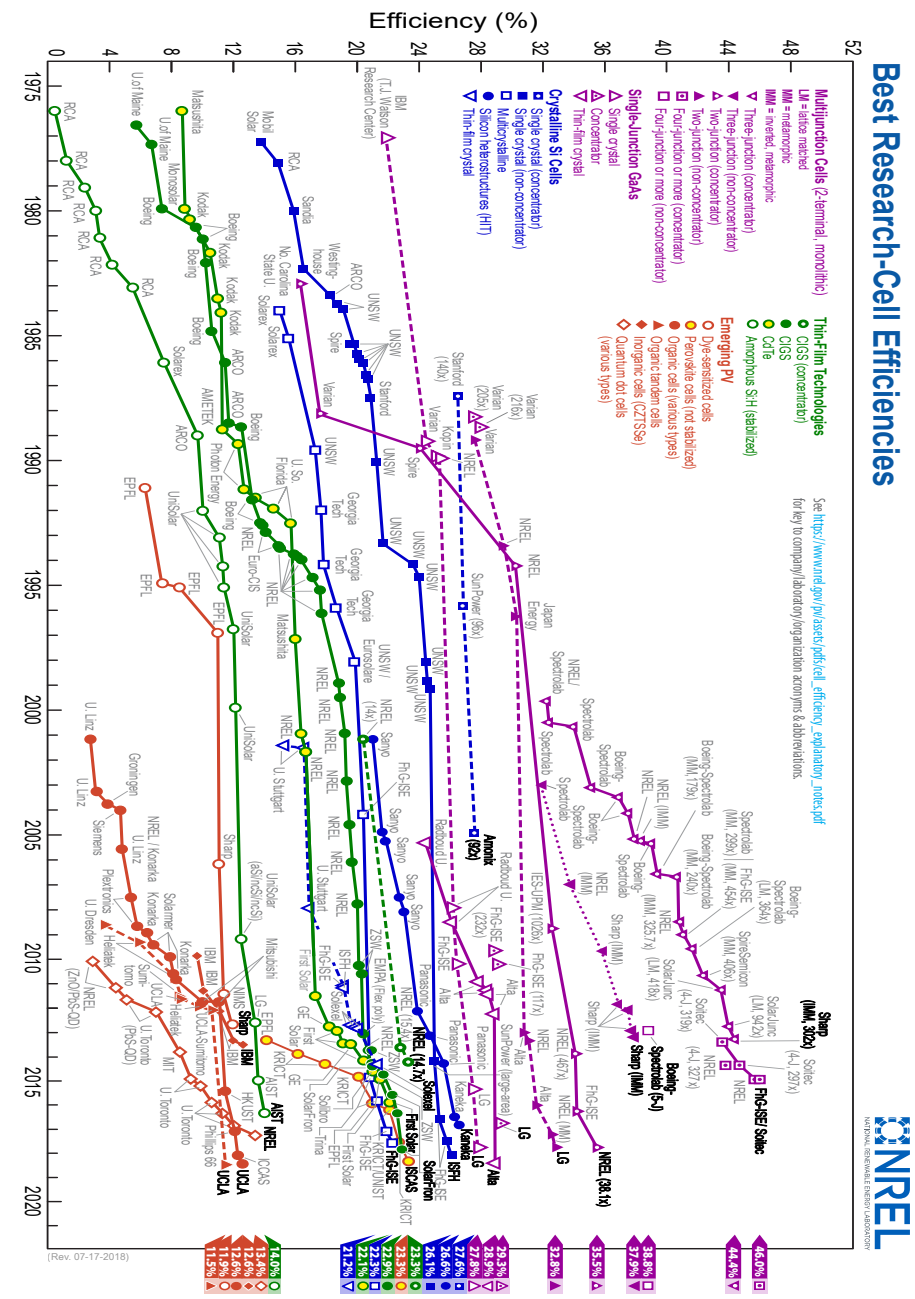

Figure 1.2: Efficiency chart of different solar cells in lab scale

nature. Researches in CZS started in 2010 by a Nigerian group. Due to the easiness of tuning the properties of CZS, material can be easily changed from absorber to buffer layer(material can show two conductivity and two band gaps i.e. n and p conductivities and two band gaps according to difference in Cu concentration). At higher concentration of Cu material can make it absorber layer and at lower Cu concentration this can become buffer layer. At lower Cu concentration material can also act as transparent conducting material(TCM) which is having attraction in transistors and LEDs.

1.5 CuZnS a novel material for photovoltaics and optoelectric devices : a brief review

CuZnS is a new material in the field of photovoltaics. Basically it is a mixture of the two compounds CuS and ZnS. This material is similar to well known CZTS except the element Tin and indeed this results in variations of properties making it much more suitable for photovoltaics. Very few publications are there dealing with studies on this material. If CZTS is a well known absorber material with high coefficient of absorption and good crystalline structure, this new material CZS can act as either absorber or window layer depending up on the concentration of Copper in it.

Reports on CZS so far mainly explain the p type nature with high conductivity and transparency. Major aim of all works is to develop the material as a good p - type transparent conducting material for optoelec-

tric devices. Addition of Cu in ZnS material affects its conductivity and on increasing Cu concentration, the material becomes p type, maintaining high conductivity. Another important peculiarity is that it exhibits two different band gaps at the same time. This double band gap nature enables it to absorb different photons of different energies.

Diamond et al.[32] said about possibility of dual donor co-doping of ZnS with elements Sn and F. He also added that there are some reports supporting p type doping with elements Li and N. He also concluded that degenerate hole concentrations was achievable in sulphur rich conditions. Another important factor is that there are only very few Transparent Conducting Material(TCM) having wurtzite crystalline structure. CuZnS will definitely have crystal structure matching with so many n type buffers as wurtzite structure is found to be matching with many materials. Diamond also suggests sulphur rich, zinc deficient or Cu rich condition is favorable for p type conductivity where Fermi energy level comes very close to valance band. In this paper(from Xray diffraction pattern) it is reported that peak positions of ZnS and CZS are same, While with XPS, difference in binding energies of Cu, Zn and S in CuZnS and ZnS are very clearly depicted. Finally he succeeds in fabricating transistor using p type CuZnS and n type ZnS having high tansparency.

Uhuegbu et al.[33] explained change in absorbance, reflectance and transmittance with different ratios of Cu, Zn and S. He reported variation in thickness with increase in sulphur concentration. Absorbance

increased with increase in sulphur content(as thickness increases with sulphur content). For film having thickness of 280 nm, absorbance is double that of film having thickness about 240 nm. In this paper it is also suggested that CZS can exist like CuZnS, $CuZnS_2$, $CuZnS_3$ etc. It is also reported here that there is high transmittance in visible region and absorbance in UV and infrared region of the spectrum. He suggested that, this property of transmitting visible light makes these films useful for solar transmitting films especially in solar thermal systems. Que et al.[34] explained possibility of using CuZnS as green light emitting devices. He explained the green luminescence as due to transition between conduction band to Cu^{2+} level in ZnS band gap. It has emission from 490 nm to 530 nm.

Ichimura et al.[35] studied CuZnS in detail and reported many optical properties. He reported variation in absorption with variation of Cu and Zn concentration and also calculated composition of different samples deposited with different concentration of elements in solution. This study showed that there is large variation of composition of samples which is proportional to concentration of elements in solution(Here it is Cu and Zn). Along with these he reported variation of band gaps of different samples having different concentrations of elements. Band gap is varying from 2 eV to 3.6 eV with variation of Cu and Zn concentration in solution. Variation of pH was another study he has done and explained complexity of deposition as well as precipitation. Structural study with XRD analysis indicated that samples are amorphous in nature. With Photo Electro Chemical(PEC) measurements Ichimura proved capability of material to

generate carriers with illumination and strongly recommends for using in solar cells. Using photosensitivity study of samples increase in generation of carriers was also proved.

Yang et al.[36]reported preparation of CuZnS using electrochemical deposition method. He deposited different samples at different pH values using lactic acid, and there film formation occurred at different deposition potentials. He suggests occurance of material is like alloy and phases of CuS and ZnS are there. PEC measurements indicated that the material was very much light sensitive and with illumination, more minority carriers were generated contributing to photo current. Morphological analysis using SEM showed good compact and continuous surface. Raman analysis showed very good peak of CuS and this befits the fact that material exists as mixture of CuS and ZnS. Transmission spectra of samples show a gradual decrease in transmission with decrease in Zn/Cu ratio. PEC measurements showed considerable increase in negative current with illumination which means that minority carriers (electrons) are generated with light absorption and increase in current density is also very clear. Here Yang et al. confirmed the capability of this material to respond to light.

In another article, Yang et al.[37] explained about p type conducting possibility of this material (i.e. CuZnS) in the future. Even with very small amount of Cu one can make CuZnS a transparent conducing material. The band gap comes around 3.3 eV which is very near to the band gap of ZnS and ZnO. It is to be specifically noted here that

electrical properties are very much varied with Cu doping. He studied transmission spectra of CuZnS which clearly showed that the material has transmission in visible region. CuZnS films show transmissions of around 60 to 80% which is considered to be high in case of transparent conducting materials. He also strongly suggested that the material is an alloy and the high transmission also show that Cu is not existing as CuS.

Kitagaw et al.[38]suggested that there was drastic variation of resistivity with decrease in Cu concentration. He noted that when concentration of Cu is below 18% the material became highly resistive so that it could not be measured using normal conductivity measurements. Band gap varied from 2.3 eV to 3.4 eV and carrier concentration was in the order of $10^{21}cm^{-3}$. Mobility was around 10^{-1}, which was low. He fabricated a solar cell with CZS and Indium Sulphide in which he claimed the formation of Copper Indium Sulphide, which was not present in Xray diffraction analysis because of low thickness of the interlayer formed between CZS and Indium Sulphide. This paper proved how spray pyrolysed CZS acted as good absorber with Indium sulphide buffer. Cell having higher Cu concentration had higher efficiency. When percentage of Cu was about 20% to 33% efficiency was about 0.5%. But When the cells had Cu concentration of 55% to 60%, efficiency was about 1.5%.

W.Q. Peng et al.[39] studied photoluminescence of Cu doped ZnS. Doping was done using very small quantity of Cu (about a maximum of 2%). Structural characterization gave good crystalline structure of ZnS and no peaks of Cu or CuS were observed. In transmission electron mi-

croscope image particle size was observed around 3 nm and lattice fringes were very clear, which indicated crystallinity of the particles. Particles exhibited blue emission; but here along with blue emission a green emission was also observed. Peak around 450 nm was attributed to trap states emission due native Zinc vacancy in ZnS. He suggested that with more Cu^{2+} chances for defect level formation was high. This was confirmed with peaks around 411 nm and 455 nm which enhanced with doped samples.

Tong et al.[40] deposited CuZnS using photochemical deposition method and studied structural and optical characterizations. Structural studies of annealed samples indicated peaks corresponding to ZnS (zinc blend). For lower temperature annealing crystallinity was not observed(no peaks of ZnS were observed). From Augur Electron Spectroscopy(AES), composition of samples was measured. It showed increase in Sulphur content after annealing of samples. But in optical band gap measurements, there was no considerable variation in bangaps and transmission spectra. He suggested that Cu would be distributed throughout CuZnS phase and no chances of CuS formation was there. In PEC measurements, annealed samples gave more negative photo current which clearly indicated that the response was definitely p type. Cu could be acting as acceptor and in amorphous samples(i.e. comparing to annealed samples) role of Cu is not clear.

Wei-Shih Ni and Yow-Jon Lin[41] reported different properties of CuZnS films prepared using solution method. They found that Cu con-

tent in the films were lower than that in the solution. Higher resistive samples were not showing any response towards Hall measurement setup. It was also suggested that hole concentration increased with increase in Cu concentration. Another interesting observation was that concentration of sulfur changed with increase in Cu concentration; simultaneously donor density reduced. This paper revealed relation of concentrations of Cu, Zn and S with sulfur vacancies.

Uhuegbu et al.[42] reported CuZnS deposited using chemical solution method. In this paper it was reported that there was increase in transmittance with decrease in thickness(transmittance varying from 60% to 20%). Authors proved that there was a probability for formation of materials like $CuZnS_1$, $CuZnS_2$ and $CuZnS_3$. Through a plot between absorption coefficient and photon energy, it had been proved that for all compositions of Cu, Zn and S the value increased with photon energy. Interestingly this material has different nature in band gap properties; some showed both direct band gap while others had indirect band gaps. In the same way, optical conductivity of the material is increasing with increase in photon energy. But in lower energy region i.e. around 1.5 eV, the conductivity shows opposite nature where it is decreasing with increase in photon energy. Extinction coefficient of the material is decreasing with increase in photon energy.

Very recently in 2017, Jose et al.[43] deposited CuZnS films "SILAR" method and characterized. They observed a 'petal-like' structure for Cu rich samples and for Zn rich samples, these were aggregated to form

clusters. Very nice 'petal like flower' structure was reported in the manuscript. Basic trend was that when Cu increases, grains become small. Using XPS analysis Jose et al. found out that major portion of material was CuS phase and hence there was large chance for Cu atoms replacing Zn. When Zn is introduced normal CuS phase get distorted and non stoichiometric phase of Cu, Zn and S would be formed. Then whole material behaves like an alloy where major portion was CuS. XRD analysis also showed characteristic peak of CuS and in Zn rich samples, an extra peak was formed indicating the material existed as "Zn incorporated CuS" or non stoichiometric CuZnS. They could see some change of CuS peaks in Raman analysis, when Zn is incorporated. The Raman shift towards left side of original peak indicated that bond strength between Cu, Zn and S changed. This paper also reports that all samples show p type conductivity.

Corrado et al.[44] studied photoluminescence properties of ZnS(which is Cu doped). They could find blue shift in emission and red emission. This is very clear evidence of Cu^{+}. Eventhough Cu doping is in low percentage, CuS is formed with bond length around $2.27A^{0}$. They compared the PL emission properties of this Cu doped ZnS nano cystals with bulk Cu doped ZnS. In both materials the PL peaks(CuS peaks) are broadening with temperature indicating increase of bond length.

Innocenti et al. deposited CuZnS films using electrochemical process, on Ag substrate, in two sequences. Stripping voltammetry studies gave exact conditions for deposition of CuS and ZnS. Apart from that,

these authors described exact condition for formation of CuZnS material using stripping voltammetry. Films grown with this had low Zn concentration. The material fabricated on Ag substrate had band gap of 1.6 eV which is very suitable for solar cell fabrication.

Yildirim et al.[45] reported on CuZnS films, grown using "SILAR" method on glass substrate.They characterized samples after annealing at different temperatures and found that maximum temperature which it could withstand was 400^oC. From XRD analysis it was observed that all films were amorphous. In morphological analysis using SEM, CuZnS was found to be non uniform on glass substrates. These samples were photosensitive and it increases with increase in intensity of light and decreased with increase in annealing temperature.

Ramos et al.[46] deposited Cu doped ZnS as transparent conducting material using CBD. In this work they first deposited ZnS and then doped Cu which brought some changes in ZnS. Though ZnS deposited was crystalline(cubic) in nature, introduction of Cu made it amorphous. Also there was decrease in transparency of the films from 80% to 60%. In the case of band gap, doping resulted in slight decrease from 3.8 eV to 3.76 eV. All samples were electrically p type in nature and resistivity was in KΩcm.

Ichimura et al.[47] in 2015 reported fabrication of a heterostructure between CuZnS and ZnO on ITO. They used transparent CuZnS having 60% transparency and the ZnO layer had transmission about 80%; the combined structure exhibited transmission of about 30%. The whole

setup exhibited efficiency about 10^{-4}, with short circuit current of about 0.01 mA/cm^2 and open circuit voltage of about 200 mV. This was the pioneering work on transparent cells.

Ichimura et al.[48] reported heterojunction Cu_xZn_y S/ZnS using photochemical deposition method and the heterostructure was totally transparent in nature. These samples were having high transmission about 70% in visible region. The peculiarity was that the junction showed rectification and photo response properties in AM 1.5 irradiation.

Xu et al.[49] reported on chemical bath deposited CuS and ZnS nano composite and their combination with Si, forming hetero junctions. Rasoul et al.[50] reported on Ni and Cu doped ZnS particles prepared using solution method. Kim et al.[51] reported possibility of Ga and Cu doping in ZnS. Similarly Owens et al.[52] found high temperature magnetic order in ZnS doped with Cu. Different properties like 'mechanoluminesense' were also found in Cu doped ZnS which was reported by Shin et al.[53]. Photoconductive properties of Cu doped ZnS, which was reported by Shrivastava et al.[54] gave clear confirmation of the material to be used in solar cells. Behavior of Cu doping in ZnS is totally different from doping in nano structures like quantum dots. Behavior of Cu doping in quantum dot ZnS was reported by Lee et al.[55].

References

[1] Historical Data Workbook. Bp statistical review of world energy:[6]. 2014.

[2] Indu Ambat, Varsha Srivastava, and Mika Sillanpa. Recent advancement in biodiesel production methodologies using various feedstock: A review. *Renewable and Sustainable Energy Reviews*, 90:356–369, 2018.

[3] Shuai Han, Hong Chen, Ruyin Long, and Xiaotong Cui. Peak coal in china: A literature review. *Resources, Conservation and Recycling*, 129:293–306, 2018.

[4] J Lin, D Fridley, H Lu, L Price, and N Zhou. Near-term trends in china's coal consumption. 2018.

[5] Lennart Soder, Peter D Lund, Hardi Koduvere, Torjus Folsland Bolkesjo, Geir Hoyvik Rossebo, Emilie Rosenlund-Soysal, Klaus Skytte, Jonas Katz, and Dagnija Blumberga. A review of demand side flexibility potential in northern europe. *Renewable and Sustainable Energy Reviews*, 91:654–664, 2018.

[6] Siddharth Suman. Hybrid nuclear-renewable energy systems: a review. *Journal of Cleaner Production*, 181:166–177, 2018.

[7] Omkar P Kedar and Ganesh Fodase. A review on under water windmill. 2018.

[8] Patrick Moriarty and Damon Honnery. Global renewable energy resources and use in 2050. pages 221–235. Elsevier, 2019.

[9] Godfrey Boyle. Renewable energy. *Renewable Energy*, page 456, 2004.

[10] Samuel Gyamfi, Nana S A Derkyi, Emmanuel Y Asuamah, and Israel J A Aduako. Renewable energy and sustainable development. pages 75–94. Elsevier, 2018.

[11] Markus Munz, Alexander Mokros, and Christian Beidl. Ome in the diesel engine–a concept for co 2 neutrality and lowest pollutant emissions. pages 445–458. Springer, 2018.

[12] Vincenzo Bianco and Federico Scarpa. Impact of the phase out of french nuclear reactors on the italian power sector. *Energy*, 150: 722–734, 2018.

[13] Elina Brutschin and Jessica Jewell. 23 international political economy of nuclear energy. *Handbook of the International Political Economy of Energy and Natural Resources*, page 322, 2018.

[14] Junxia Liu. China's renewable energy law and policy: A critical review. *Renewable and Sustainable Energy Reviews*, 99:212–219, 2019.

[15] Daria Freier, Roberto Ramirez-Iniguez, Tahseen Jafry, Firdaus Muhammad-Sukki, and Carlos Gamio. A review of optical concentrators for portable solar photovoltaic systems for developing countries. *Renewable and Sustainable Energy Reviews*, 90:957–968, 2018.

[16] Arif Hepbasli and Yildiz Kalinci. A review of heat pump water heating systems. *Renewable and Sustainable Energy Reviews*, 13: 1211–1229, 2009.

[17] Dennis W Van der Meer, Joakim Widn, and Joakim Munkhammar. Review on probabilistic forecasting of photovoltaic power production and electricity consumption. *Renewable and Sustainable Energy Reviews*, 81:1484–1512, 2018.

[18] Ehsanul Kabir, Pawan Kumar, Sandeep Kumar, Adedeji A Adelodun, and Ki Hyun Kim. Solar energy: Potential and future prospects. *Renewable and Sustainable Energy Reviews*, 82:894–900, 2018.

[19] Ingmar Hoger, Martin Schaper, Ansgar Mette, Benjamin G Lee, Fabian Fertig, Ronny Lantzsch, Stefan Peters, Andreas Eidner, Klaus Duncker, Matthias Bartzsch, et al. Boosting module power by advanced interconnection and p-type cz silicon solar cell efficiencies exceeding 22% in mass production. volume 1999, page 110003, 2018.

[20] Martin A Green, Yoshihiro Hishikawa, Ewan D Dunlop, Dean H Levi, Jochen Hohl Ebinger, Masahiro Yoshita, and Anita WY Ho-Baillie. Solar cell efficiency tables (version 53). *Progress in Photovoltaics: Research and Applications*, 27:3–12, 2019.

[21] Simon P Philipps, Frank Dimroth, and Andreas W Bett. High-efficiency iii–v multijunction solar cells. In *McEvoy's Handbook of Photovoltaics*, pages 439–472. Elsevier, 2018.

[22] Michelle Vaisman, Nikhil Jain, Qiang Li, Kei May Lau, Emily Makoutz, Theresa Saenz, Willian E McMahon, Adele C Tamboli, and Emily L Warren. Gaas solar cells on nanopatterned si substrates. *IEEE Journal of Photovoltaics*, 8:1635–1640, 2018.

[23] Amit H Munshi, Jason M Kephart, Ali Abbas, Tushar M Shimpi, Kurt L Barth, John M Walls, and Walajabad S Sampath. Polycrystalline cdte photovoltaics with efficiency over 18% through improved absorber passivation and current collection. *Solar Energy Materials and Solar Cells*, 176:9–18, 2018.

[24] Christopher P Muzzillo, Jonathan D Poplawsky, Ho Ming Tong, Wei

Guo, and Tim Anderson. Revealing the beneficial role of k in grain interiors, grain boundaries, and at the buffer interface for highly efficient cuinse2 solar cells. *Progress in Photovoltaics: Research and Applications*, 2018.

[25] Alexander R Uhl, Adharsh Rajagopal, James A Clark, Anna Murray, Thomas Feurer, Stephan Buecheler, Alex K Y Jen, and Hugh W Hillhouse. Solution-processed low-bandgap cuin(s,se)2 absorbers for high-efficiency single-junction and monolithic chalcopyrite-perovskite tandem solar cells. *Advanced Energy Materials*, 8: 1801254, 2018.

[26] Wenqin Shi, Mirjam Theelen, Veronique Gevaerts, Andrea Illiberi, Nicolas Barreau, Maik Butterling, Henk Schut, Werner Egger, Marcel Dickmann, Christoph Hugenschmidt, et al. Positron annihilation studies on the damp heat degradation of zno: Al transparent conductive oxide layers for cigs solar cells. *IEEE Journal of Photovoltaics*, pages 1–5, 2018.

[27] Shreyash H Hadke, Sergiu Levcenko, Stener Lie, Charles J Hages, Jose A Marquez, Thomas Unold, and Lydia H Wong. Synergistic effects of double cation substitution in solution-processed czts solar cells with over 10% efficiency. *Advanced Energy Materials*, 8: 1802540, 2018.

[28] Dharmendar Kumar, Jaykumar Patel, and Kshitij Bhargava. Theoretical investigation of the influence of defect states on the power conversion efficiency of cztsse solar cells. In *2018 3rd International Conference for Convergence in Technology(I2CT)*, pages 1–4. IEEE, 2018.

[29] Junhua Long, Meng Xiao, Xinping Huang, Zhiwei Xing, Xuefei Li, Pan Dai, Ming Tan, Yuanyuan Wu, Minghui Song, and Shulong Lu. High efficiency thin film gainp/gaas/ingaas inverted metamorphic (imm) solar cells based on electroplating process. *Journal of Crystal Growth*, 2019.

[30] Kumar Mallem, Yong Jun Kim, Shahzada Qamar Hussain, Subhajit Dutta, Anh Huy Tuan Le, Minkyu Ju, Jinjoo Park, Young Hyun Cho, Youngkuk Kim, and Eun-Chel Cho. Molybdenum oxide: A superior hole extraction layer for replacing p-type hydrogenated amorphous silicon with high efficiency heterojunction si solar cells. *Materials Research Bulletin*, 110:90–96, 2019.

[31] Nam Joong Jeon, Hyejin Na, Eui Hyuk Jung, Tae-Youl Yang, Yong Guk Lee, Geunjin Kim, Hee-Won Shin, Sang Il Seok, Jaemin Lee, and Jangwon Seo. A fluorene-terminated hole-transporting material for highly efficient and stable perovskite solar cells. *Nature Energy*, 3:682, 2018.

[32] Anthony M Diamond, Luca Corbellini, KR Balasubramaniam, Shiyou Chen, Shuzhi Wang, Tyler S Matthews, Lin-Wang Wang, Ramamoorthy Ramesh, and Joel W Ager. Copper-alloyed zns as ap-type transparent conducting material. *physica status solidi (a)*, 209:2101–2107, 2012.

[33] C C Uhuegbu and E B Babatunde. Spectral analysis of copper zinc sulphide ternary thin film grown by solution growth technique. *American Journal of Scientific and Industrial Research*, 1:397–400, 2010.

[34] Wenxiu Que, Y Zhou, Y L Lam, Y C Chan, C H Kam, B Liu, L M Gan, C H Chew, G Q Xu, and S J Chua. Photoluminescence

and electroluminescence from copper doped zinc sulphide nanocrystals/polymer composite. *Applied physics letters*, 73:2727–2729, 1998.

[35] Man Dula, Kai Yang, and Masaya Ichimura. Photochemical deposition of a p-type transparent alloy semiconductor cuxznys. *Semiconductor Science and Technology*, 27:125007, 2012.

[36] Kai Yang and Masaya Ichimura. Fabrication of transparent p-type cuxznys thin films by the electrochemical deposition method. *Japanese Journal of Applied Physics*, 50:040202, 2011.

[37] Kai Yang, Yuki Nakashima, and Masaya Ichimura. Electrochemical deposition of cuxs and cuxznys thin films with p-type conduction and photosensitivity. *Journal of The Electrochemical Society*, 159: H250–H254, 2012.

[38] Noriyuki Kitagawa, Seigo Ito, Duy-Cuong Nguyen, and Hitoshi Nishino. Copper zinc sulfur compound solar cells fabricated by spray pyrolysis deposition for solar cells. *Natural Resources*, 4:142, 2013.

[39] W Q Peng, G W Cong, S C Qu, and Z G Wang. Synthesis and photoluminescence of zns: Cu nanoparticles. *Optical Materials*, 29: 313–317, 2006.

[40] Bayingaerdi Tong and Masaya Ichimura. Annealing of p-type wide-gap cu x zn y s thin films deposited by the photochemical deposition method. *Japanese Journal of Applied Physics*, 55:098004, 2016.

[41] Wei-Shih Ni and Yow-Jon Lin. Conduction behavior conversion for cu-doped zns/n-type si devices with different cu contents. *Applied Physics A*, 119:1127–1132, 2015.

[42] Chidi Chukwuemeka Uhuegbu, Elisha Bamidele Babatunde, and Cornelius O Oluwafemi. The study of copper zinc sulphide (cuzns2) thin films. *Turkish Journal of Physics*, 32:39–47, 2008.

[43] Edwin Jose and M C Santhosh Kumar. Room temperature deposition of highly crystalline cuzns thin films for solar cell applications using silar method. *Journal of Alloys and Compounds*, 712:649–656, 2017.

[44] Carley Corrado, Yu Jiang, Fadekemi Oba, Mike Kozina, Frank Bridges, and Jin Z Zhang. Synthesis, structural, and optical properties of stable zns: Cu, cl nanocrystals. *The Journal of Physical Chemistry A*, 113:3830–3839, 2009.

[45] M Ali Yildirim and Ate. Annealing and light effect on structural, optical and electrical properties of cus, cuzns and zns thin films grown by the silar method.

[46] Daniela E Ortz-Ramos, Luis A Gonzlez, and Rafael Ramirez-Bon. p-type transparent cu doped zns thin films by the chemical bath deposition method. *Materials Letters*, 124:267–270, 2014.

[47] Masaya Ichimura and Yosuke Maeda. Heterojunctions based on photochemically deposited cuxznys and electrochemically deposited zno. *Solid-State Electronics*, 107:8–10, 2015.

[48] Masaya Ichimura and Yosuke Maeda. Fabrication of transparent cuxznys/zns heterojunction diodes by photochemical deposition. *physica status solidi (c)*, 12:504–507, 2015.

[49] Xiaojie Xu, James Bullock, Laura T Schelhas, Elias Z Stutz, Jose J Fonseca, Mark Hettick, Vanessa L Pool, Kong Fai Tai, Michael F

Toney, Xiaosheng Fang, et al. Chemical bath deposition of p-type transparent, highly conducting (cus)–(zns)nanocomposite thin films and fabrication of si heterojunction solar cells. *Nano letters*, 16: 1925–1932, 2016.

[50] Khalid T Al Rasoul, Nada K Abbas, and Zainb J Shanan. Structural and optical characterization of cu and ni doped zns nanoparticles. *Int. J. Electrochem. Sci*, 8:5594–5604, 2013.

[51] Melody Kimi, Leny Yuliati, and Mustaffa Shamsuddin. Preparation of high activity ga and cu doped zns by hydrothermal method for hydrogen production under visible light irradiation. *Journal of Nanomaterials*, 16:200, 2015.

[52] Frank J Owens, L Gladczuk, R Szymczak, P Dluzewski, A Wisniewski, H Szymczak, A Golnik, Ch Bernhard, and Ch Niedermayer. High temperature magnetic order in zinc sulfide doped with copper. *Journal of Physics and Chemistry of Solids*, 72:648–652, 2011.

[53] Seung Wook Shin, Jeung Pyo Oh, Chang Woo Hong, Eun Mi Kim, Jeong Ju Woo, Gi-Seok Heo, and Jin Hyeok Kim. Origin of mechanoluminescence from cu-doped zns particles embedded in an elastomer film and its application in flexible electro-mechanoluminescent lighting devices. *ACS applied materials & interfaces*, 8:1098–1103, 2015.

[54] Rajneesh K Srivastava, Nitin Pandey, and Sheo K Mishra. Effect of cu concentration on the photoconductivity properties of zns nanoparticles synthesized by co-precipitation method. *Materials Science in Semiconductor Processing*, 16:1659–1664, 2013.

[55] Gang-Juan Lee, Hui-Chuan Chen, and Jerry J Wu. (in, cu) co-doped

zns nanoparticles for photoelectrochemical hydrogen production. *International Journal of Hydrogen Energy*, 44:110–117, 2019.

Chapter 2

Deposition of thin film CuZnS using Chemical Bath Deposition and characterization

2.1 Introduction

Nowadays different research groups all over the world are deeply involved in developing eco-friendly and economic thin film solar cells[1]. These groups try to incorporate earth abundant materials in solar cells. CZTS is a well known absorber material which has only earth abundant and eco-friendly elements. Like CZTS, we tried to develop a new material called Copper Zinc Sulphide(CZS) where the material is simply a new one which is 'CZTS without Tin'. CuZnS is a good candidate for the development of TCM(Transparent Conducting Material) and here we try to develop the material CZS as an absorber material for solar cell fabrication[2, 3].

Most of the research groups started fabricating the material through doping Cu in ZnS and then slowly increasing the concentration of Cu[4, 5]. At lower concentration of Cu, material behaves like TCM whereas at higher concentration of Copper, material generally behaves as absorber material and in appearance it would not be transparent too. As we are interested in solar cell fabrication we concentrated on making a good absorber layer.

CuZnS material was fabricated using different methods by different groups, some of the deposition techniques are photochemical deposition[6], pulsed vapor deposition[7], electrodeposition[8], SILAR[9], spray pyrolysis [10] and chemical bath deposition[11, 12]. Here we started depositing material using chemical bath deposition technique as it is very simple and cost effective for thin film deposition[13, 14]. Materials like CdS, ZnS and CuS are very common candidates being deposited using this method[15, 16]. Here there is no need of vacuum and high power electricity. Deposition conditions can be easily changed for different compounds. Almost 18%[12] efficiency is reported for ZnS - Cu(In,GA)Se_2 solar cell prepared using chemical bath deposition. It is worth mentioning here that for methods like electrodeposition we need to use conducting material like ITO or FTO while for pulsed laser deposition and sputtering we need to use different targets at the same time. But in the case of CBD, it is a matter of using a solution containing necessary elements as constituents; ofcourse one need to maintain the pH and temperature of the solution carefully. In this particular chapter we describe CuZnS material deposition using CBD technique, their characterization and device

fabrication.

2.2 Experimental techniques

Soda lime glass was the substrate that we used for deposition of CuZnS films. Deposition conditions were decided from deposition of CuS and ZnS reported in various articles[17, 18, 19]. First we smeared substrates with alcohol, using tissues made wet with propanol and water. Then sonicated the substrates in fresh propanol for 15 minutes and finally boiled in chromic acid for 20 minutes. All substrates were rinsed properly using deionized water to assure that there is no acid droplets. Copper sulphate, Zinc sulphate, Thiourea and Sodium thiosulphate were the precursors used for deposition of CZS. As complexing agents Triethanolamine(TEA) and Ammonia solutions were used.

Sample	$CuSO_4$ (ml)	$ZnSO_4$(ml)	Thiourea(ml)	$Na_2S_2O_3$(ml)
S1	2	4	2	4
S2	2.5	4	2	4
S3	3	4	2	4
S4	3.5	4	2	4
S5	4	4	2	4

Table 2.1: Experimental details of the deposition of CuZnS

The reaction bath was prepared by mixing 4 ml of(0.1 M) $ZnSO_4$, 0.4 ml of(0.5 M) Sodium Thiosulphate, 3 ml of(1 M) NaOH, 10 ml of ammonia solution, 0.4 ml of TEA, 0.5 ml of(0.1 M) $CuSO_4$ and 2 ml of(1M) Thiourea[20, 21]. $CuSO_4$(varied from 2 ml to 4 ml in steps of 0.5 ml in each set) and $ZnSO_4$ were added first followed by Thiourea

and TEA at the end. After adding all precursors it was made up to 60 ml using deionized water and was again placed in hot water bath for maintaining temperature of 85^{o}C[22]. The glass plates were vertically arranged inside the bath using nonreactive steel sample holder. When temperature gradually increases from room temperature, solution color slowly changes from blue to brown which shows that reaction is taking place.

The solution was kept there for 1 hr at the same temperature and samples were taken out without disturbing the solution. Samples were dried at room temperature after rinsing in fresh deionized water and then sonicating in propanol for 5 minutes. This step did not satisfy sufficient thickness for the film and deposited samples were again treated for two more dips in freshly prepared solutions, keeping all the bath parameters constant to attain sufficient thickness.

In the present study we varied volume of Cu precursor from 2 ml to 4 ml in steps of 0.5 ml keeping all other parameters constant. Different samples prepared were named S1, S2, S3, S4 and S5. The specifications are depicted in the Table 2.1. Structural, electrical and optical characterizations of prepared films were studied using different techniques. Thickness of deposited samples were measured using thickness profilometer.

Structural analysis of the films was carried out using Rigaku (D. Max.C X-ray diffractometer and Ni filter). UV-Visible absorption analysis was done using UV-Vis-NIR spectrophotometer(Jasco-V 570). Raman analysis was done employing Horiba Jobin Yvon LabRAM micro

spectrometer. Composition of the CZS thin film was studied with the help of XPS[Kratos Analytical AMICUS spectrometer fitted with the Mg Ka/Al Ka dual anode X-ray source]. Hall measurements(Ecopia HMS-5300)and thickness(Stylus profiler Dektak 6M) were measured for all samples. Solar cell J-V characterization was done using Photo Emission(Tec SS550AAA) solar simulator (100 mW/cm^2 illumination) and National Instruments Source Measure Unit.

2.3 Results and discussion

2.3.1 Structural studies

Samples S2 to S4 show very little response towards XRD analysis(Fig.2.1). S1 shows peaks of hexagonal Zinc Sulphide at 2θ values 16.42, 18.12, and 24.67 where planes are (009) (0010) and (0014) respectively(Table 2.2). Here samples S1 and S5 show crystallinity in which Zinc and Cu are rich in quantity respectively. In Cu rich sample (S5), there are peaks of hexagonal covellite CuS planes at 2θ value 48.02 which corresponds to (110) plane of CuS. Moving from sample S1 to S2 the crystallinity slowly decreases and peaks corresponding to ZnS phase disappeared. All the samples from S2 to S4 are amorphous in nature.

Again on increasing the concentration of Cu material begins to show crystalline planes of CuS. In sample S5, (110) plane of CuS appears at 2θ value 48.02 and this is a common peak of CuS. In thin films, this phenomenon (disappearance of one crystalline phase and appearance of other)can be seen frequently, where amorphous phase will come in between two different crystalline phases[23]. According to variation in

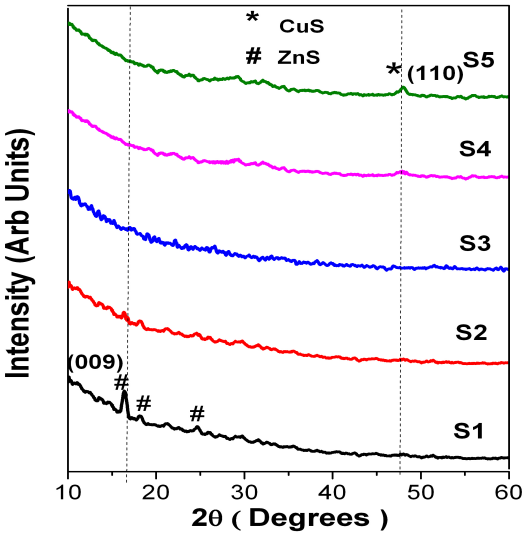

Figure 2.1: XRD plot of different samples deposited at different Cu concentrations (Samples S1 to S5)

copper concentration transition of crystalline nature from one to other, shows the potential of material to have different properties at different elemental concentration.

sample	2θ (in degrees)	Material	Orientation
	16.42	ZnS (H)	[00 09]
S1	18.12	ZnS (H)	[00 10]
	24.67	ZnS (H)	[00 14]
S5	48.02	CuS (H)	[1 1 0]

Table 2.2: Angle peak positions of different CuZnS samples

2.3.2 Optical studies

Samples show two different absorptions at different wavelengths (Fig. 2.2). That is, same sample exhibits two different band gap values or material is capable to absorb two different photons of different energies. Samples S1 and S2 have band gaps at 3.2 eV, 2.5 eV and 3.1, 2.7 eV respectively. Samples S3 and S4 have at 3.1 eV, 2.4 eV and 2.8 eV, 2.4 eV respectively. For sample S5 plot show a single band gap which is about 2.1 eV(Table 2.3). For all samples Tauc plot can be extrapolated from two different points which intercepts at different points on X axis. Two band gaps is due to the co-existence of different phases of same substance or of different substances.

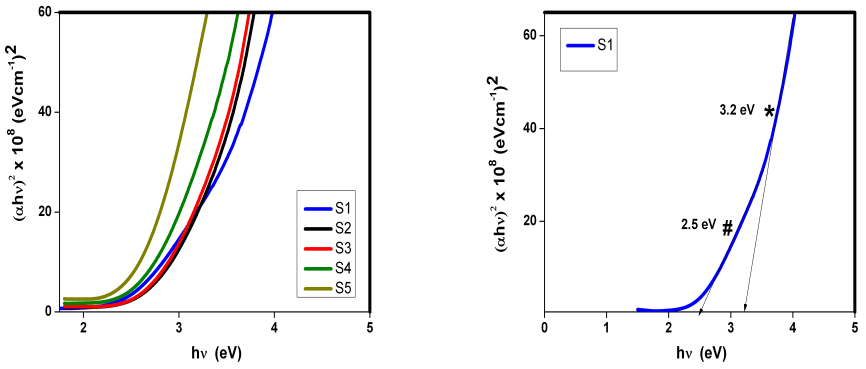

(a) (b)

Figure 2.2: $(\alpha h\nu)^2$ Vs h ν spectra of (a) different samples deposited at different Cu concentration (b)Plot of sample S1

This double band gap nature probably will help the material to be used in tandem solar cells in future as it absorbs two photons of two

Sample	Band	gap (eV)
S1	2.5	3.2
S3	2.4	3.1
S5	2.1	–

Table 2.3: Double band gap values of different samples

different energies at the same time. Two band gap phenomenon takes place due to formation of two phases. The band gap values are not the exact characteristic band gap values of either CuS, Cu_2S or ZnS. May be presence of new elements (in case of CuS, Zn is outsider and for ZnS, Cu is the extra element) shifts the band. The deviation from actual atomic ratio cause difference in band gaps. At higher Cu concentrations the material exhibits only single band gap(S5 -2.1 eV), which may be due to domination of CuS at this particular Cu concentration and quantity of Zn present is so small that it could not contribute anything to the material.

2.3.3 Raman analysis

From XRD, it was observed that two phases CuS and ZnS are not existing together; hence we moved to Raman analysis which is more sensitive for identification of different phases even if the sample behaves like amorphous[24]. Excitation wavelength was 325 nm. Raman analysis of samples S1 to S5 show two peaks near 472 cm^{-1} and 264 cm^{-1} which correspond to CuS[25] and ZnS respectively[26]. We could find presence of two different phases in XRD also but both phases were in two different samples. Here we see both CuS and ZnS in same sample(Fig.2.3).

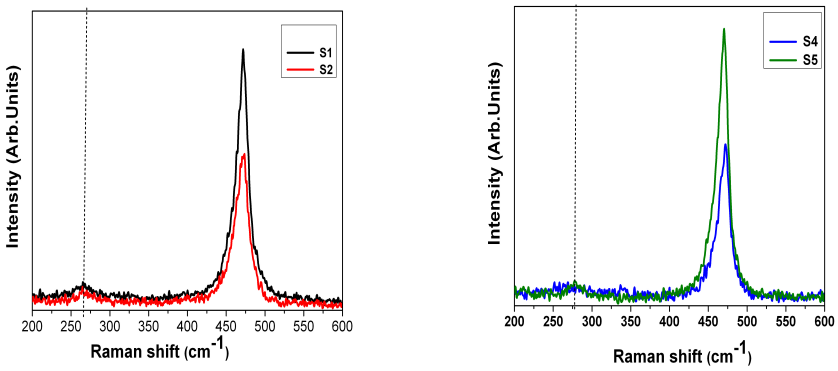

(a) (b)

Figure 2.3: Raman analysis plots of different samples deposited

Sample	Peak position (cm^{-1}) (CuS)	(ZnS)
S1	473	264
S2	471	265
S4	470	278
S5	472	278

Table 2.4: Raman shift of different CuZnS samples

Hence Raman analysis confirms simultaneous existence of CuS and ZnS. For sample S1, Raman peaks are found at 473 cm^{-1} and 264 cm^{-1}. In case of Zinc rich sample (S1) Raman peak 473 cm^{-1} is distributed at two different points or which can be deconvoluted to two peaks, one is at 473 cm^{-1} and other at 471 cm^{-1}. Here mainly Raman shift of 470 cm^{-1} corresponds to CuS phase and slight deviation from 470 cm^{-1} may be due to the presence of Zn atom between Cu and S.

In some cases stress due to presence of other neighbour atoms cause

this deviation in Raman shift[27, 28]. In case of Cu rich samples also, this deviation is clear when go from S4 to S5. In the case of S4, peak is at 470 cm^{-1} and for S5, it is at 472 cm^{-1}. It can be noted that in all cases main peak seems to be due to CuS phase and whatever the case be, presence of Zinc definitely affects Raman shift. Another very interesting thing is that Raman peaks corresponding to ZnS in samples S1 and S2 are at 264 cm^{-1} and 265 cm^{-1} where in S4 and S5 these are at 278 cm^{-1}. Here ZnS peaks at 264 cm^{-1} and 265 cm^{-1} correspond to Second Order Raman Scattering while the one at 278 cm^{-1} is due to First Order Raman Scattering in Zinc blend structure[29, 30].

2.3.4 XPS analysis

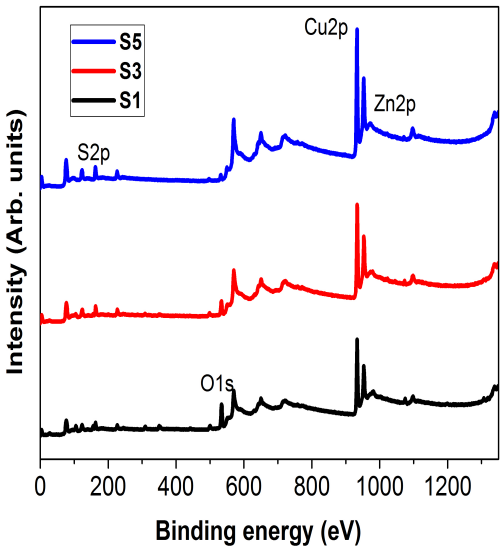

Figure 2.4: XPS survey spectra of different CuZnS samples deposited at different Cu concentrations

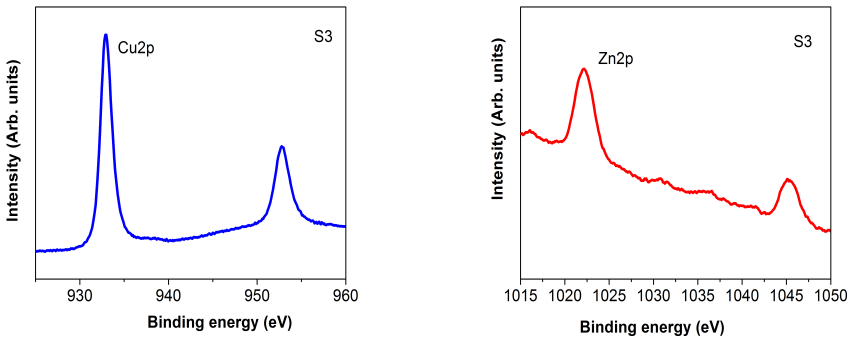

(a) (b)

Figure 2.5: Binding energies of (a)Cu2p and (b)Zn2p using XPS

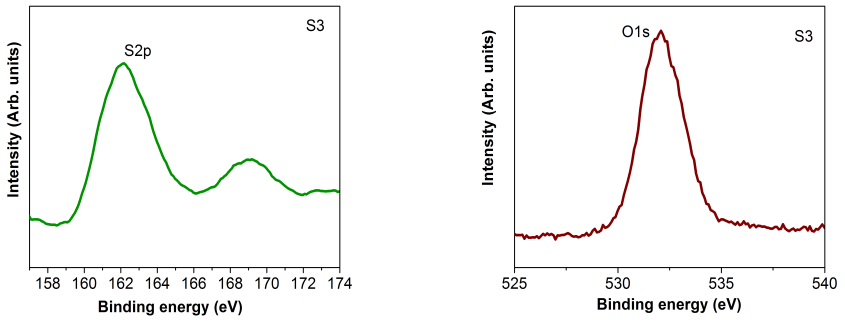

(a) (b)

Figure 2.6: Binding energies of (a)S2p and (b)O1s using XPS

XPS analysis shows binding energies corresponding to different chemical states of the elements which constitute CuZnS. Survey spectrum of samples S1, S3 and S5 prove presence of CuS and ZnS where the binding energy values of Cu2p and Zn2p are near to energies of Cu2p and Zn2p in CuS and ZnS[31, 32]. Fig.2.5 and Fig.2.6 show that binding energies of $Cu2p_{3/2}$ and $Cu2p_{1/2}$ are at 932.98 eV and 952.78 eV respectively in sample S3.

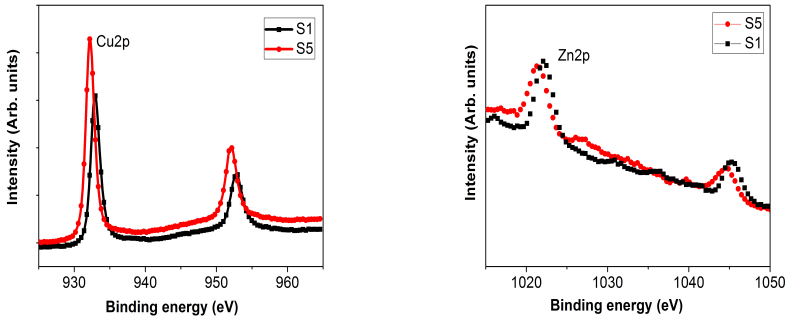

(a) (b)

Figure 2.7: Binding energies of (a)Cu2p and (b)Zn2p in samples S1 and S5

For $Zn2p_{1/2}$ and $Zn2p_{1/2}$ energy values are at 1022.18 eV and 1045.18 eV respectively. For O1s binding energy is at 532.08 eV and for $S2p_{1/2}$ and $S2p_{3/2}$, binding energies are at 162.08 eV and 168.98 eV respectively. In Fig.2.7 binding energies of Cu and Zn have slight shift in energy values towards low energy. In Cu2p, a shift of 0.70 eV and in Zn2p, 0.30 eV energy difference were observed. Shift of Zn2p towards low energy side indicates that some Zn atoms in the material are replaced with Cu atoms[31, 33]. In chemical bath deposition technique, incorporating external elements(doping) is very difficult; but change in binding energies of Cu and Zn supports existence of CuZnS, and uniqueness of this material. Influence of S2p is still to be investigated as Sulfur is constant in concentration in solution. Some reports says that Sulfur vacancies can influence the binding energy shifts of Cu and Zinc in complex materials like CZTS[34].

2.3.5 Photoluminescence studies

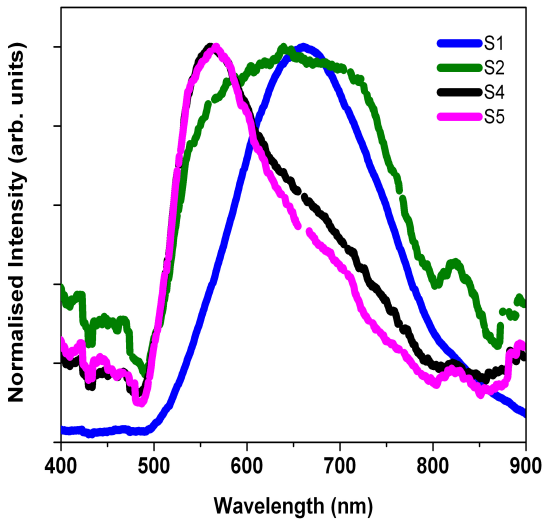

Figure 2.8: Photoluminescence studies of samples S1, S2, S4 and S5

The photoluminescence studies(Fig.2.8) of samples gave clear picture of formation of ZnS and CuS[35]. Sample S1 where Zinc is very rich in composition, exhibited emission around 650 nm, which is reported to be defect related emission in ZnS[36]. Similarly in sample S5 when the peak is deconvoluted, two peaks are obtained in which one is at 550 nm and other at 650 nm. Peak at 550 nm is reported to be emission from Cu related compounds[37, 38]. When we move from sample S1 to S5, gradually the emission corresponding to ZnS is reduced and Cu related emission started to appear and dominates. We see in sample S2 contribution of each emission is almost equal. From samples S2 to S4 and then to S5, clearly CuS emission becomes more dominating with minimum ZnS emission.

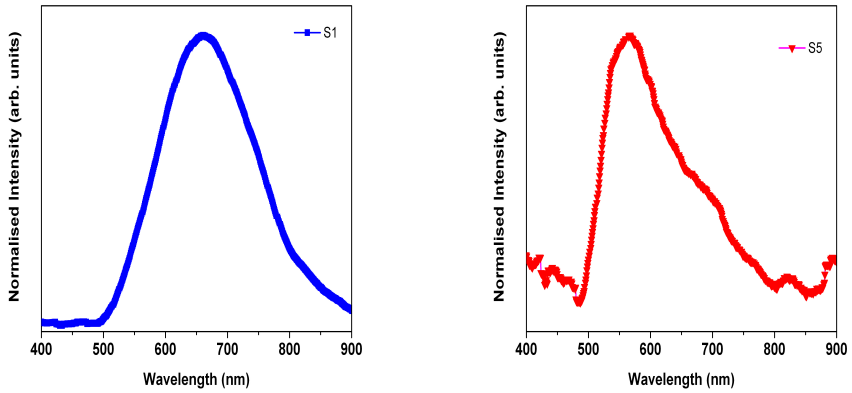

(a) (b)

Figure 2.9: Photoluminescence plots of samples (a) S1 and (b) S5

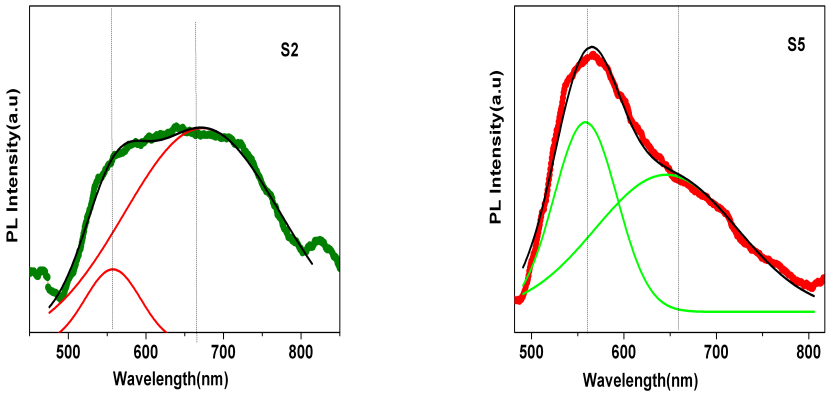

(a) (b)

Figure 2.10: Deconvoluted PL plots of samples (a)S2 and (b) S5

2.3.6 Hall measurements

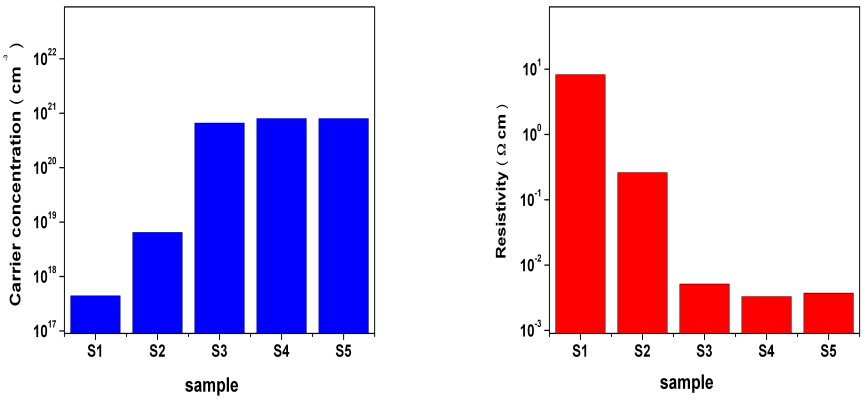

(a) (b)

Figure 2.11: (a)Bulk carrier concentration and (b) Resistivity of samples S1 to S5

When resistivity of sample is very high(i.e. of the order of 10^5 Ωcm or more) it is too difficult to take Hall measurements. Here CZS samples deposited with volume of $CuSO_4$, less than 2 ml is resistive and do not respond to Hall measurement. All samples show p type conductivity in Hall analysis. Variation in the carrier concentration is very clear in Fig.2.11(a) and carrier concentration increases with increase in Cu concentration in the solution. Gradual increase in carrier concentration is linear till the volume of Cu in the solution is 3 ml and then the value remains constant with further increase in Cu concentration. A complimentary decrease in resistivity indicates this(Fig.2.11(b)). Variation in mobility with volume of Cu precursor solution is shown in Fig.2.12(a). In general, mobility values are very low for CBD thin film samples and

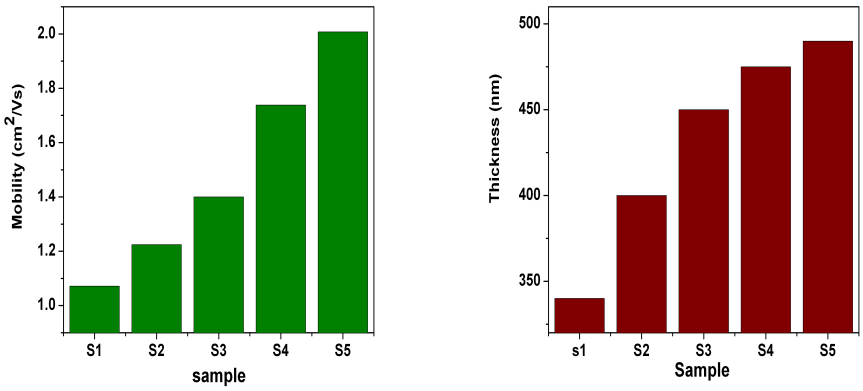

(a) (b)

Figure 2.12: (a) Mobility and (b) Thickness of samples S1 to S5

Sample	Bulk Con.(cm^{-3})	Resistivity(Ω cm)	Mobility (cm^2 /Vs)
S1	4.43×10^{17}	8.25	1.07
S2	6.44×10^{18}	0.26	1.22
S3	6.60×10^{20}	0.005	1.40
S4	7.97×10^{20}	0.0032	1.73
S5	7.95×10^{20}	0.0037	2.00

Table 2.5: Electrical properties of samples S1 to S5 measured using Hall measurement setup

lie only in range of 0 to 2 cm^2/Vs. The variation is like mobility increases with increase in Cu volume in precursor solution. Mobility values lies between 1 and 2 cm^2/Vs. As we see in carrier concentration plot, a reverse behavior is seen in resistivity. When Cu concentration increases resistivity decreases where decrease in resistivity is sudden at the beginning and then it becomes constant. When Cu concentration changes(from 2 ml to 4 ml) resistivity changes by 4 orders.

2.3.7 Morphological studies

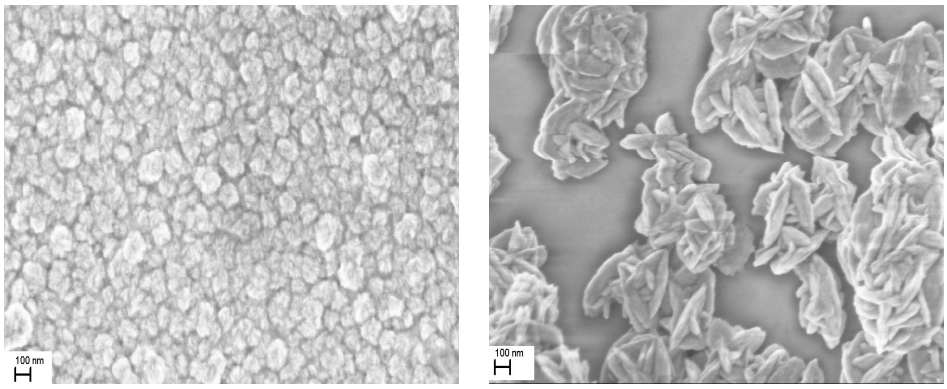

(a) (b)

Figure 2.13: SEM images of samples (a) S5 (b) S3

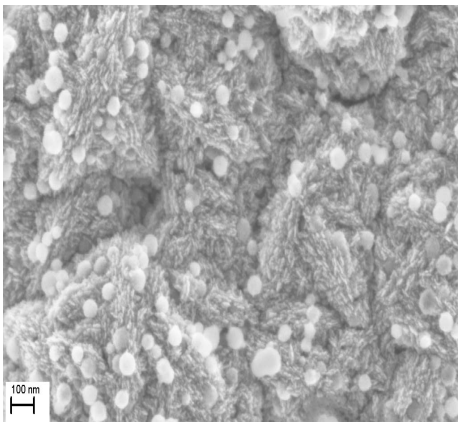

Figure 2.14: SEM image of samples S1

Surface morphology of sample S5, S3 and S1 are depicted in Fig.2.13 and Fig.2.14 where all samples show different nature. In sample S1, granule-like structure is seen which is attributed to presence of Cu and in sample S3 structure is changing to petal-like structure[39]. Sample S5 is more or less uniform in nature and grain-like structure is clear with

clear grain boundaries. Hall measurements indicated that mobility values are comparatively high for sample S5.

2.3.8 Device fabrication

Devices were fabricated with all the CZS samples deposited and the buffer layer chosen for junction fabrication was Indium Sulphide as it is a well studied material in our lab(With In_2S_3, our group could fabricate successful devices using different absorber layers[40]). Properties of In_2S_3 is similar to well known Cadmium Sulphide and highly photosensitive in nature.

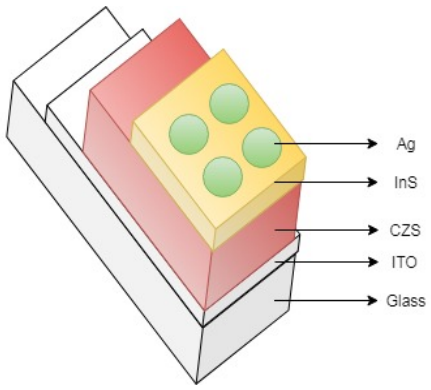

Figure 2.15: Device structure of CZS/InS devices

Solar cell structure was 'substrate structure' and structure of device is showed in Fig.2.15. On ITO coated glass (Geomaatec, Japan), CZS was deposited first using chemical bath deposition technique and In_2S_3 layer was deposited over CZS layer using chemical spray pyrolysis technique. Five devices were deposited where all the layers except CZS were constant(constant in thickness and composition in nature). Devices were named like S1, S2, S3, S4 and S5 according to the increasing order of Cu

concentration in CZS samples. From thickness measurements, it is clear that from samples S1 to S5, thickness was increasing and in devices also, thickness of CZS layers were increasing when moving from device S1 to S5(Fig.2.12(b)).

For the deposition of In_2S_3, Indium chloride and Thiourea were used; 60 ml(to get 200 nm thickness) of solution was sprayed on CZS with spray rate of 4 ml/min at temperature of 350^{o}C. Light was illuminated through the absorber layer. In earlier studies of absorbers like CZTS, $CuInS_2$ and $CuInSe_2$ by our group, it was already proved that this particular structure seems more promising for light activity. For top electrodes Ag(area about 0.03 cm^2 and thickness of about 50 nm) was deposited on In_2S_3 layer using vacuum deposition technique. About 50 mg of Ag wire was taken in evaporating boat to get thickness of 50 nm electrode and pressure was set about 10^{-6} mbar.

In Fig.2.16 J-V characteristics of devices are depicted. Cells S1, S2 and S3 showed junction behavior in which S1 and S2 showed better junction parameters. Here moving to S4 and S5 junction property totally disappeared. S4 and S5 were shorted or ohmic in nature. Here most probably increase in Cu content in absorber i.e. cells with Cu rich CZS samples, surely enhance diffusion of Cu to Indium Sulphide buffer layer. Thickness of Indium Sulphide buffer layer was around 200 nm and there is a tendency that Cu easily diffuse into Indium Sulphide[41, 42]. This diffusion may lead to the direct contact between absorber layer and electrode on the buffer layer which is Ag. When we see cells S1 and S2, they

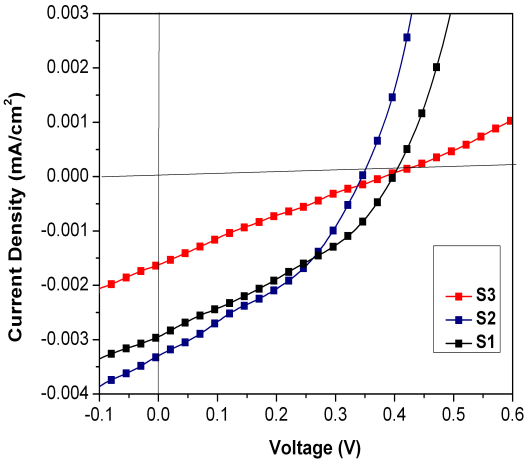

Figure 2.16: J-V characteristics of devices S1 to S3

cell	$V_oc(mV)$	$J_sc(mA/cm^2)$	FF
S1	406	0.002	40
S2	350	0.003	37
S3	421	0.001	24

Table 2.6: J-V characteristics of devices fabricated using different CuZnS samples with Indium sulphide buffer layer

have comparatively good fill factors and open circuit voltage.

Junctions were good to give light activity with good voltage(open circuit voltage values were near to 400 mV which is considerably good for solar cells). Short circuit current values were in micro amperes only, but 40% of fill factor value indicates the device can definitely be improved with more variations in absorber and buffer layer properties.

2.4 Conclusion

We could successfully deposit p-type CuZnS films using chemical bath deposition technique. All samples were showing(particularly at lower Cu concentration) double band gap nature i.e. two different band gaps at the same time. We could vary properties (optical as well as electrical) by varying the concentration of elements in the material. Raman analysis says material exists like mixture of two different phases of CuS and ZnS. From photoluminescence studies, it was found that Cu and Zn related emissions varies in intensity with variation in concentration of elements. Devices were fabricated using these CZS films; however these exhibited only very low device parameters. Though the solar cell parameters are low we could prove that the material is capable to form junction with buffer layers and to give light activity.

References

[1] Alireza Goudarzi, Ghaffar Motedayen Aval, Reza Sahraei, and Hiva Ahmadpoor. Ammonia-free chemical bath deposition of nanocrystalline zns thin film buffer layer for solar cells. *Thin Solid Films*, 516:4953–4957, 2008.

[2] Jiyeon Hong, Donghwan Lim, Young-Joo Eo, and Changhwan Choi. Chemical bath deposited zns buffer layer for cu (in,ga) se2 thin film solar cell. *Applied Surface Science*, 432:250–254, 2018.

[3] P K Nair, M T S Nair, V M Gara, O L Arenas, Y Pena, A Castillo, I T Ayala, O Gomezdaza, A Sanchez, and J Campos. Semiconduc-

tor thin films by chemical bath deposition for solar energy related applications. *Solar Energy Materials and Solar Cells*, 52:313–344, 1998.

[4] K A Aduloju and A I Mukolu. Optical absorption and transmission in cuzns alloys. *Global Journal of Pure and Applied Sciences*, 15, 2009.

[5] Sandeep Kumar Maurya, Ya Liu, Xiaojie Xu, Rachel Woods-Robinson, Chandan Das, Joel W Ager III, and KR Balasubramaniam. High figure-of-merit p-type transparent conductor, cu alloyed zns via radio frequency magnetron sputtering. *Journal of Physics D: Applied Physics*, 50:505107, 2017.

[6] Masaya Ichimura and Yosuke Maeda. Fabrication of transparent cuxznys/zns heterojunction diodes by photochemical deposition. *physica status solidi (c)*, 12:504–507, 2015.

[7] Anthony M Diamond, Luca Corbellini, KR Balasubramaniam, Shiyou Chen, Shuzhi Wang, Tyler S Matthews, Lin-Wang Wang, Ramamoorthy Ramesh, and Joel W Ager. Copper-alloyed zns as ap-type transparent conducting material. *physica status solidi (a)*, 209:2101–2107, 2012.

[8] Kai Yang and Masaya Ichimura. Fabrication of transparent p-type cuxznys thin films by the electrochemical deposition method. *Japanese Journal of Applied Physics*, 50:040202, 2011.

[9] Edwin Jose and M C Santhosh Kumar. Room temperature deposition of highly crystalline cuzns thin films for solar cell applications using silar method. *Journal of Alloys and Compounds*, 712:649–656, 2017.

[10] Noriyuki Kitagawa, Seigo Ito, Duy-Cuong Nguyen, and Hitoshi Nishino. Copper zinc sulfur compound solar cells fabricated by spray pyrolysis deposition for solar cells. *Natural Resources*, 4:142, 2013.

[11] Xiaojie Xu, James Bullock, Laura T Schelhas, Elias Z Stutz, Jose J Fonseca, Mark Hettick, Vanessa L Pool, Kong Fai Tai, Michael F Toney, Xiaosheng Fang, et al. Chemical bath deposition of p-type transparent, highly conducting (cus)–(zns)nanocomposite thin films and fabrication of si heterojunction solar cells. *Nano letters*, 16: 1925–1932, 2016.

[12] Tokio Nakada and Masayuki Mizutani. 18% efficiency cd-free cu (in,ga) se2 thin-film solar cells fabricated using chemical bath deposition (cbd)-zns buffer layers. *Japanese Journal of Applied Physics*, 41:L165, 2002.

[13] Fabiana Lisco, Piotr M Kaminski, Ali Abbas, Kevin Bass, Jake W Bowers, Gianfranco Claudio, Maria Losurdo, and J M Walls. The structural properties of cds deposited by chemical bath deposition and pulsed direct current magnetron sputtering. *Thin solid films*, 582:323–327, 2015.

[14] E Guneri, C Ulutas, F Kirmizigul, G Altindemir, F Gode, and C Gumus. Effect of deposition time on structural, electrical, and optical properties of sns thin films deposited by chemical bath deposition. *applied surface science*, 257:1189–1195, 2010.

[15] Aixiang Wei, Jun Liu, Mixue Zhuang, and Yu Zhao. Preparation and characterization of zns thin films prepared by chemical bath deposition. *Materials Science in Semiconductor Processing*, 16:1478–1484, 2013.

[16] So Ra Kang, Seung Wook Shin, Doo Sun Choi, A V Moholkar, Jong-Ha Moon, and Jin Hyeok Kim. Effect of ph on the characteristics of nanocrystalline zns thin films prepared by cbd method in acidic medium. *Current Applied Physics*, 10:S473–S477, 2010.

[17] M T S Nair and P K Nair. Chemical bath deposition of cuxs thin films and their prospective large area applications. *Semiconductor Science and Technology*, 4:191, 1989.

[18] Yongjuan Lu, Xu Meng, Gewen Yi, and Junhong Jia. In situ growth of cus thin films on functionalized self-assembled monolayers using chemical bath deposition. *Journal of colloid and interface science*, 356:726–733, 2011.

[19] Taisuke Iwashita and Shizutoshi Ando. Preparation and characterization of zns thin films by the chemical bath deposition method. *Thin Solid Films*, 520:7076–7082, 2012.

[20] M Mnari, N Kamoun, J Bonnet, and M Dachraoui. Chemical bath deposition of tin sulphide thin films in acid solution. *Comptes Rendus Chimie*, 12:824–827, 2009.

[21] Mudi Xin, KunWei Li, and Hao Wang. Synthesis of cus thin films by microwave assisted chemical bath deposition. *Applied Surface Science*, 256:1436–1442, 2009.

[22] WGC Kumarage, L B D R P Wijesundara, V A Seneviratne, C P Jayalath, and B S Dassanayake. Influence of bath temperature on cbd-cds thin films. *Procedia Engineering*, 139:64–68, 2016.

[23] F Gode, Gum C, and M Zor. Investigations on the physical properties of the polycrystalline zns thin films deposited by the chemical

bath deposition method. *Journal of Crystal Growth*, 299:136–141, 2007.

[24] N Wada, SA Solin, J Wong, and S Prochazka. Raman and ir absorption spectroscopic studies on α, β, and amorphous si3n4. *Journal of Non-Crystalline Solids*, 43:7–15, 1981.

[25] P A Fernandes, P M P Salom, and A F Da Cunha. Growth and raman scattering characterization of cu2znsns4 thin films. *Thin solid films*, 517:2519–2523, 2009.

[26] Andrew Fairbrother, Victor Izquierdo-Roca, Xavier Fontan, Maria Ibez, Andreu Cabot, Edgardo Saucedo, and Alejandro Perez-Rodrguez. Zns grain size effects on near-resonant raman scattering: optical non-destructive grain size estimation. *CrystEngComm*, 16: 4120–4125, 2014.

[27] F Cerdeira, C J Buchenauer, Fred H Pollak, and Manuel Cardona. Stress-induced shifts of first-order raman frequencies of diamond-and zinc-blende-type semiconductors. *Physical Review B*, 5:580, 1972.

[28] Jian Chen and Ingrid De Wolf. Study of damage and stress induced by backgrinding in si wafers. *Semiconductor science and technology*, 18:261, 2003.

[29] J H Kim, H Rho, J Kim, Y J Choi, and J G Park. Raman spectroscopy of zns nanostructures. *Journal of Raman Spectroscopy*, 43: 906–910, 2012.

[30] J Serrano, A Cantarero, M Cardona, N Garro, R Lauck, R E Tallman, T M Ritter, and B A Weinstein. Raman scattering in β-zns. *Physical Review B*, 69:014301, 2004.

[31] S K Chawla, N Sankarraman, and J H Payer. Diagnostic spectra for xps analysis of cuosh compounds. *Journal of electron spectroscopy and related phenomena*, 61:1–18, 1992.

[32] G Gordillo, C Calderon, and P Bartolo Perez. Xps analysis and structural and morphological characterization of cu2znsns4 thin films grown by sequential evaporation. *Applied Surface Science*, 305: 506–514, 2014.

[33] E Z Kurmaev, J Van E k, D L Ederer, L Zhou, TA Callcott, RCC Perera, VM Cherkashenko, S N Shamin, V A Trofimova, St Bartkowski, et al. Experimental and theoretical investigation of the electronic structure of transition metal sulphides: Cus, and. *Journal of Physics: Condensed Matter*, 10:1687, 1998.

[34] W C Liu, B L Guo, X S Wu, F M Zhang, C L Mak, and K H Wong. Facile hydrothermal synthesis of hydrotropic cu2znsns4 nanocrystal quantum dots: band-gap engineering and phonon confinement effect. *Journal of Materials Chemistry A*, 1:3182–3186, 2013.

[35] K Jayanthi, S Chawla, H Chander, and D Haranath. Structural, optical and photoluminescence properties of zns: Cu nanoparticle thin films as a function of dopant concentration and quantum confinement effect. *Crystal Research and Technology: Journal of Experimental and Industrial Crystallography*, 42:976–982, 2007.

[36] N Poornima and C Sudha Kartha. *Non-destructive evaluation of photovoltaic materials and solar cells using Photoluminescence*. PhD thesis, Cochin University Of Science And Technology, 2013.

[37] W Q Peng, G W Cong, S C Qu, and Z G Wang. Synthesis and

photoluminescence of zns: Cu nanoparticles. *Optical Materials*, 29: 313–317, 2006.

[38] K Manzoor, S R Vadera, N Kumar, and T R N Kutty. Synthesis and photoluminescent properties of zns nanocrystals doped with copper and halogen. *Materials Chemistry and physics*, 82:718–725, 2003.

[39] Seppo Lindroos, Alexandre Arnold, and Markku Leskel. Growth of cus thin films by the successive ionic layer adsorption and reaction method. *Applied Surface Science*, 158:75–80, 2000.

[40] Teny Theresa John, K C Wilson, P M Ratheesh Kumar, C Sudha Kartha, K P Vijayakumar, Y Kashiwaba, T Abe, and Y Yasuhiro. Cuins2 films using repeated chemical spray pyrolysis. *physica status solidi (a)*, 202:79–84, 2005.

[41] V G Rajeshmon, N Poornima, C Sudha Kartha, and K P Vijayakumar. Modification of the optoelectronic properties of sprayed in2s3 thin films by indium diffusion for application as buffer layer in czts based solar cell. *Journal of Alloys and Compounds*, 553:239–244, 2013.

[42] S Bini, K Bindu, M Lakshmi, C Sudha Kartha, K P Vijayakumar, Y Kashiwaba, and T Abe. Preparation of cuins2 thin films using cbd cuxs films. *Renewable Energy*, 20:405–413, 2000.

Chapter 3

Deposition of CuZnS thin films using Chemical Spray Pyrolysis and characterization

3.1 Introduction

Nowadays people are trying to replace silicon solar cells with other cells using inorganic compound semiconductor materials, organic materials or perovskite materials[1, 2, 3]. Disposal of silicon wafers and panels, will be a big problem after few decades. In parallel, material cost of silicon panels are still on the higher side. Only very few organic materials are there almost ready for solar cell production commercially. It is expected that thin film solar cells will have very good market due to low cost of material, high durability and comparatively good efficiencies. CIGS, CdTe, GaAs and CZTS[4] based cells are becoming very popular. Among these, CZTS is very promising due to its non-toxic and earth abundant nature. CZTS is usually deposited using vacuum deposition technique along with

sulfurization[5], PLD[6], sputtering[7], chemical spray pyrolysis[8, 9] etc. Here we are trying to deposit CuZnS which is more economically viable than CZTS and is novel material in photovoltaics. The details of importance as well as properties are included in first chapter.

Among different deposition techniques, vacuum techniques are more effective and promising for high efficiency devices. Here we deposit the material CuZnS using Chemical Spray Pyrolysis(CSP) technique which is a popular non vacuum technique for thin film deposition[10]. In spray pyrolysis different salts for different elements are mixed together in suitable solvent like water, methanol or propanol and solution is sprayed on to the substrate. Pyrolysis itself means reaction taking place in the presence of heat. Here substrate temperature can easily be controlled using a heater and thermocouple. This particular technique reduces the cost of thin film production because there is no need of vacuum or the whole process is taking place with the assistance of atmospheric air. Pressure of carrier gas as well as spray rate of the solution can be adjusted to the needs. Large area coating can be easily done using spray pyrolysis which is another advantage.

3.2 Experimental techniques

Sample	$CuCl_2$ (×0.01 M)	$ZnCl_2$ (×0.01 M)	Thiourea (×0.01 M)
C1	0.1	1	4
C2	0.2	1	4
C3	0.4	1	4
C4	0.6	1	4
C5	0.8	1	4
C6	1	1	4

Table 3.1: Experimental details of CuZnS samples deposited at different Cu concentrations

Soda lime glass is used as substrate material for deposition of CuZnS. In the case of CSP method, temperature is an important parameter as it decides compound formation as well as composition of material[11]. Here deposition temperature is fixed at 350^{o}C, because we have good case references of CZTS from our own group. Rajeshmon et al. reported that, this particular temperature is optimum for CZTS deposition[12]. Even for cell fabrication also the same temperature seems to be the best, giving good junction parameters in devices.

Precursors used for deposition of the material were $CuCl_2$, $ZnCl_2$ and Thiourea. $CuCl_2$ is for Cu, Zinc chloride is for Zn and Thiourea for S. Aqueous solution containing $CuCl_2$(0.01M), $ZnCl_2$ (0.01M) and Thiourea(0.04M) were sprayed at spray rate of 4 ml/min on to the substrate. Here we kept the concentration of Zn and S constant and varied the concentration of Cu in solution. At the beginning, temperature was kept at 350^{o}C. Samples were named as depicted in Table 3.1.

Cu/Zn ratio	Samples				
	250^{o}C	300^{o}C	350^{o}C	400^{o}C	450^{o}C
0.2	A2	B2	C2	D2	E2
0.4	A3	B3	C3	D3	E3
0.6	A4	B4	C4	D4	E4
0.8	A5	B5	C5	D5	E5
1.0	A6	B6	C6	D6	E6

Table 3.2: Experimental details of CuZnS samples deposited

Temperature of deposition was varied from 250^{o}C to 450^{o}C in steps of 50^{o}C(Table 3.2). Each set was named as set A, set B, set C, set D and set E(representing temperatures from 250^{o}C to 450^{o}C) and in each set the samples were named as A2 to A6, B2 to B6, C2 to C6, D2 to D6 and E2 to E6 according to variation of copper content in it(Cu/Zn ratio varying from 0.2 to 1 in steps of 0.2 in each sample of each set). Zn:S is 1:4 i.e. Sulfur is 4 times greater than Zn and this ratio is maintained in all cases. Carrier gas used here was atmospheric air(at pressure 1.5 mbar). Excess of sulfur is added in solution to compensate the loss of sulfur occurred during spray due to evaporation.

3.3 Results and discussion

3.3.1 Analysis of CuZnS samples with different Copper concentrations

3.3.1.1 Structural analysis

XRD analysis of different samples deposited at different concentration of Cu at 350°C are shown in Fig.3.1 Samples C1 to C6 show crystalline peaks of CuS at 2θ values, 29.15^0(Table 3. 3) which corresponds to (102) plane of hexagonal phase and 48.00^0 corresponding to (110) plane of hexagonal phase of CuS[13]. When we see actual peak positions of above mentioned planes in CuS, (102) plane is reported to be between 29.25^0 and 29.56^0, and (110) plane is between 47.88^0 and 48.42^0(Table 3.4).

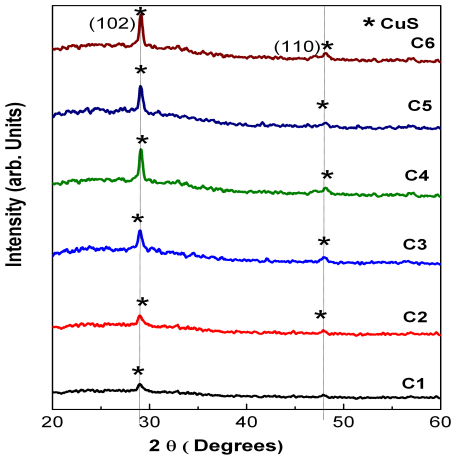

Figure 3.1: XRD plots of set of samples C1 to C6 deposited at 350^0C having different Cu concentrations

In ZnS hexagonal phase, similar planes are there near to 2θ values 29^0 and 48^0. (111) plane is between 28.49^0 and 28.55^0 while (220) plane

sample	2θ (in degrees)	Material	Orientation
C6	29.15	CuS(H)	[102]
	48.00	CuS(H)	[110]

Table 3.3: Angle peak positions of C6

is between 47.23^0 and 47.67^0(Table 3.4). For our CuZnS films, peak positions are shifted to the left side i.e. 2θ values have changed to the lower values. This phenomenon indicates presence of Zn influences the crystal structure of CuS and unit cell volume expands to some extent[14].

Actual peak position of CuS 2θ (in degrees)	Actual peak position of ZnS 2θ (in degrees)
29.25 - 29.56 (102)	28.49 - 28.55 (111)
47.88 - 48.42 (110)	47.23 - 47.67 (220)

Table 3.4: Actual peak positions of CuS and ZnS

Here we see that CuS plane corresponding to (102) orientation is shifting to the lower 2θ value while the (110) plane has no considerable change. This indicates crystal parameters "a" or "c" would have changed where "b" has no change. From second case we see "a" is not changing i.e. change would have taken place in parameter "c". In hexagonal structure, change in "c" means vertical elongation is there in crystal structure. In some case, in spite of substitution, void replacement takes place where an extra atom occupies the voids in crystal structure, that also expands the structure[15, 16].

3.3.1.2 Optical Properties

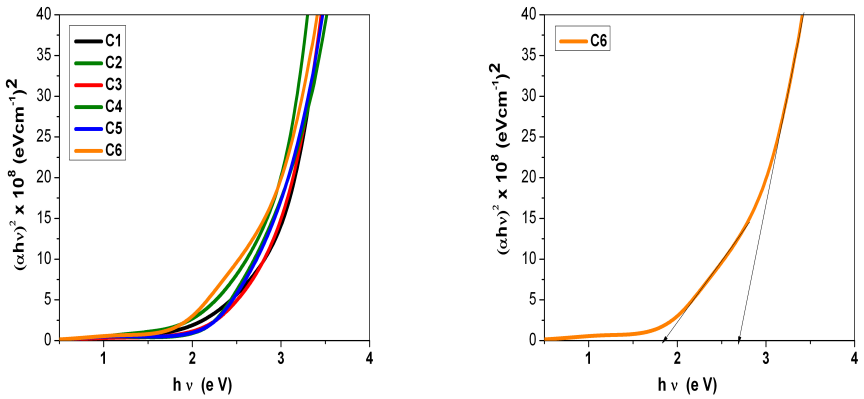

(a) (b)

Figure 3.2: $(\alpha h\nu)^2$ vs $h\nu$ plot of (a) different samples deposited at different Cu concentration (b)Extrapolated plot of sample C6 showing the cutting points on X-axis

$(\alpha h\nu)^2$ vs $h\nu$ plots of different samples from C1 to C6 are plotted in Fig.3.2. All samples showed double band gap nature and each plot can be extrapolated so as to make cuts at two different points on the X-axis and this means that they exhibit two band gaps at the same time. Interestingly for samples deposited using chemical bath deposition(which is mentioned in the previous chapter) things were a bit different. There we found that when copper concentration increases, double band gap nature slowly decreases and finally the copper rich sample show single band gap nature[17]. Materials having two band gaps are capable of absorbing two photons of different energies. For sample C1 which has the concentration of copper very low,(only about 0.1% of Zn) among the two different band gaps one was above 3 eV and other one was below 2

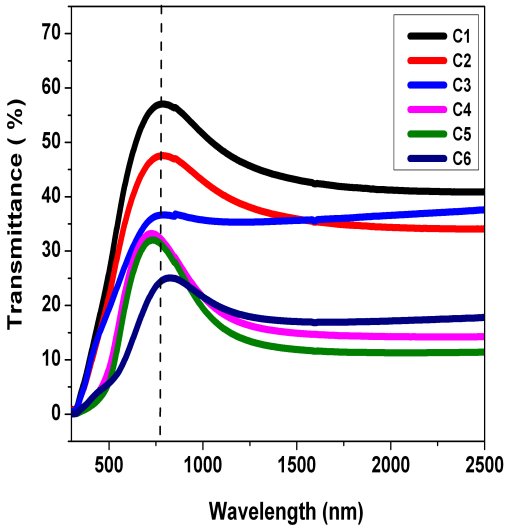

Figure 3.3: Transmission spectra of samples C1 to C6

eV[18]. Here we find the influence of ZnS is dominating and the band gap(which is corresponding to the characteristics band 8%gap of ZnS) is 3.7 eV. In copper rich sample, one band gap is below 2 eV and second one is below 3 eV; when different band gaps are present, it means that different phases are existing in the material.

In Fig.3.3 transmission spectra of samples C1 to C6 are plotted. Here transmission at 600 nm is maximum for C1 i.e. Cu is minimum in quantity. With increase in Cu concentration the transmission decreases and Cu rich sample(C6) has minimum transmission(about 25%). Among samples, maximum value is about 60% (sample C1) which is comparatively good transmission for transparent conducting materials. Here we have already mentioned that material can be used as both absorber and

window layers in solar cells and hence particularly highly transmitting CuZnS can be used as good window layers.

3.3.1.3 Raman analysis

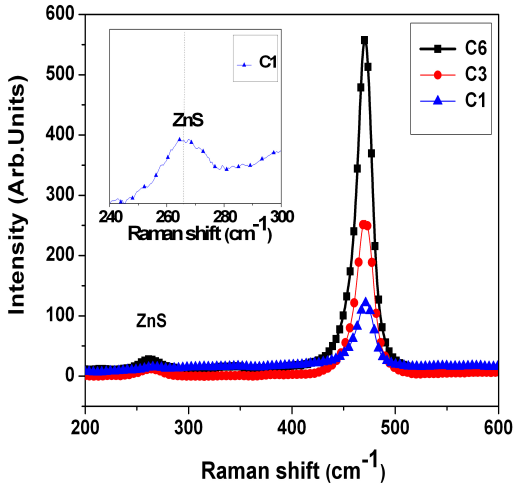

Figure 3.4: Raman shift of samples C1,C3 and C6. Zoomed portion of C1 in inset

In Raman analysis, we found that there are two peaks corresponding to CuS and ZnS [19, 20]. Peak corresponding to CuS is at 471 cm^{-1} and that of ZnS[21] is at 261 cm^{-1}(Fig.3.4). In XRD, we could not find any clue on presence of ZnS [22]. Here ZnS phase exists in the material which is very clear from Raman analysis. From the intensity of the peaks[15], itself it is clear that CuS phase is very rich in quantity and for all samples peak intensity decreases with decrease in Cu concentration[23]. In the previous chapter we saw that different samples having different Cu concentration show different peak positions in Raman analysis. Here it

is at same peak position and only intensity varies in different samples. Raman shift of samples deposited using spray pyrolysis clearly indicates the actual peak positions of concerned material(CuS and ZnS).

3.3.1.4 XPS analysis

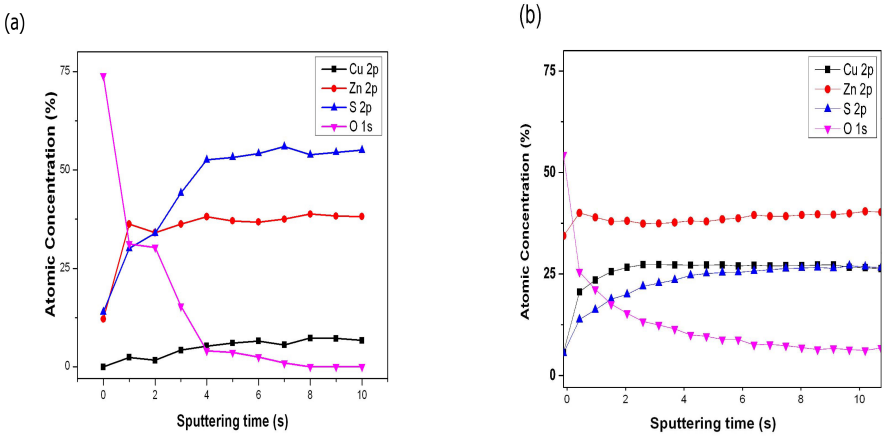

Figure 3.5: XPS analysis(depth profiling) of samples C1 (a), C3 (b)

In Fig.3.5(which shows results of "depth profiling" using XPS) variation of atomic concentration through depth or thickness of different samples C1, C3 and C6 with respect to time of sputtering is depicted. From Fig.3.5(a) it becomes very evident that concentration of Cu is very low(only about 8 % of the total elemental concentration). In samples C3 and C6 concentration of Cu is much higher. In first two samples, concentration of Zn[24, 25, 26] is almost constant while in sample C6, atomic percentage of Zn is decreasing(Fig.3.6). This simply means that some Zn atoms are replaced with Cu atoms[27]. In samples C1 and C3 the increase in Cu concentration is clear and linear in nature[28]. Sulfur

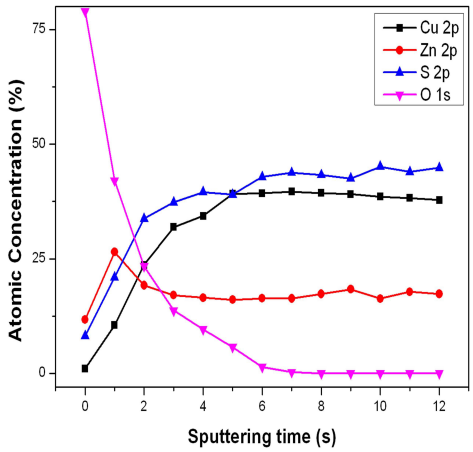

Figure 3.6: XPS analysis(depth profiling) of sample C6

is almost same in atomic percentage, in samples C1 and C6. When Cu and Zn come to equal atomic percentage, sulfur decreases. Oxygen is there at the surface and in case of spray pyrolysed films deposited, it is quite expected. However in the inner part of the film, oxygen slowly decreases. All elements are distributed uniformly and that itself shows the uniformity of films deposited.

3.3.1.5 Electrical properties

Fig.3.7 depicts results of Hall measurement[29]. When concentration of Cu increases carrier concentration increases leading to decrease in resistivity. Especially for highly resistive samples, Hall measurement setup does not respond and hence we used I-V characteristics for taking measurements. In order to take measurements using source measurement unit one has to put electrodes having width of 1 centimeter keeping dis-

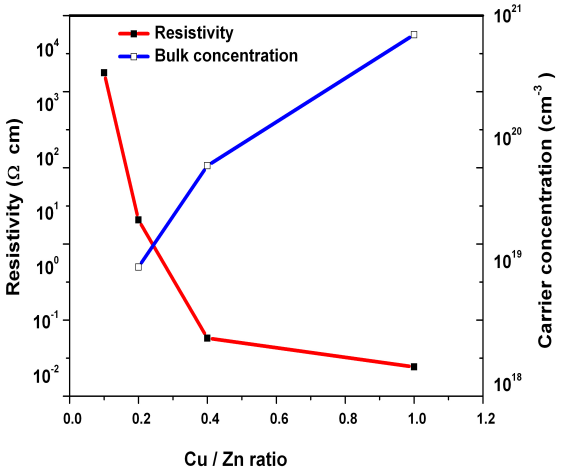

Figure 3.7: Carrier concentration and resistivity of samples C1, C2, C3 and C6

tance between electrodes the same.

Here conductivity type changed from n to p when Cu concentration changed from low to high. Sample C1 shows n type conductivity while from C2 to C6 all samples show p type conductivity. Conductivity type changes between C1 and C2 i.e. Cu/Zn ratio changes from 0.1 to 0.2. This is a promising result in semiconductor deposition. This material can be used as n type or p type semiconductor and this property can be utilized in solar cell fabrication especially in homo junction fabrication. Electrical characterization of samples with low copper concentration(where Cu concentration is only one by tenth of Zn) is done using normal source meter as these samples did not respond to Hall measurement setup due to high resistivity. Conductivity type of sample C1 was determined using hot probe method. There is 5 order difference in

both resistivity and carrier concentration from sample C1 to C6. Initially variation in carrier concentration and resistivity was very fast and later it becomes slow.

3.3.1.6 Morphological studies

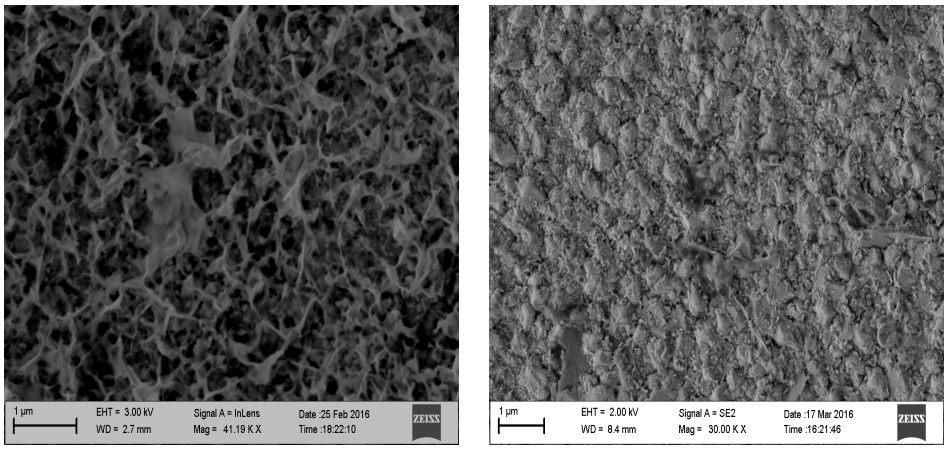

(a) (b)

Figure 3.8: SEM images of samples C3 (a)and C6 (b)

In Fig.3.8 SEM images of sample C3 and C6 are exhibited. Sample C3 shows channel-like structure which is connected through out the surface and this kind of morphology is not ever observed in spray pyrolysed films. Sample C6 is having different morphology and granule-like structures are observed.

3.3.2 Analysis of CuZnS deposited at other temperatures lower and higher than 350^{o}C

3.3.2.1 Structural analysis

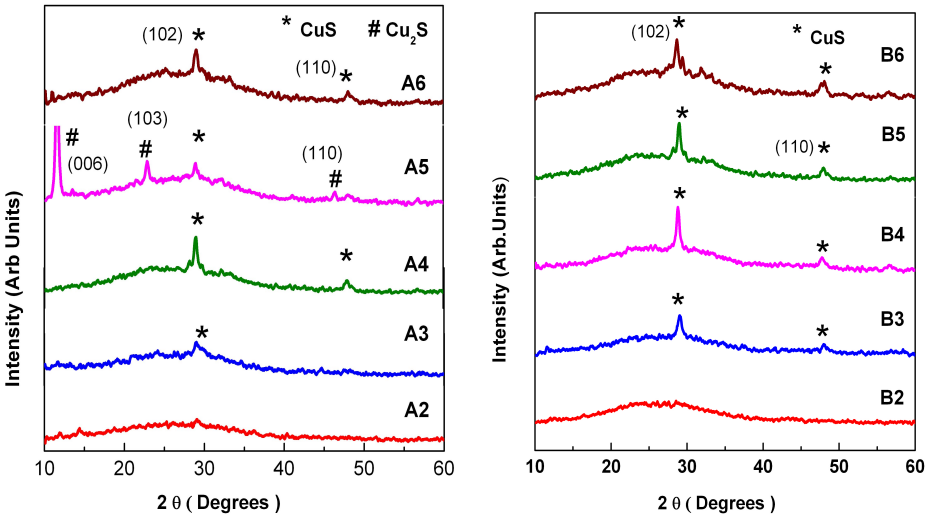

Figure 3.9: (a) XRD analysis of samples A2 to A6. (b) XRD analysis of samples B2 to B6

In Fig.3.9 XRD analysis of samples deposited at temperature 250^{o}C and 300^{o}C are shown. Apart from (102) and (110) planes of CuS phases, there are many other peaks corresponding to Cu_2S appears in samples, particularly deposited at higher Cu concentrations. Sample A5 shows (006) (103) and (110) planes of Cu_2S in addition to planes corresponding to CuS. In sample A6 also, peak corresponding to (006) plane of Cu_2S is observed. Moving to samples(deposited at temperature 300^{o}C) B5 and B6 show shoulder peaks appear near to (102) plane of CuS.

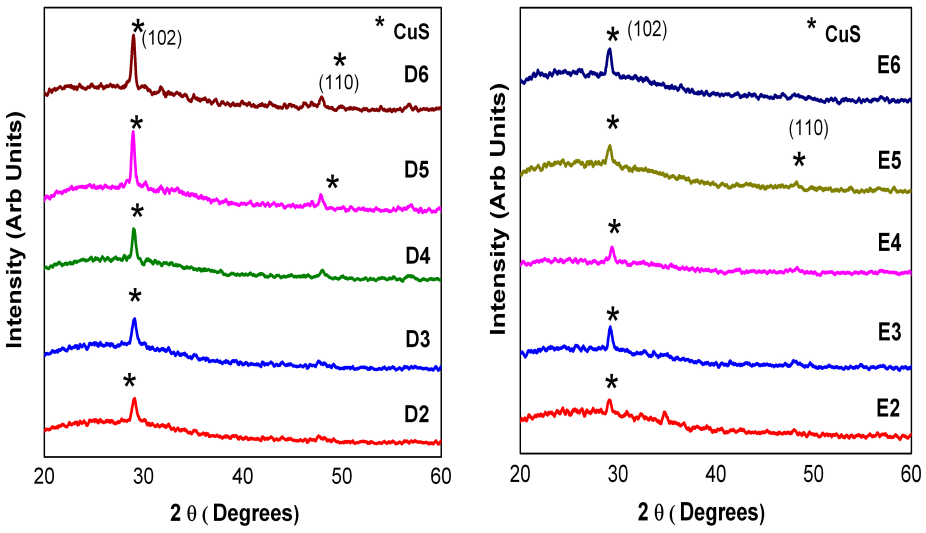

(a) (b)

Figure 3.10: a) XRD analysis of samples D2 to D6. (b)XRD analysis of samples E2 to E6

This simply means that low temperature deposition of CuZnS leads to the formation of Cu_2S phases along with CuS. In Fig.3.10 XRD plots of samples deposited at higher temperatures(400^oC and 450^oC) are shown. As we saw in the last portions, CuZnS deposited at 350^oC has peaks corresponding to only CuS and there was no trace of Cu_2S peaks in XRD plots. Samples from D2 to D6 and E2 to E6 show, peaks of CuS planes (102) and (110) only. At 450^oC, (110) plane of CuS slowly disappears and in parallel peak corresponding to (102) plane of CuS decreases its intensity, comparing to that in 400^oC and 350^oC sets.

From case histories of CZTS deposited in our own laboratory, we could see that crystalline ZnS phases forms only at higher temperatures particularly above 400^oC. For CuS, deposition temperature seems to be

below 300^{o}C(in case of spray pyrolysis) but in case of ZnS it is above 400^{o}C. CuZnS can be considered as mixture of CuS and ZnS. From set C(temperature 350^{o}C) material shows only (102) and (110) planes of CuS and no peaks of Cu_2S were found. 350^{o}C is minimum temperature from which we could deposit single crystalline CZS or we could avoid the interference of other phases.

3.3.2.2 Optical Properties

In Fig.3.11 $(\alpha h\nu)^2$ vs $h\nu$ plots and transmission plots of samples A2 to A6 are shown. All samples show double band gap nature and at higher Cu concentration double band gap nature slowly disappears, showing single band gap nature. But all other samples show two band gaps; each curve can be extrapolated at two different points intercepting at X axis. Transmission spectra also show that transmission decreases with increase in Cu concentration. In all samples, transmission decreases when moving to infrared region and in samples having higher concentration of Cu lowering of transmission in infrared region is clearer. Some reports say that this is because of absorption taking place in infrared region and this property can be made use in infrared applications. These kind of materials can be used as glass coating materials.

In Fig.3.12 absorption and transmission spectra of samples from B2 to B6 are plotted. As we saw in previous set,"double band gap" property is observed and in case of transmission, decrease in transmission with increase in Cu concentration is clear. Comparing with previous set, sam-

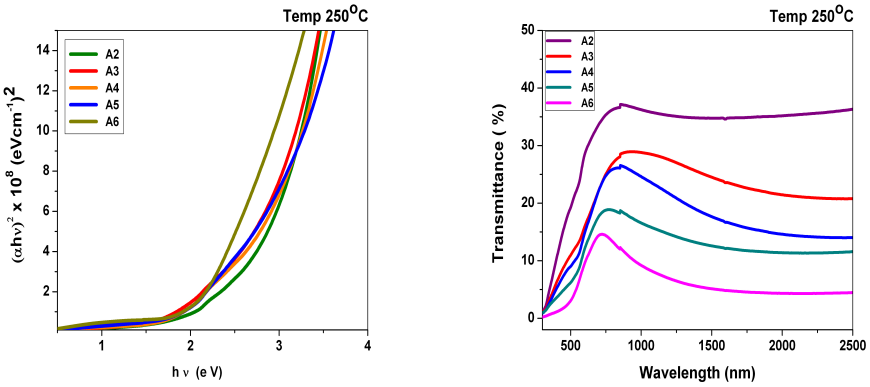

(a) (b)

Figure 3.11: (a) (α h ν)^2 vs h ν plots of samples A2 to A6 (b) Transmission spectra of samples A2 to A6

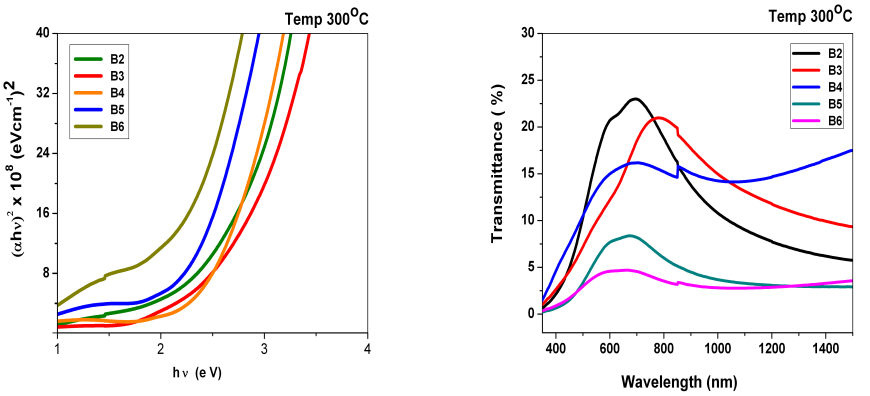

(a) (b)

Figure 3.12: (a) (α h ν)^2 vs h ν plots of samples B2 to B6 (b) Transmission spectra of samples B2 to B6

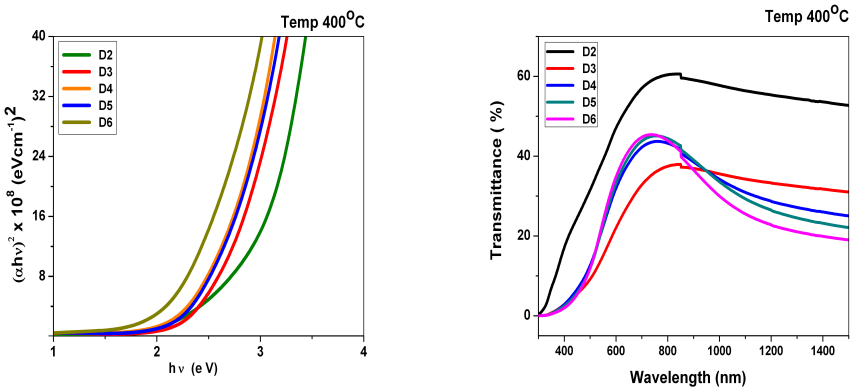

(a) (b)

Figure 3.13: (a) (α h ν)^2 vs h ν plots of samples D2 to D6 (b) Transmission spectra of samples D2 to D6

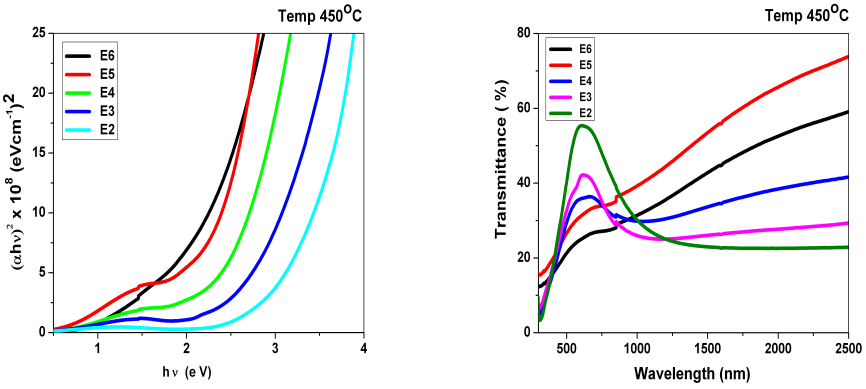

(a) (b)

Figure 3.14: (a)(α h ν)^2 vs h ν plots of samples E2 to E6 (b) Transmission spectra of samples E2 to E6

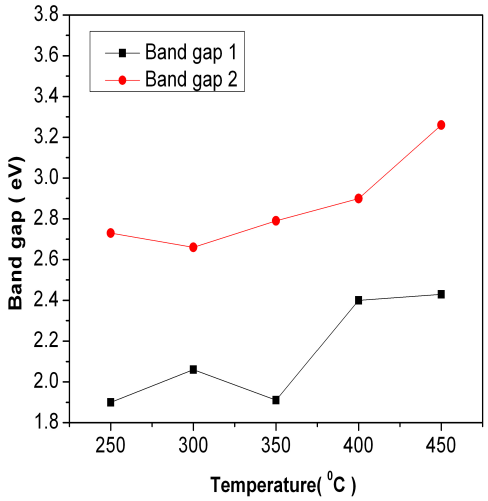

Figure 3.15: Variations of two band gaps of Cu poor samples with respect to temperature(Cu/Zn=0.2)

ples B2 to B6 show sudden decrease of transmission in infrared region. The absorption of infrared is more clear and prominent in this particular set[30]. In $(\alpha$ h $\nu)^2$ vs h ν plots, absorption of each sample has considerable gap between each other(band gap values of each sample is much different from that of the others). In set A, plots are very near to each other.

Fig.3.13 and Fig.3.14 show absorption and transmission of samples D2 to D6 and E2 to E6 respectively. Both sets show same double band gap behavior and transmission decreases with increase in Cu concentration. When we come to samples deposited at higher temperatures(400^oC and 450^oC), transmission is comparatively more than that of low temperature samples(250^oC and 300^oC). In Fig.3.15 variations in band gap

values with respect to temperature of different samples deposited at different temperatures are plotted. We have already mentioned that there are two band gaps for each CuZnS sample. One will be near to 2 eV and second one near to 3 eV. In Fig.3.15 variation of these two band gap values in different CuZnS samples(minimum Cu concentration)with respect to temperature and both band gaps are increasing to higher energy values.

3.3.2.3 Electrical properties

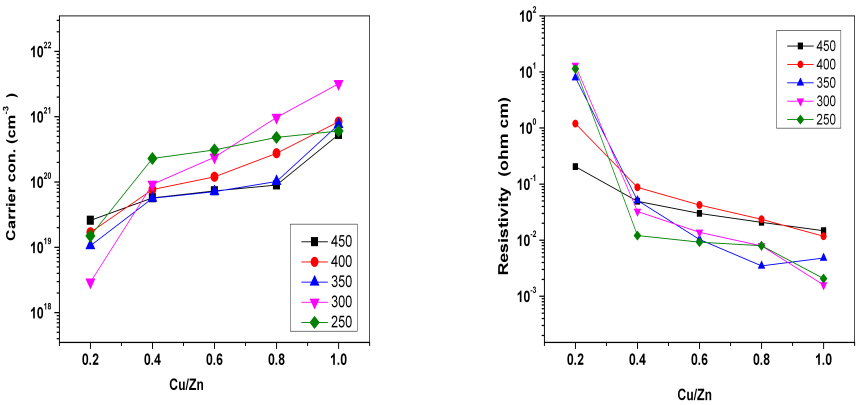

(a) (b)

Figure 3.16: (a) Carrier concentration of samples deposited at different temperatures (b) Resistivity of samples deposited at different temperatures

In Fig.3.16 and Fig.3.17 electrical properties of different samples are plotted. The properties were measured using Hall measurement setup. Bulk carrier concentration, resistivity and mobility were plotted in different graphs[31]. We could see that samples deposited at all temper-

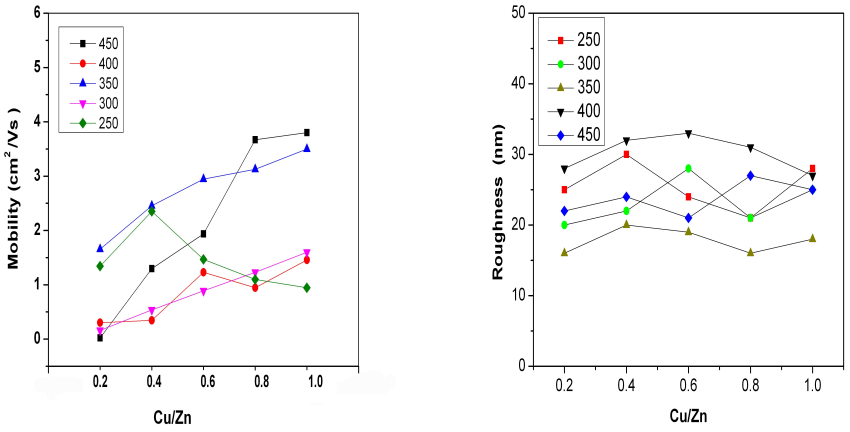

(a) (b)

Figure 3.17: (a) Mobility of different samples deposited at different temperature (b) Roughness of different samples deposited at different temperature.

atures show almost linear variations in carrier concentration and resistivity. Bulk concentration is increasing with respect to increase in Cu concentration in sample. Complimentary decrease in resistivity is clear and graphs of resistivity and carrier concentration are complimentary in nature[32]. For all samples mobility[33] is in the rage of 0 to 10 cm^2/Vsec. Except for low temperature set A, all other sets show increase in mobility with increase in Cu concentration. The variation is not linear in nature. Comparatively set C i.e. the set of samples deposited at temperature 350^{o}C has more mobility. Samples C2 to C6 show mobility values from 2 cm^2/Vsec to 4 cm^2/Vsec.

All other sets have lower mobilities which are below 1 cm^2/Vsec. In Fig.3.17(b) roughness with respect to concentration of Cu is shown. All

sets have average roughness between 20 nm to 30 nm. Set C samples have minimum roughness which are below 20 nm.

3.4 Conclusion

CuZnS material was deposited using CSP technique in the temperature range of 250^{o}C to 450^{o}C and also varying the Cu/Zn ratio in each case. From XRD analysis we could see that the material consists of crystalline CuS and amorphous ZnS. Lower temperature samples have tendency of forming Cu_2S phases along with CuS and from temperature 350^{o}C onwards, Cu_2S phases slowly disappears. In optical characterization all samples showed double band gap nature and when temperature increases from 250^{o}C to 450^{o}C both band gaps(double band gaps) shift to higher energy side or band gap values increase with increase in temperature. Raman analysis confirmed presence of ZnS phase along with CuS phase. XPS analysis clearly showed compositions of samples where presence of Zn was very much evident. From Hall measurements, we saw that there is a tendency to show higher carrier concentrations at higher copper concentrations. Likewise in resistivity values we found a decrease with increase in carrier concentration. Very interesting property that we observed in the material is, n to p conversion in conductivity type. Low Cu concentrated samples show n type conductivity and Cu rich samples show p type conductivity. 350^{o}C deposited samples have high mobility values comparing to other sets and the same set has minimum roughness. For junction fabrication using CZS we choose set C because of high mobility and minimum roughness. Inspite of minimum roughness and good

mobility, 350^{o}C is the minimum temperature at which we could deposit CZS samples free from Cu_2S.

References

[1] Yichuan Chen, Linrui Zhang, Yongzhe Zhang, Hongli Gao, and Hui Yan. Large-area perovskite solar cells–a review of recent progress and issues. *RSC Advances*, 8:10489–10508, 2018.

[2] Shida Yang, Weifei Fu, Zhongqiang Zhang, Hongzheng Chen, and Chang-Zhi Li. Recent advances in perovskite solar cells: efficiency, stability and lead-free perovskite. *Journal of Materials Chemistry A*, 5:11462–11482, 2017.

[3] Kiran Diwate, Kakasaheb Mohite, Manish Shinde, Sachin Rondiya, Amit Pawbake, Abhijit Date, Habib Pathan, and Sandesh Jadkar. Synthesis and characterization of chemical spray pyrolysed czts thin films for solar cell applications. *Energy Procedia*, 110:180–187, 2017.

[4] Tejas Prabhakar and J Nagaraju. Ultrasonic spray pyrolysis of czts solar cell absorber layers and characterization studies. In *Photovoltaic Specialists Conference (PVSC), 2010 35th IEEE*, pages 001964–001969. IEEE, 2010.

[5] K V Gurav, S M Pawar, Seung Wook Shin, G L Agawane, P S Patil, Jong-Ha Moon, J H Yun, Jin Hyeok Kim, et al. Electrosynthesis of czts films by sulfurization of czt precursor: Effect of soft annealing treatment. *Applied Surface Science*, 283:74–80, 2013.

[6] A V Moholkar, S S Shinde, A R Babar, Kyu-Ung Sim, Ye-bin Kwon, K Y Rajpure, P S Patil, C H Bhosale, and J H Kim. Development

of czts thin films solar cells by pulsed laser deposition: influence of pulse repetition rate. *Solar Energy*, 85:1354–1363, 2011.

[7] Tooru Tanaka, Takeshi Nagatomo, Daisuke Kawasaki, Mitsuhiro Nishio, Qixin Guo, Akihiro Wakahara, Akira Yoshida, and Hiroshi Ogawa. Preparation of cu2znsns4 thin films by hybrid sputtering. *Journal of Physics and Chemistry of Solids*, 66:1978–1981, 2005.

[8] N Kamoun, H Bouzouita, and B Rezig. Fabrication and characterization of cu2znsns4 thin films deposited by spray pyrolysis technique. *Thin Solid Films*, 515:5949–5952, 2007.

[9] Sheng Huang, Wenjun Luo, and Zhigang Zou. Band positions and photoelectrochemical properties of cu2znsns4 thin films by the ultrasonic spray pyrolysis method. *Journal of Physics D: Applied Physics*, 46:235108, 2013.

[10] Thi Hiep Nguyen, Wilman Septina, Shotaro Fujikawa, Feng Jiang, Takashi Harada, and Shigeru Ikeda. Cu2znsns 4 thin film solar cells with 5.8% conversion efficiency obtained by a facile spray pyrolysis technique. *RSC Advances*, 5:77565–77571, 2015.

[11] Swati J Patil, Vaibhav C Lokhande, Dong-Weon Lee, and Chandrakant D Lokhande. Electrochemical impedance analysis of spray deposited czts thin film: Effect of se introduction. *Optical Materials*, 58:418–425, 2016.

[12] V G Rajeshmon, C Sudha Kartha, K P Vijayakumar, C Sanjeeviraja, T Abe, and Y Kashiwaba. Role of precursor solution in controlling the opto-electronic properties of spray pyrolysed cu2znsns4 thin films. *Solar Energy*, 85:249–255, 2011.

[13] Lei Zhang, Lei Xu, Qingfang Li, Jing Su, and Jingfa Li. Double-edged sword effects of cation rotation and additive passivation on perovskite solar cell performance: an ab initio investigation. *Solar Energy Materials and Solar Cells*, 186:349–355, 2018.

[14] Feng Zhang, Siu-Wai Chan, Jonathan E Spanier, Ebru Apak, Qiang Jin, Richard D Robinson, and Irving P Herman. Cerium oxide nanoparticles: size-selective formation and structure analysis. *Applied physics letters*, 80:127–129, 2002.

[15] Leonid V Azaroff and Leonid V Azaroff. *Elements of X-ray Crystallography*, volume 323. McGraw-Hill New York, 1968.

[16] M Sabeena, Alphy George, S Murugesan, R Divakar, E Mohandas, and M Vijayalakshmi. Microstructural characterization of transformation products of bcc β in ti-15 mo alloy. *Journal of Alloys and Compounds*, 658:301–315, 2016.

[17] Sana Riyaz, Azra Parveen, and Ameer Azam. Microstructural and optical properties of cus nanoparticles prepared by sol–gel route. *Perspectives in Science*, 8:632–635, 2016.

[18] AK Sahoo, P Mohanta, and A S Bhattacharyya. Structural and optical properties of cus thin films deposited by thermal co-evaporation. In *IOP Conference Series: Materials Science and Engineering*, volume 73, page 012123. IOP Publishing, 2015.

[19] W G Nilsen. Raman spectrum of cubic zns. *Physical Review*, 182: 838, 1969.

[20] Y C Cheng, C Q Jin, F Gao, X L Wu, W Zhong, S H Li, and Paul K Chu. Raman scattering study of zinc blende and wurtzite zns. *Journal of Applied Physics*, 106:123505, 2009.

[21] Radmila Kostic, Duanka Stojanovic, Jelena Traji, and P Balav. Off-resonant raman spectroscopy of zns quantum dots. In *Proceedings of the IV Advanced Ceramics and Applications Conference*, pages 203–215. Springer, 2017.

[22] J H Kim, H Rho, J Kim, Y J Choi, and J G Park. Raman spectroscopy of zns nanostructures. *Journal of Raman Spectroscopy*, 43: 906–910, 2012.

[23] M Abdulkhadar and Binny Thomas. Study of raman spectra of nanoparticles of cds and zns. *Nanostructured materials*, 5:289–298, 1995.

[24] M P Seah, I S Gilmore, and Graham Beamson. Xps: binding energy calibration of electron spectrometers 5âĂŤre-evaluation of the reference energies. *Surface and Interface Analysis*, 26:642–649, 1998.

[25] Davide Barreca, Alberto Gasparotto, Cinzia Maragno, Eugenio Tondello, and Trevor R Spalding. Analysis of nanocrystalline zns thin films by xps. *Surface Science Spectra*, 9:54–61, 2002.

[26] G Deroubaix and P Marcus. X-ray photoelectron spectroscopy analysis of copper and zinc oxides and sulphides. *Surface and Interface Analysis*, 18:39–46, 1992.

[27] M J Guittet, J P Crocombette, and M Gautier Soyer. Bonding and xps chemical shifts in zrsio4 versus sio2 and zro2: Charge transfer and electrostatic effects. *Physical Review B*, 63:125117, 2001.

[28] K S Kim and N Winograd. X-ray photoelectron spectroscopic binding energy shifts due to matrix in alloys and small supported metal particles. *Chemical Physics Letters*, 30:91–95, 1975.

[29] David C Look, J R Sizelove, S Keller, Y F Wu, U K Mishra, and S P DenBaars. Accurate mobility and carrier concentration analysis for gan. *Solid state communications*, 102:297–300, 1997.

[30] Lihua Xiao, Jianming Wu, Jingyu Ran, Yike Liu, Wei Qiu, Fanghai Lu, Fang Shao, Dongsheng Tang, and Ping Peng. Near-infrared radiation absorption properties of covellite (cus) using first-principles calculations. *AIP Advances*, 6:085122, 2016.

[31] Sheng S Li. The dopant density and temperature dependence of hole mobility and resistivity in boron doped silicon. *Solid-State Electronics*, 21:1109–1117, 1978.

[32] S M Sze and J C Irvin. Resistivity, mobility and impurity levels in gaas, ge, and si at 300 k. *Solid-State Electronics*, 11:599–602, 1968.

[33] Julius Lange. Method for hall mobility and resistivity measurements on thin layers. *Journal of Applied Physics*, 35:2659–2664, 1964.

Chapter 4

Device fabrication using CuZnS with different buffer layers

4.1 Introduction

In this chapter we focus on device fabrication using CuZnS material. Among many efficient solar cell materials, CuZnS is considered to be a good replacement for CZTS and CIGS as the elements in CZS are earth abundant, nontoxic and eco-friendly. In previous chapters, we have already seen potential of CZS for using in solar cells. Moreover CZS can be used as p type or n type layer in solar cells. Nowadays eco-friendly solar cells have good demand due to the crisis developed in silicon solar cell disposal and recycling. Among them solar cells based on organic materials, Perovskite[1, 2] and CZTS [3, 4] are the major ones. A group from Japan proved capability of CZS as absorber layer in solar cell, and efficiency of about 1.7% already reported for CZS/In_2S_3 solar cell[5].

In a solar cell basically two layers are most important; one is absorber

layer and the other is buffer layer[6, 7]. We are interested in making CZS a good absorber layer and are also interested to find good buffer layer to function in combination with CuZnS. Most established buffer layers in thin film field are CdS, ZnS, In_2S_3 and ZnO.

Device with CdS and CuS are the earlier junctions in photovoltaic field achieving efficiency around 9%. But CdS/CuS cells had major issue related with the diffusion of Cu into CdS creating extra phase like CuCdS, that damages devices. In parallel, Cd is highly toxic in nature. On the other hand, Zinc related materials are having high band gap and devices fabricated using these buffer layers will have high open circuit voltage. Like CdS and ZnS, In_2S_3 is another potential buffer layer and band gap of Indium sulphide is almost equal to that of CdS. Some good case histories say that the material could contribute attractive results in spray pyrolysed devices[8]. In this chapter, we discuss about combinations of CuZnS with different buffer layers and fabrication of devices. These buffer layers are as above mentioned, CdS[9], ZnS and In_2S_3[10].

4.2 Junction between CuZnS and CdS

In junction fabrication mainly two different kinds of materials are needed; one is n type and other is p type in conductivity. Normally absorbers[11] would be p type in nature. In the present case CuZnS is p type in nature and CdS is well known buffer layer for junction fabrication[12]. CdS with CdTe[13] is good combination for cell production. Only due to toxic nature of Cadmium, this material was being tried to be replaced with some other alternatives. But it is a good window material with large band gap and easy to deposit using simple technique viz., Chemical Bath Deposition(CBD); hence we started trying junction with CdS buffer material.

4.2.1 Experimental techniques

In the previous chapter, deposition of CuZnS using spray pyrolysis is explained in detail. Devices were fabricated on ITO coated glass (Geomaatec, Japan) substrate. CdS was deposited first on ITO and above this layer, CuZnS was deposited, using CSP(Fig.4.1). This particular structure was selected because, during chemical bath deposition, there is a chance of reaction taking place between deposited layer and CBD solution. This would end in peeling of the first layer. In the proposed structure, we could avoid the risk of interaction between precursor solution and deposited layer.

In order to deposit CdS, precursors used were 8 ml of(0.05M) $CdSO_4$, 2 ml of(1M) thiourea, 3 ml of(1M) NaOH, 10 ml of NH_4OH and 1 ml

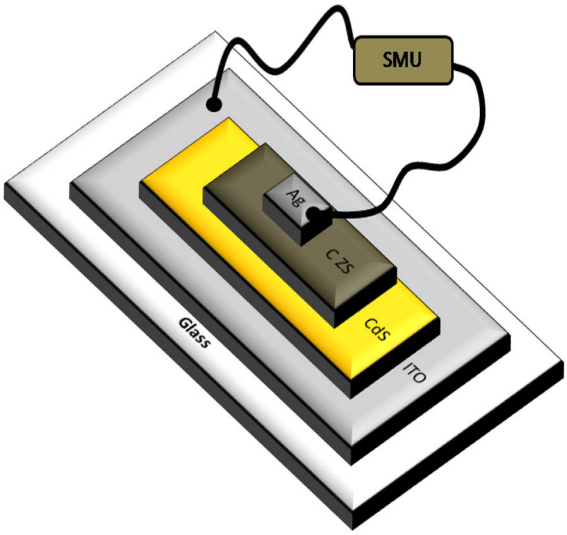

Figure 4.1: Device structure of CdS/CZS device.

of(13M) Triethanolamine(TEA) as complexing agent. The solution was made up to 100 ml using deionized water. Four pieces of ITO coated glasses were kept(vertically using a support of stand) in the reaction solution for different time periods at room temperature for getting films having different thickness(mainly in CBD technique there are two ways to vary thickness of films, one is by varying concentration, other is varying deposition time). These samples were named Cd1, Cd2, Cd3 and Cd4 which were deposited with CdS for 6 hours, 12 hours, 18 hours and 24 hours respectively. Such long timings were selected for deposition as molarity used was very low for Cd and S. Thickness of CdS films varied between 30 nm to 120 nm when deposition time varies from 6 hours to 24 hours.

These samples were taken out after required time, and washed with

distilled water; finally dried for junction fabrication. Then cleaned the films with propanol using ultra sonic cleaner which makes the films clear and uniform. Normally after the deposition using CBD technique, unwanted CdS(which is not the part of film) get precipitated on films which can easily be removed using ultra sonic cleaner.

In the case of CuZnS deposition details are the same as explained in Chapter 3. Atomic concentration ratio of Cu:Zn:S was 1:1:4. Temperature was kept at 350^{o}C(we have already seen that at this particular temperature CZS samples have minimum roughness with maximum mobility). At least 2 to 3 minutes of heating was required to make the film and substrate uniform in temperature. After CZS deposition, Ag electrodes were deposited on CZS using vacuum deposition. Area of electrodes was fixed as 0.03 cm^2. Samples were illuminated through ITO side because illumination through metal electrodes masks light.

4.2.2 Properties of CdS deposited

In Fig.4.2 properties of Cd4 is depicted; films were transparent and uniform having greenish yellow color in appearance. Measured band gap was 2.4 eV which is exactly the characteristic band gap of CdS. Peaks corresponding to (111) plane of cubic CdS was observed in XRD analysis of Cd4(Fig.4.2(b)). CZS material has hexagonal structure and CdS is cubic in nature. There are reports on hexagonal CdS, but the deposition techniques though which they deposited were not CBD. Normally we get cubic CdS through CBD[14].

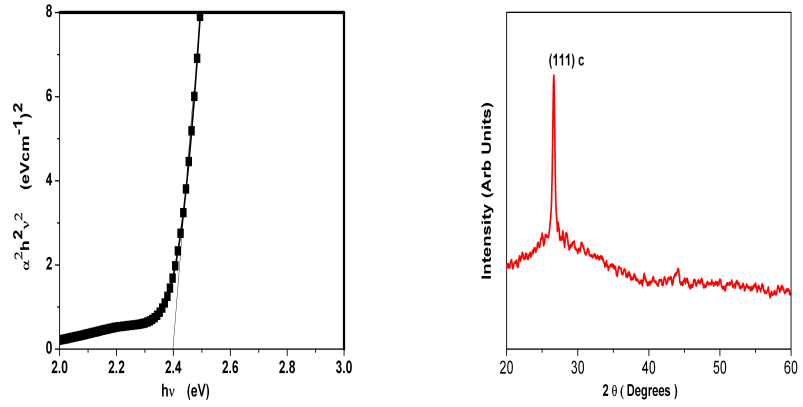

(a) (b)

Figure 4.2: (a)(α h ν)^2 Vs h ν plot of Cd4 (b)XRD plot of Cd4

Resistivity was measured using I-V source measuring unit. As the samples are highly resistive, it is impossible to measure using Hall measurement setup(resistivity comes to 350 KΩ). CdS has very high photosensitivity(around 10^3)[15]. From samples Cd1 to Cd4, thickness is increasing with respect to deposition time. Cd1, Cd2, Cd3 and Cd4 have thickness 30 nm, 60 nm, 90 nm and 120 nm respectively. Maximum thickness of Cds layer is 120 nm which is considered to be very low and light can easily pass through it. Normally for material characterization 120 nm films would not give clear peaks of the material in XRD analysis. Here we fixed maximum thickness limit around 120 nm because thicker films would affect performance of devices. We have already mentioned that resistivity of films was very high and carriers will have to move more distance if thickness becomes high. Simultaneously thickness will affect transparency which negatively affects the light availability in junctions.

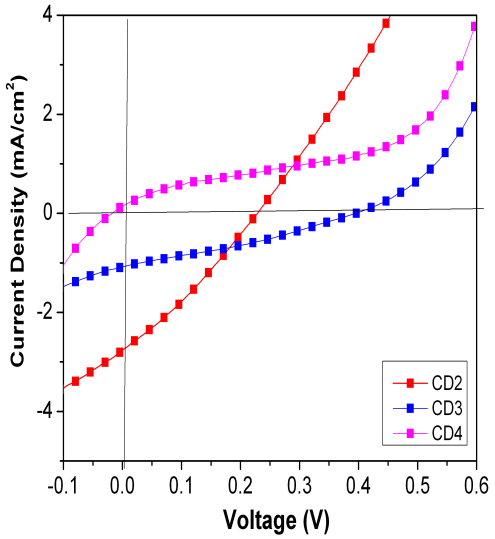

Figure 4.3: J-V characteristics of different devices fabricated using CZS and CdS buffer layers

In Fig.4.3 J-V characteristic of devices fabricated using CuZnS and CdS buffer layer are depicted. Here thickness and concentration of CuZnS layer were constant and CdS thickness was varied from 30 nm to 120 nm in steps of 30 nm. Four devices were fabricated and named as CD1, CD2, CD3 and CD4 respectively. From the figure it is clear that junction properties of devices CD2 and CD3 are better as they show light activity. Device CD1 was shorted probably due to lack in thickness of buffer layer; this is because when thickness of buffer is lower than a limit, there is a chance that Cu from CuZnS diffuse to get direct contact with lower electrode(ITO). Devices CD2 and CD3 show comparatively good junction behavior with light activities. When thickness of buffer layer is low open circuit voltage is low. At the same time, with increase in

Cell	$V_oc(mV)$	$J_sc(mA/cm^2)$	$F.F.(\%)$	$Eff.(\%)$
CD1		shorted		
CD2	213	2.72	32	0.01
CD3	401	1.04	30	0.12
CD4		No light activity		

Table 4.1: Parameters of devices fabricated using different CuZnS samples with CdS buffer layers

buffer thickness short circuit current decreases. For device CD2 open circuit voltage of about 213 mV was obtained which increases to 401 mV with the increase of 30 nm in buffer layer thickness. On the other side short circuit current decreased with increase in buffer thickness(decrease from 2.72 mA/cm^2 to 1.04 mA/cm^2). Fill factor values of CD2 and CD3 are 32% and 30% respectively which are also not good. Due the bad performance of junction with CdS, we decided not to proceed further in improving the junction.

4.3 Junction between CuZnS and ZnS

ZnS[16] and ZnO[17] are good buffer layers useful for solar cells. Both have transparency and can be made resistive[18] or conducting too[19, 20]. Highly conducting ZnO films(doping with trivalent metals or Chlorine) are being used in solar cells for collection of carriers to increase short circuit current. In the present work, we tried fabricating CuZnS/ZnS junction without any additional layers. Our expectation was that for CuZnS, ZnS would be having good lattice matching. Interestingly so far there are not much reports on CuZnS. Probably we are the first group reported about crystalline behavior properties of CuZnS[21].

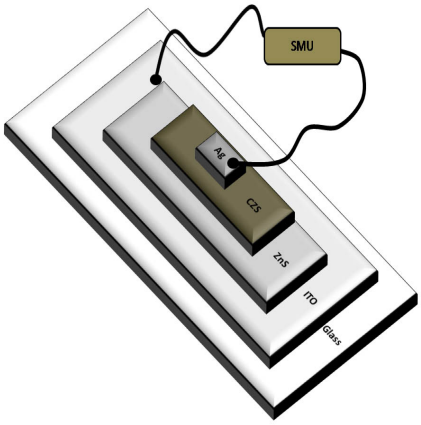

Figure 4.4: Device structure of ZnS/CZS device

ZnS can be considered as parent material of CuZnS and combination between CuZnS and ZnS would definitely favor approximately homo junction formation. Here the cell structure is like buffer layer on ITO and absorber layer on the top of buffer layer. Light illumination is through buffer layer so that absorber can utilize maximum light for minority carrier production.

4.3.1 Experimental techniques

In the previous section on CdS deposition it was stated that CdS was deposited first and absorber layer was deposited on that. In the case of ZnS buffer layer also we followed this device structure(Fig.4.4). In CSP technique one usually deposit ZnS material only at higher temperature for good crystalline nature [22, 23, 24]. It gives crystalline behavior only above 400^oC in case of spray pyrolysis deposition technique. Above ZnS, CuZnS was deposited with the same conditions as we mentioned(temp.

350^{o}C) in the previous section. ZnS was deposited using same precursor salts that of CZS, except $CuCl_2$. Ratio between Zn and S was 1:4.

Temperature was fixed at 450^{o}C and aqueous solution containing $ZnCl_2$ (0.01M) and thiourea(0.04M) was sprayed at spray rate of 4 ml/min. Different devices were deposited named according to thickness of ZnS in the device. Thickness of ZnS was controlled by varying total volume of spray solution from 40 ml to 85 ml in steps of 15 ml. Samples were named as Zn1, Zn2, Zn3 and Zn4 in ascending order of ZnS solution volume.

4.3.2 Properties of ZnS deposited

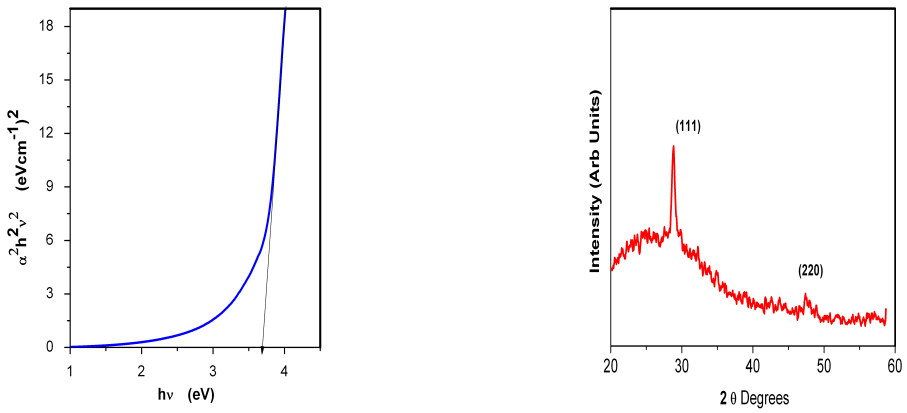

(a) (b)

Figure 4.5: (a)(α h ν)^2 Vs h ν plot of Zn4 (b) XRD plot of Zn4

Properties of sample Zn4 are showed in Fig.4.5(a). Samples had band gap around 3.7 eV and high transparency(around 78%). 3.6 eV to 3.7 eV is the characteristic band gap reported for ZnS[25]. XRD analysis(Fig.4.5(b)) shows good crystallinity with (111) and (220) planes

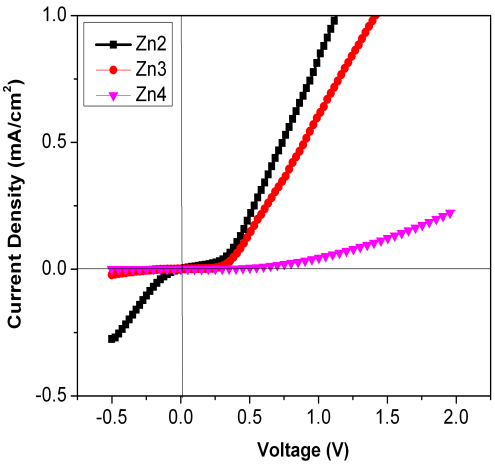

Figure 4.6: J-V characteristics of devices fabricated using different CuZnS samples with ZnS buffer layer

which correspond to hexagonal ZnS where (111) is more intense than (220). Films deposited above 450^{o}C would have given more intense peaks of crystalline ZnS, but we were forced to restrict the temperature at 450^{o}C because of some technical issues. Comparing to ZnO, ZnS has high resistivity(10^5 to 10^7 Ωcm) and in the present work we got resistivity of about 1100 KΩ cm, which was measured using source measuring unit.

In Fig.4.6 J-V characteristics of junction devices with CZS and ZnS (for illumination 100 mW/cm^2) are showed. Device having very low thickness of ZnS i.e. Zn1 was shorted due to lack of thickness of buffer layer. Usually it is difficult for Cu to diffuse through ZnS and ZnO; but here for this sample, ZnS thickness is very low and hence Cu can diffuse easily out of CuZnS and making direct contact with electrode[26]. Device Zn2 shows junction behavior with small leakage in 3^{rd} quadrant of plot in

Fig.4.6. Again thicker ZnS device, Zn3 showed better junction without any leakage current in 3^{rd} quadrant. Finally for device with thickest buffer(Zn4), showed very low current. No devices showed light activity in general.

4.4 Junction between CuZnS and In_2S_3

Eventhough junction between CdS and CZS have showed light activity, as we mentioned in the previous section, toxicity of CdS is a serious problem. Indium sulphide(InS) is a material having band gap which is very close to CdS and its resistivity is also almost of the same order. Peculiar thing is that it is highly photosensitive like CdS. Though cost of Indium is on the higher side, its eco-friendly nature as well as good opto-electronic properties prompted us to try junction with this material. Moreover spray pyrolysed Indium sulphide is well studied in our lab and we could deposit buffer and absorber with same technique[8, 27].

4.4.1 Experimental techniques

Deposition conditions of CZS is exactly the same as that of previous cases. Here the device structure is different from previously mentioned absorber-buffer combinations. Absorber layer was deposited first using CSP technique and above absorber layer, buffer layer was deposited(Fig.4.7). The precursors used for In_2S_3 were Indium chloride(0.025 M) and thiourea(0.1 M). Spray rate was fixed at 4 ml/min. We fabricated 4 different devices having similar CuZnS layers with different thickness of Indium sulphide. Thickness of Indium sulphide was varied by varying

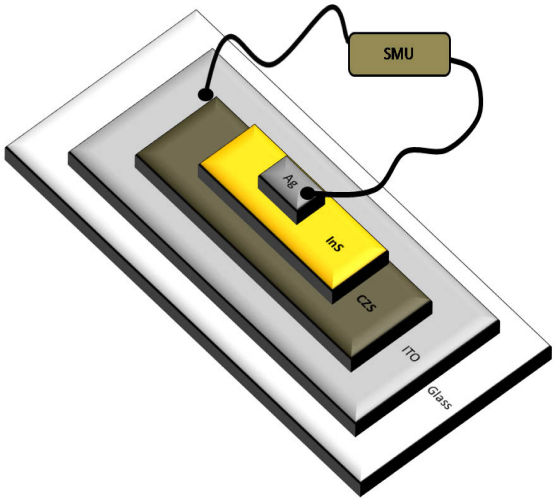

Figure 4.7: Device structure of InS/CZS device.

volume of spray solution. Four different samples were deposited(named like Ins1, Ins2, Ins3 and Ins4) by varying solution volume from 20 ml to 35 ml in steps of 5 ml.

Ag electrodes having area of 0.03 cm^2 were deposited over the Indium sulfide layer by vacuum evaporation. Total 4 electrodes were deposited on each cell and each electrode was separated from others; hence each electrode was on a separate cell. Deposition temperature was 350°C. Illumination was through ITO i.e. through the absorber. Some case histories from our own group(especially in case of CIS/InS and CZTS/InS solar cells) says this particular kind of illumination give better results.

4.4.2 Properties of In_2S_3 deposited

In Fig.4.8 (a)$(\alpha h\nu)^2$ Vs hν plot of Indium sulphide deposited is shown. The material deposited has band gap around 2.2 eV which is almost near the characteristic band gap of In_2S_3. XRD analysis shows clear peaks correspond to (112) and (220) planes of tetragonal Indium sulphide(fig.4.8(b)). These two peaks are very intense in nature and this indicates crystallinity of material.

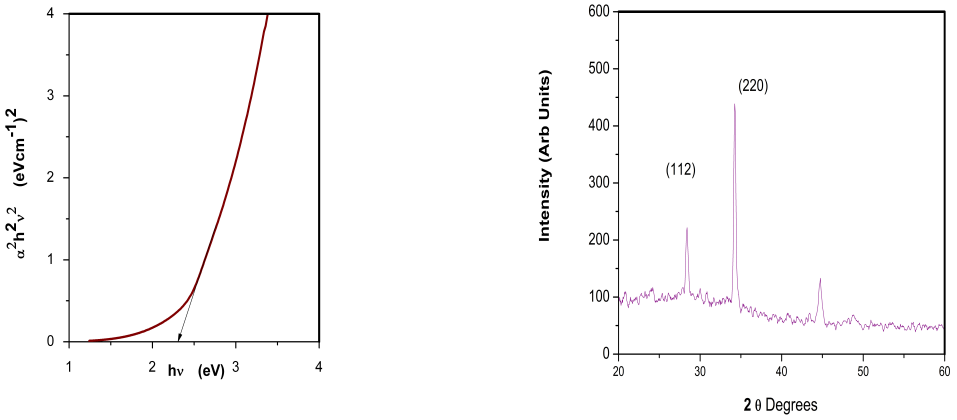

(a) (b)

Figure 4.8: (a)$(\alpha$ h $\nu)^2$ Vs h ν plot of Ins4 (b) XRD plot of Ins4

Electrical properties show material has resistivity around 630 KΩcm. Comparing to CdS mentioned in the previous section, sulphide has more resistivity. Along with resistivity films show good photo sensitivity also which is around 10^3. Different Indium sulphide layers have thicknesses in the range of 100 nm to 250 nm with steps of approximately 50 nm and devices were fabricated using these samples(Ins1 to Ins4). Each sample was deposited on CZS layer having thickness of 250 nm(deposition con-

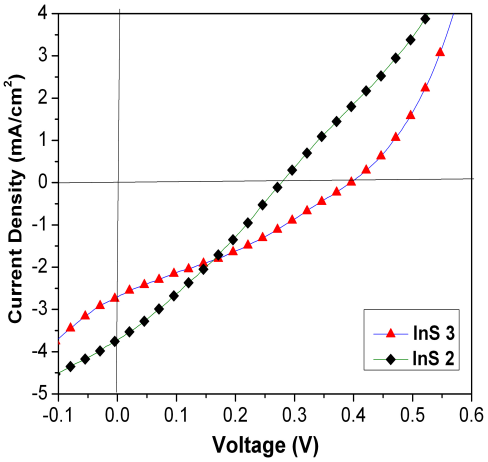

Figure 4.9: J-V characteristics of devices fabricated using different CuZnS samples with In_2S_3 buffer layers

ditions are same as in earlier case). Devices were named InS1, InS2, InS3 and InS4 according to ascending order of thickness of Indium sulphide layers.

Cell	$V_oc(mV)$	$J_sc(mA/cm^2)$	$F.F.(\%)$	$Eff.(\%)$
InS1		shorted		
InS2	280	3.71	33	0.10
InS3	404	2.62	32	0.33
InS4		Not measurable		

Table 4.2: J-V characteristics of devices fabricated using different CuZnS samples with In_2S_3 buffer layers

J-V characteristics of these junctions are shown in Fig.4.9. Devices with lower thickness of Indium sulfide InS1(100 nm) were shorted due to lack in thickness of In_2S_3 and Cu would have diffused through Indium sulphide layer to reach Ag electrodes. There is a chance that Ag elec-

trode may diffuse through Indium sulphide and reach CZS and/or ITO which also causes shorting of device. InS2 and InS3 show good junction behavior with light activity. InS2 has more current density but open circuit voltage is low. But in case of InS3 open circuit voltage is higher than InS2 with low short circuit current. This kind of behavior is seen in CuZnS/CdS devices which was mentioned in previous section. Devices which have higher buffer layer thickness,(as resistance is high) will have higher shunt resistance making junction better. This leads to higher open circuit voltage. In case of thinner buffer layer devices, separated carriers can easily reach electrodes and short circuit current increases. However device with InS4 was too resistive to measure current and voltage (J-V characteristics are done using source measuring unit and this particular setup has sensitivity only above 10^{-8}A) .

4.5 Junction between CuZnS and In_2S_3 - a detailed analysis by varying both thickness of In_2S_3 layer as well as Cu concentration in CZS layer

4.5.1 Experimental techniques

Devices were fabricated using CuZnS samples deposited with different Cu concentrations. In_2S_3 layers were divided into three different sets according to thickness. Device specifications are shown in the Table 4.3 below. For each thickness of In_2S_3, five different devices were fabricated having five different concentrations of Cu in CuZnS(thickness of CZS was varied from 300 nm to 400 nm). Hence in total, 15 devices were fabricated. For each combination 16 devices were fabricated to get accurate average value of cell parameters. Spray solutions and spray parameters were exactly same as those mentioned in previous sections.

$CuCl_2$ (×0.01M)	Thiourea (×0.01M)	$ZnCl_2$ (×0.01M)	In_2S_3 (nm)		
			200	250	300
0.2	4	1	CA1	CB1	CC1
0.4	4	1	CA2	CB2	CC2
0.6	4	1	CA3	CB3	CC3
0.8	4	1	CA4	CB4	CC4
1.0	4	1	CA5	CB5	CC5

Table 4.3: Experimental details of the deposition of different sets of CuZnS/In_2S_3 devices

4.5.2 Junction Properties

In Fig.4.10 J-V characteristics of devices CA1 to CA5 are depicted. All devices showed junction behavior with light activity. Open circuit voltage was very low,(only about 100 mV to 200 mV) and short circuit current varied from 1 mA/cm^2 to 3 mA/cm^2. Fill factor was also very low (only below 30%) which is considered to be due to bad device performance; efficiencies were only in decimals. According to increase in Cu concentration of CuZnS, current value was increasing; however V_{oc} varied in random manner.

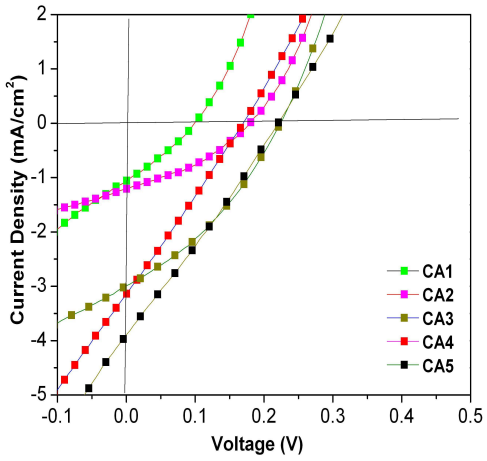

Figure 4.10: J-V characteristics of devices CA1 to CA5

Basically if a device shows low fill factor means that it would not be delivering much power to a load in practical. Low value of V_{oc} is due to lack of sufficient thickness for buffer layer. For a device to exhibit good open circuit voltage the generated carriers should be properly separated

Cell	$V_oc(mV)$	$J_sc(mA/cm^2)$	$F.F.(\%)$	$Eff.(\%)$
CA1	106±24	1.17±0.17	27±2	0.02±0.002
CA2	186±24	1.24±0.11	35±2	0.08±0.007
CA3	190±30	3.02±0.29	35±1	0.19±0.002
CA4	162±14	3.31±0.09	29±4	0.13±0.002
CA5	206±18	3.65±0.28	27±2	0.15±0.005

Table 4.4: J-V characteristics of devices CA1 to CA5

at junction. Here thickness of buffer layer(resistive layer) is very low and hence there can be 'shortings' in buffer layer enabling carriers to easily reach top electrodes. Lower fill factor also shows lack of good shunt resistance at junction of devices leading to leakage/shorting.

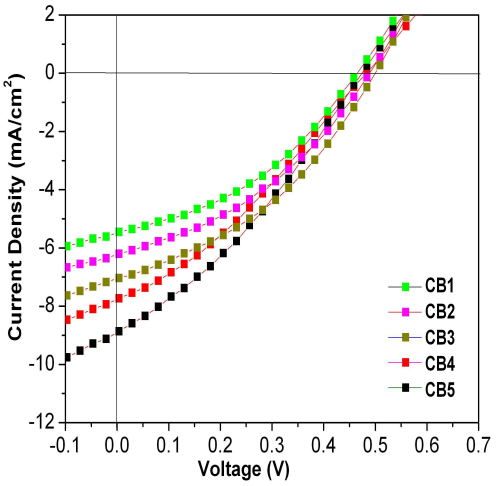

Figure 4.11: J-V characteristics of devices CB1 to CB5

In Fig.4.11 J-V characteristics of devices CB1 to CB5 are depicted. Devices CB1 to CB5 show considerable increase in voltage and current on comparing with previous set(CA1 to CA5). Open circuit voltage is

Cell	$V_oc(mV)$	$J_sc(mA/cm^2)$	$F.F.(\%)$	$Eff.(\%)$
CB1	444±20	5.60±0.19	37±1	0.89±0.04
CB2	462±27	6.28±0.19	38±3	1.08±0.08
CB3	478±21	7.08±0.17	37±2	1.27±0.05
CB4	483±12	7.62±0.16	34±2	1.28±0.08
CB5	478±12	8.64±0.20	34±2	1.41±0.12

Table 4.5: J-V characteristics of devices CB1 to CB5

high(almost near to 450 mV to 480 mV). Short circuit current density is between 5 mA/cm^2 and 9 mA/cm^2. Fill factor also improved from previous set and present values come around 35% to 38%. Efficiencies of devices exceeds 1% and having highest Cu concentration device has maximum current and efficiency which is about 1.41%. Devices CB1 to CB5 exhibit increase in short circuit current, corresponding to increase in Cu concentration. Since devices in this set have high open circuit voltage along with good current, efficiency values hiked suddenly.

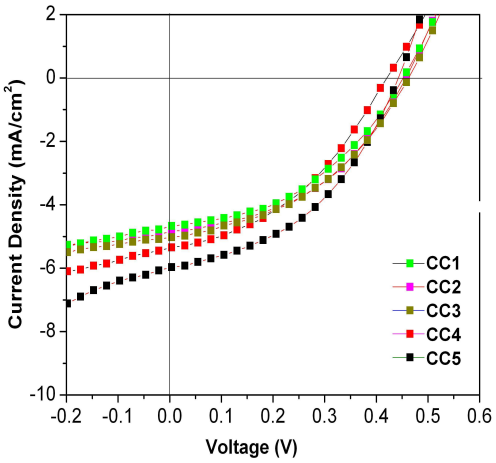

Figure 4.12: J-V characteristics of devices CC1 to CC5

Cell	$V_oc(mV)$	$J_sc(mA/cm^2)$	$F.F.(\%)$	$Eff.(\%)$
CC1	445±12	4.70±0.14	37±2	0.72±0.04
CC2	452±6	4.70±0.04	42±2	0.88±0.09
CC3	454±8	5.26±0.11	37±1	0.87±0.02
CC4	423±10	5.20±0.17	35±1	0.78±0.05
CC5	427±14	6.00±0.19	37±1	0.92±0.04

Table 4.6: J-V characteristics of devices CC1 to CC5

In Fig.4.12, J-V characteristics of devices from CC1 to CC5 are depicted. Unlike two previous sets this set has slightly high fill factor. Open circuit voltage is in the range 430 to 450 mV and current density values are in the range 3 to 4.8 mA/cm^2. Fill factor is around 40% which means that devices have good potential to deliver electricity. Comparing to previous set, I_{sc} is low which reduces the conversion efficiency values also. This decrease in short circuit current is probably due to increase in thickness of buffer layer due to which generated carriers in the junction have to travel more to reach electrodes. May be in previous set, current values are high because carriers travelled smaller distances to reach electrodes and this considerably reduced the loss of carriers due to recombination.

4.6 Conclusion

Using CuZnS absorber material different devices were tried with different buffer layers. Among them CdS and In_2S_3 showed junction behavior and light activity. Eventhough it was expected that ZnS may be good buffer layer especially for CuZnS, no device showed light activity. Comparing CdS and In_2S_3 as buffer layers, In_2S_3 was selected for further studies on CuZnS devices. Cd is toxic in nature and people are trying to

avoid the material.

The extended works on CZS/InS devices showed good improvements in device parameters. Mainly the short circuit current and open circuit voltage values were affected by both the thickness of buffer layer and concentration of Cu in CZS. Improvement in V_{oc} of devices with increase in buffer thickness and increase in I_{sc} with increase in concentration of Cu in CZS were observed.

References

[1] Huanping Zhou, Qi Chen, Gang Li, Song Luo, Tze-bing Song, Hsin-Sheng Duan, Ziruo Hong, Jingbi You, Yongsheng Liu, and Yang Yang. Interface engineering of highly efficient perovskite solar cells. *Science*, 345:542–546, 2014.

[2] Mingzhen Liu, Michael B Johnston, and Henry J Snaith. Efficient planar heterojunction perovskite solar cells by vapour deposition. *Nature*, 501:395, 2013.

[3] Hironori Katagiri, Kazuo Jimbo, Satoru Yamada, Tsuyoshi Kamimura, Win Shwe Maw, Tatsuo Fukano, Tadashi Ito, and Tomoyoshi Motohiro. Enhanced conversion efficiencies of cu2znsns4-based thin film solar cells by using preferential etching technique. *Applied physics express*, 1:041201, 2008.

[4] F Z Boutebakh, M Lamri Zeggar, N Attaf, and M S Aida. Electrical properties and back contact study of czts/zns heterojunction. *Optik-International Journal for Light and Electron Optics*, 144:180–190, 2017.

[5] Noriyuki Kitagawa, Seigo Ito, Duy-Cuong Nguyen, and Hitoshi Nishino. Copper zinc sulfur compound solar cells fabricated by spray pyrolysis deposition for solar cells. *Natural Resources*, 4:142, 2013.

[6] Born Arvid Schubert, Born Marsen, Sonja Cinque, Thomas Unold, Reiner Klenk, Susan Schorr, and Hans Werner Schock. Cu2znsns4 thin film solar cells by fast coevaporation. *Progress in Photovoltaics: Research and Applications*, 19:93–96, 2011.

[7] Kannan Ramanathan, Miguel A Contreras, Craig L Perkins, Sally Asher, Falah S Hasoon, James Keane, David Young, Manuel Romero, Wyatt Metzger, Rommel Noufi, et al. Properties of 19.2% efficiency zno/cds/cuingase2 thin-film solar cells. *Progress in Photovoltaics: research and applications*, 11:225–230, 2003.

[8] Teny Theresa John, K C Wilson, P M Ratheesh Kumar, C Sudha Kartha, K P Vijayakumar, Y Kashiwaba, T Abe, and Y Yasuhiro. Cuins2 films using repeated chemical spray pyrolysis. *physica status solidi (a)*, 202:79–84, 2005.

[9] Arturo Morales Acevedo. Thin film cds/cdte solar cells: research perspectives. *Solar Energy*, 80:675–681, 2006.

[10] Negar Naghavi, Stefani Spiering, Michael Powalla, Bruno Cavana, and Daniel Lincot. High-efficiency copper indium gallium diselenide (cigs) solar cells with indium sulfide buffer layers deposited by atomic layer chemical vapor deposition (alcvd). *Progress in Photovoltaics: Research and Applications*, 11:437–443, 2003.

[11] S T Lakshmikumar and A C Rastogi. Selenization of cu and in thin films for the preparation of selenide photo-absorber layers in solar

cells using se vapour source. *Solar Energy Materials and Solar Cells*, 32:7–19, 1994.

[12] O Vigil Gan, A Morales Acevedo, Francisco Cruz-Gandarilla, MG Jimenez Escamilla, J Aguilar-Hernandez, G Contreras Puente, J Sastre Hernandez, E Sanchez-Meza, and M L Ramon Garcia. Characterization of cbd–cds layers with different s/cd ratios in the chemical bath and their relation with the efficiency of cds/cdte solar cells. *Thin Solid Films*, 515:6085–6088, 2007.

[13] Zhou Fang, Xiao Chen Wang, Hong Cai Wu, and Ce Zhou Zhao. Achievements and challenges of cds/cdte solar cells. *International Journal of Photoenergy*, 2011, 2011.

[14] Hoi Sing Kwok, J P Zheng, Sarath Witanachchi, P Mattocks, Lei Shi, Q Y Ying, X W Wang, and D T Shaw. Growth of highly oriented cds thin films by laser-evaporation deposition. *Applied physics letters*, 52:1095–1097, 1988.

[15] M T S Nair, P K Nair, Ralph A Zingaro, and E A Meyers. Conversion of chemically deposited photosensitive cds thin films to n-type by air annealing and ion exchange reaction. *Journal of applied physics*, 75:1557–1564, 1994.

[16] Alireza Goudarzi, Ghaffar Motedayen Aval, Reza Sahraei, and Hiva Ahmadpoor. Ammonia-free chemical bath deposition of nanocrystalline zns thin film buffer layer for solar cells. *Thin Solid Films*, 516:4953–4957, 2008.

[17] Muhammad Aftab Akram, Sofia Javed, Mohammad Islam, Mohammad Mujahid, and Amna Safdar. Arrays of czts sensitized zno/zns

and zno/znse core/shell nanorods for liquid junction nanowire solar cells. *Solar Energy Materials and Solar Cells*, 146:121–128, 2016.

[18] Wen-Yuan Chang, Chin An Lin, Jr Hau He, and Tai-Bor Wu. Resistive switching behaviors of zno nanorod layers. *Applied Physics Letters*, 96:242109, 2010.

[19] Jin Hong Lee and Byung Ok Park. Transparent conducting zno: Al, in and sn thin films deposited by the sol–gel method. *Thin solid films*, 426:94–99, 2003.

[20] Devendra Goyal, Parag Solanki, Balkrishna Marathe, Murlidhar Takwale, and Vishnu Bhide. Deposition of aluminum-doped zinc oxide thin films by spray pyrolysis. *Japanese journal of applied physics*, 31:361, 1992.

[21] M S Sreejith, D R Deepu, C Sudha Kartha, K Rajeevkumar, and K P Vijayakumar. Tuning the properties of sprayed cuzns films for fabrication of solar cell. *Applied Physics Letters*, 105:202107, 2014.

[22] Xin Zeng, Kong Fai Tai, Tianliang Zhang, Chun Wan John Ho, Xiaodong Chen, Alfred Huan, Tze Chien Sum, and Lydia H Wong. Cu2znsn(s,se)4 kesterite solar cell with 5.1% efficiency using spray pyrolysis of aqueous precursor solution followed by selenization. *Solar Energy Materials and Solar Cells*, 124:55–60, 2014.

[23] N M Shinde, R J Deokate, and C D Lokhande. Properties of spray deposited cu2znsns4 (czts) thin films. *Journal of Analytical and Applied Pyrolysis*, 100:12–16, 2013.

[24] N Kamoun, H Bouzouita, and B Rezig. Fabrication and characterization of cu2znsns4 thin films deposited by spray pyrolysis technique. *Thin Solid Films*, 515:5949–5952, 2007.

[25] PE Lippens and M Lannoo. Calculation of the band gap for small cds and zns crystallites. *Physical Review B*, 39:10935, 1989.

[26] L Huang, P K Nair, M T S Nair, R A Zingaro, and E A Meyers. Interfacial diffusion of metal atoms during air annealing of chemically deposited zns-cus and pbs-cus thin films. *Journal of The Electrochemical Society*, 141:2536–2541, 1994.

[27] Teny Theresa John, S Bini, Y Kashiwaba, T Abe, Y Yasuhiro, C Sudha Kartha, and K P Vijayakumar. Characterization of spray pyrolysed indium sulfide thin films. *Semiconductor Science and Technology*, 18:491, 2003.

Chapter 5

Junction fabrication using CuZnS thin films having different Zinc concentration

5.1 Introduction

In previous chapters studies on effects due to variations of Cu concentration in CuZnS were discussed. Junction fabrication using CZS material in combination with different buffer layers were also examined, and found that Indium sulfide is a possible buffer layer for CuZnS. Here in this chapter, we investigate how concentration of Zn influences properties of CuZnS. In previous chapters, we explained about variation of Cu and we could see that concentration of Cu readly affects optical and electrical properties of CuZnS. The material properties particularly electrical properties are mostly related with Cu dominance in CZS[1, 2]. Like Cu variation, Zn concentration may also influence properties in definitely[3].

In last chapter we have already seen that in case of devices fabricated with Cu rich CuZnS material, there is improvement in short circuit current and efficiency. Hence CZS devices may need higher Cu for better absorption; but practically there are some limitations for depositing the films with higher concentration of Cu[4]. After a particular concentration spray solution precipitates and would not be usable for spraying [5]. Reducing Zn in CZS would be an alternate solution(by reducing Zn, the ratio between Cu and Zn would be high) for fabricating Cu rich CZS [6, 7]. Hence we tried varying concentration of Zn in CuZnS, by keeping the concentration of Cu constant and devices were fabricated using these CuZnS samples to examine the variation in junction parameters.

5.2 Experimental techniques

As stated in chapter 3, precursor salts used for CuZnS are $CuCl_2$, $ZnCl_2$ and thiourea for Copper, Zinc and Sulfur respectively[8, 9]. Aqueous solution containing $CuCl_2$(0.01 M) , $ZnCl_2$(0.01 M) and thiourea(0.04 M) was sprayed at the spray rate of 4 ml/min on to the substrate kept at temperature of 350^{o}C [10, 11, 12]. Carrier gas used here was atmospheric air(at pressure 1.5 mbar). Excess of Sulfur was sprayed to compensate loss of Sulfur during spray due to evaporation. At the beginning, we discuss about samples deposited at temperature 350^{o}C. Different samples were deposited with different Zn concentrations keeping Cu concentration constant. Here two Cu concentrations are there where molarities are 0.008M and 0.01M respectively and for each Cu concentration, 4 different Zn concentrations are there, so 8 samples in total. The sample details are

$CuCl_2$ (×0.01M)	Thiourea (×0.01M)	$ZnCl_2$ (×0.01M)			
		1	0.75	0.50	0.25
0.8	4	ZA1	ZA2	ZA3	ZA4
1	4	ZB1	ZB2	ZB3	ZB4

Table 5.1: Details of the CuZnS films

$CuCl_2$ (×0.01M)	$ZnCl_2$ (×0.01M)			
	1	0.75	0.50	0.25
0.8	A1	A2	A3	A4
1	B1	B2	B3	B4

Table 5.2: Details of cells fabricated using CuZnS having different Zn concentrations

mentioned in the Table 5.1. This was to find out the variation of properties of CZS samples due to Cu variation too. Since the only difference between these two sets is the concentration difference, major analysis were conducted on the set having higher Cu concentration. Devices were fabricated using all the samples mentioned above. Indium sulphide was used as buffer layer for device fabrication. The precursors used for In_2S_3 were Indium chloride(0.025 M) and thiourea(0.1 M). Ag electrodes(area of 0.03 cm^2) were deposited over the Indium Sulfide layer using vacuum evaporation[13, 14].

Deposition temperature of In_2S_3 was 310^{o}C. In the previous chapters devices were fabricated at 350^{o}C and here temperature is lowered because normally when buffer layer deposits on Cu rich CuZnS samples, there is a chance of Indium sulphide layer getting peeled off and gradually the

CZS layer too gets damaged. In order to solve this issue, temperature of deposition of buffer layer was reduced to lower temperature(310°C) and it worked quite well. Details of the devices are listed in Table 5.2.

5.3 Results and discussion

5.3.1 Raman analysis

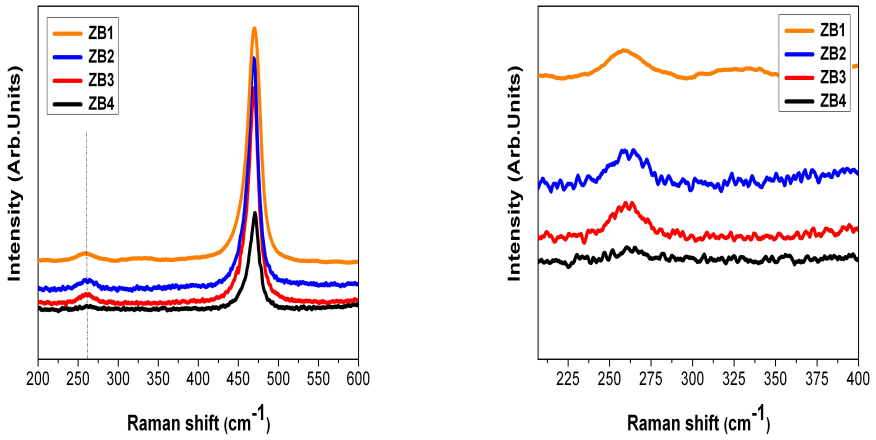

(a) (b)

Figure 5.1: Raman specra of (a) different samples deposited at different Zn concentrations (b)zoomed version of Figure 5.1(a)

In Fig.5.1(a) results of Raman analysis of samples ZB1 to ZB4 are depicted and in Fig.5.1(b) gives magnified version of peak at 260 cm^{-1} region. Here samples(having higher to lower concentration of zinc) show almost same behavior in Raman plots. When moving from sample ZB1 (Cu and Zn are maximum in concentration)to ZB4, peak intensities of Raman shifts are decreasing. Normally we expect more intense peak of CuS(around 470 cm^{-1}) in sample ZB4 because Zinc is minimum in

Sample	Peak	position (cm^{-1})
ZB1	470	261
ZB2	469	261
ZB3	469	261
ZB4	469	-

Table 5.3: Raman shift of different CuZnS samples deposited at different Zn concentration

molarity[15, 16]. Naturally Zinc sulphide peak reduces in intensity; but at the same time CuS peak also lowers its intensity. This is very striking phenomenon as it simply indicates that, for the formation of crystalline phase of CuS in CZS, presence of zinc is necessary or zinc helps the material to maintain crystallinity of CuS formed in it[17]. In later portions also we can see same phenomenon(in structural analysis).

5.3.2 Structural Analysis

In Fig.5.2 XRD plots of different samples(ZB1 to ZB4) are depicted. Here Cu concentration in samples are maximum and Zn varies in concentration. Sample ZB1 shows peaks at 2θ value 29.15 and 48.00 which correspond to (102) and (110) planes of CuS[18, 19, 20]. Moving from sample ZB1 to ZB2, we get crystalline peaks of Cu_2S also, in addition to CuS[21, 22]. The main CuS planes (102) and (110) are there; but peak intensities are low comparing to those in ZB1. The intensity of peaks of Cu_2S are more intense than CuS peaks. Again for ZB3, all peaks correspond to Cu_2S are disappeared and simultaneously peaks corresponding to CuS lowered their intensities.

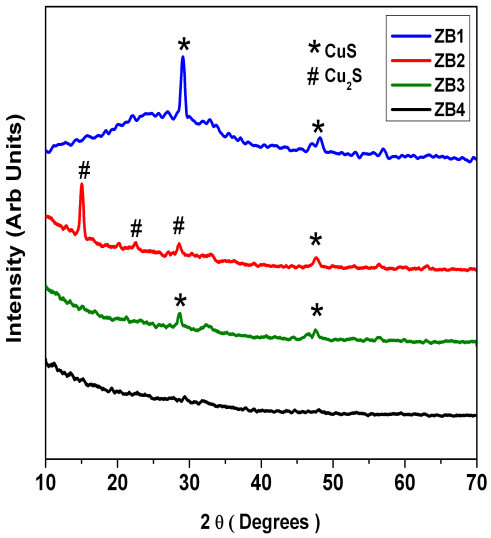

Figure 5.2: XRD plots of different samples deposited at different Zn concentrations

Finally for sample ZB4 all crystalline peaks disappeared indicating amorphous nature[23]. From Raman analysis, we already saw that there is a tendency of loosing CuS phase in CuZnS at the absence of Zn. Here, in case of structural analysis also, crystalline phase of CuS slowly disappear at lower Zn concentration. Zinc somehow influences formation of CuS. There are case histories and reports, about spray deposited CuS films which say that the material forms at lower temperature(particularly below 300^{o}C)[24, 25]. At higher temperatures, there is no chance of forming CuS but here at 350^{o}C we get good crystalline phase of CuS in CZS. In the absence of Zinc, CuS peaks slowly disappear and this probably means that Zinc has some influence in the formation of CuS at higher temperature.

sample	2θ (in degrees)	Material	Orientation
ZB1	29.15	CuS (H)	[102]
	46.88	Cu_2S	[110]
	48.00	CuS	[110]
ZB2	15.11	Cu_2S	[008]
	22.63	Cu_2S	[103]
	48.00	CuS	[110]
ZB3	29.05	CuS (H)	[102]
	48.05	CuS	[110]

Table 5.4: Peak positions of different CuZnS samples deposited at different Zn concentrations

5.3.3 Electrical properties

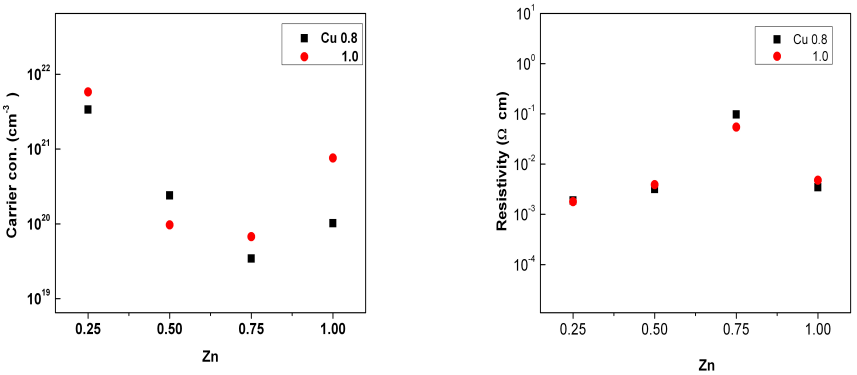

(a) (b)

Figure 5.3: Hall measurements of samples (a) Carrier concentration (b)Resistivity

In Fig 5.3 results of Hall measurements of CZS samples deposited at different Zn concentration are depicted. Carrier concentration of samples deposited at two different Cu concentrations, show a dip at the Zn concentration of 0.75 and again increases. Resistivity has compli-

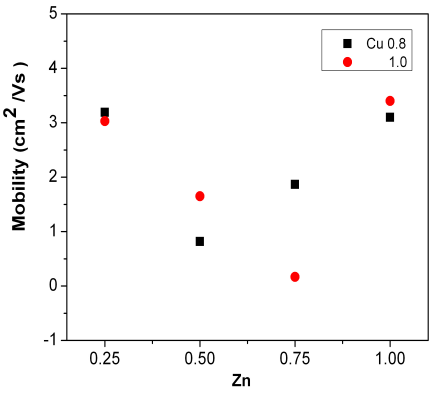

Figure 5.4: Mobility values of CZS samples deposited at different Zn concentrations

mentary behavior with increase in Zn concentration[26]. Mobility also show(Fig.5.4) same behavior like, a dip in the region of Zn concentration around 0.5 to 0.75 and then increases[27]. At both Cu concentrations, same behavior is seen with variation in Zn concentrations.

5.3.4 Morphological studies

SEM photographs of different samples deposited at different Zn concentration are shown in Fig.5.5. Samples ZB1 to ZB4 show almost similar morphologies but for sample ZB4 surface is more uniform. Grain-like structures are clear in sample ZB4 and size is around 100 nm. In sample ZB1, different particle distributions are seen where big grain-like structures are equally separated with clear grain boundaries. This morphological studies are not sufficient to determine the actual behavior of different CuZnS films, as all different samples show almost similar surface morphologies. But the SEM analysis of different CZS samples deposited

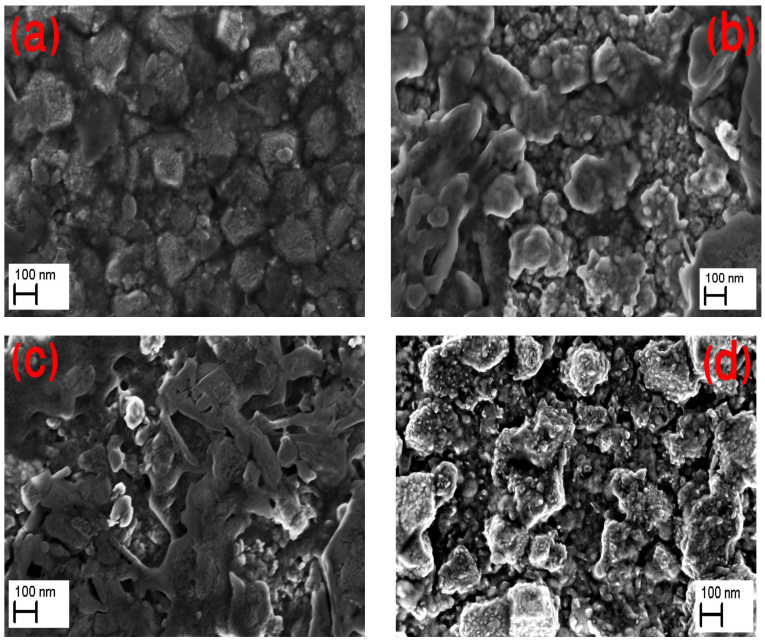

Figure 5.5: SEM images of different samples deposited at different Zn concentrations

at different Zn concentrations proves that material is capable to appear like well defined crystals having grain boundaries.

5.3.5 Junction fabrication using CZS

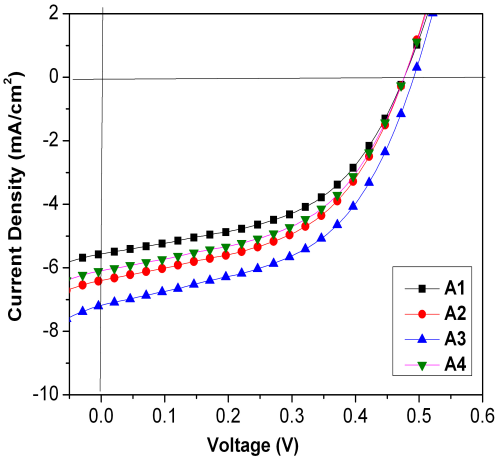

Figure 5.6: J-V characteristics of devices A1 to A4

Cell	$V_oc(mV)$	$J_sc(mA/cm^2)$	F.F. (%)	$Eff.(\%)$
A1	485±7	5.61±0.17	50±2	1.33 ±0.11
A2	467±9	6.28±0.17	51±2	1.47 ±0.06
A3	478±11	6.12±0.22	50±2	1.46 ±0.06
A4	486±5	7.06± 0.17	49±2	1.68 ±0.003

Table 5.5: J-V characteristics of devices A1 to A4

J-V characteristics of devices from A1 to A4 are tabulated in Table 5.5 Devices show good junction behavior with good open circuit voltage and short circuit current. All devices have V_{oc} around 450 mV and J_{sc} around $6(mA/cm^2)$. We have already seen that devices mentioned in the previous chapter show gradual increase in J_{sc} with increase in Cu concentration. Here with decrease in Zn concentration, current density is increasing from $5(mA/cm^2)$ to $7(mA/cm^2)$. Along with increase in

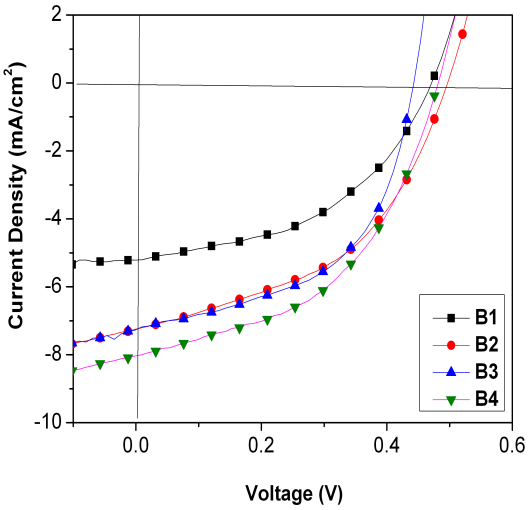

Figure 5.7: J-V characteristics of devices B1 to B4.

Cell	$V_oc(mV)$	$J_sc(mA/cm^2)$	FF	$Eff.(\%)$
B1	469±7	5.15±0.19	50±1	1.21 ±0.07
B2	430±9	7.26±0.14	49±1	1.54±0.04
B3	490±5	7.24±0.20	49±1	1.73 ±0.06
B4	477±4	8.13±0.27	48±1	1.86 ±0.03

Table 5.6: J-V characteristics of devices B1 to B4.

short circuit current density, fill factor of devices are improved very much comparing to the previous devices(mentioned in chapter 4) where Zinc concentration in CuZnS was very high. All devices have fill factors around 50% which is considerably good fill factor value of an efficient solar cell or at least we can assure the device could give better performances with further variations in preparation methods and precursors.

Devices B1 to B4(Fig.5.7 and Table 5.6) show good junction behavior

as well as light activity. Like in the previous set, where Cu concentration was 0.008M, all devices have good open circuit voltage around 460 mV and short circuit current density between 5(mA/cm^2) to 8(mA/cm^2). Fill factors are near to 50% and efficiency values around 1.8%. In conclusion, all devices having high Cu and low Zn in absorber layer give good junction parameters. This is how concentration of Cu and Zn in CuZnS work in devices. Devices described in previous chapter(Cu and Zn concentrations were very high) behave like good devices with good short circuit current and open circuit voltage. But fill factors were very low,(only around 35%). Here fill factor is considered to be the most important parameter which can give a picture about the power transfer capacity of solar devices. More the fill factor, more power can be transfered from a device to load.

5.3.6 XPS analysis of Zn poor-Cu rich cell

XPS analysis was done on cell B4, and Fig.5.8 depicts variation of binding energies of Cu, Zn, S and O through the film thickness of cell. Here it is very clear that Cu is present almost throughout the cell(even though Cu is expected only in CZS region which is near ITO) proving diffusion of Cu into the(top) In_2S_3 layer too. Probably, this might have resulted in the formation of $CuInS_2$ phase(CIS) in the In_2S_3 layer near the interface between In_2S_3 and CZS. Interestingly(in the top layer where we have In_2S_3), the peaks corresponding to Cu2p have been shifted by 0.6 eV which may be due to the formation of $CuInS_2$. However, in case of Zn, diffusion is very little and is concentrated only at the centre,

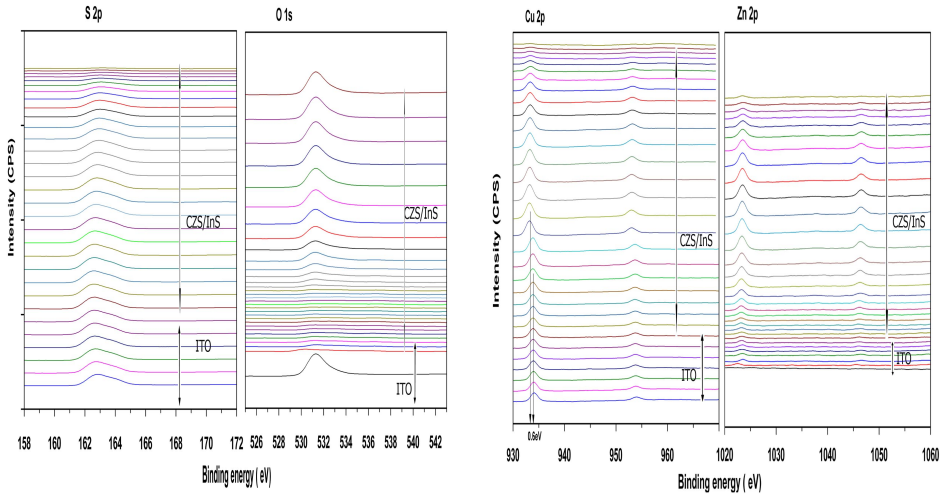

Figure 5.8: Depth profiling of cell B4 using XPS (a) Sulfur and Oxygen (b)Copper and Zinc

where it is expected (i.e. in the region of CZS) making the cell structure as ITO/CZS/CIS/InS/Ag. In Fig.5.8 binding energies of S and O are plotted. Naturally S is distributed throughout In_2S_3-CZS layers, but oxygen is present only at the surface of In_2S_3 layer(in few layers) and in the ITO layer.

Fig.5.9(a) and Fig.5.9(b) depict XPS depth profile giving variation of atomic concentration through thickness/depth of cells B4 and CB2(in the previous chapter). Here atomic concentrations of different elements are plotted against etching time(Zero on X-axis corresponds to In_2S_3 surface of the cells). We are comparing two different cells, where one is the best cell we have got from the Table 5.6 i.e. the cell B4 which has maximum Cu and minimum Zn, concentration(Cu/Zn = 4). In second

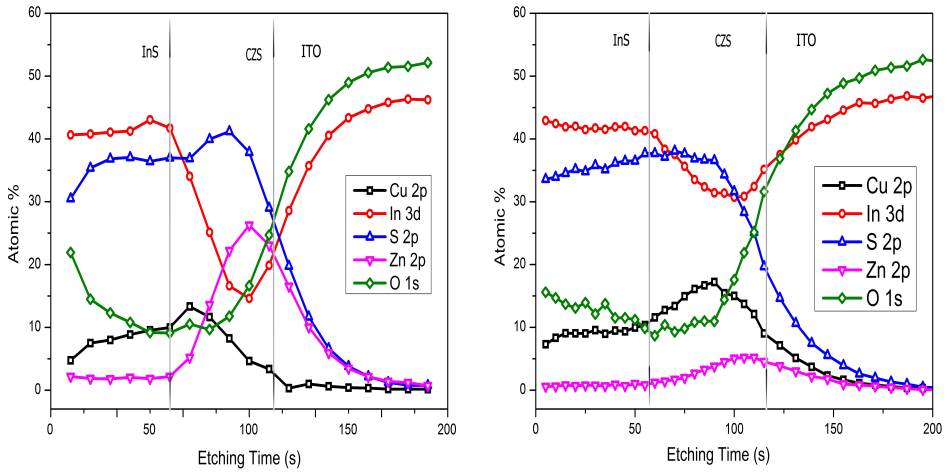

Figure 5.9: Atomic concentrations of different elements through the depth of cells using XPS (a) CB2 (in the chapter 4) (b)B4

cell i.e. cell CB2, concentrations of Zn is maximum and Cu concentration is minimum(Cu/Zn = 0.4). In two different cases Cu to Zn ratios are in two extremes.

CuZnS/InS junction is very clear from the atomic concentration plot of cell B4. Atomic percentage of S is almost same in both cells, while that of Oxygen is bit lower in B4. Cu concentration is really enhanced in B4(as expected); due to Cu diffusion into In_2S_3 layer is observed in both the plots making it quite clear that there is formation of $CuInS_2$ phase near the junction. This results in having multiple band gaps(due to the presence of CuZnS and $CuInS_2$) in the absorber layer, enhancing absorption of photons of two different energies. Transmittance studies on sample ZB4 and exact energy values are to be find out in future studies.

5.3.7 Raman analysis of Zn poor cell

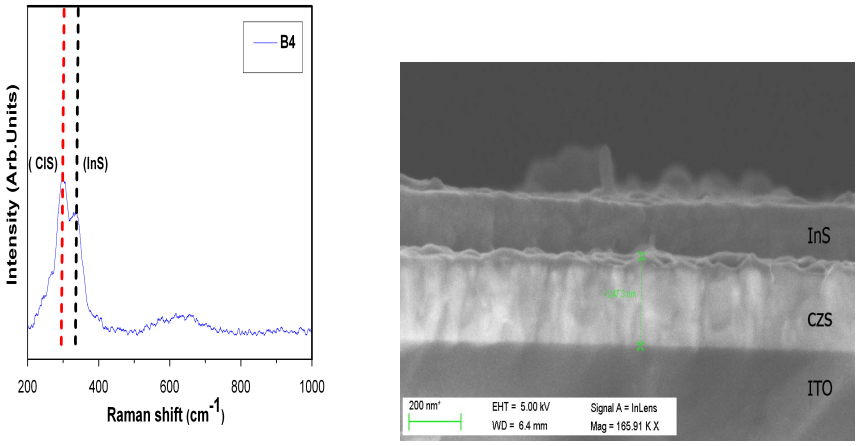

(a) (b)

Figure 5.10: (a) Raman spectrum of cell B4(b)Cross sectional SEM of cell B4

Fig.5.10(a) shows Raman analysis of cell B4 is showed where we find Raman shifts corresponding to $CuInS_2$ and In_2S_3. Though we have not purposefully deposited Copper Indium sulphide, we could get $CuInS_2$ phase. From the previous results of XPS, we had suspected about the formation of $CuInS_2$ which is very evident in XPS depth profiling picture. Cu is diffused to Indium sulphide and extra phase of $CuInS_2$ is formed between In_2S_3 and CuZnS. We know the characteristics band gap of CZS is more, comparing to $CuInS_2$ and this would definitely enhance performance of Cu rich cells. Unfortunately Raman shift corresponds to CuS is not seen in the case and this is probably because the CuS layer would be there below $CuInS_2$ and laser(excitation laser) could not penetrate into the depth of cell. Here in spray pyrolysis method, we

utilize diffusion tendency of different elements which actually enhances the performance parameters[28].

5.3.8 Effect in current density and efficiency with respect to Cu-Zn concentration in CZS devices

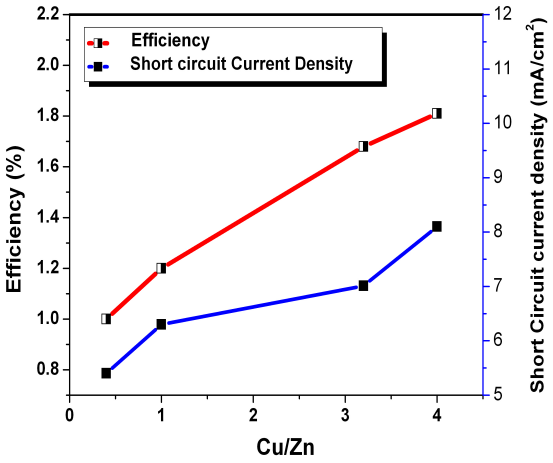

Figure 5.11: Variation of Current density and efficiency of devices with respect to Cu/Zn ratio

Fig.5.11 shows variation of efficiency and current density with respect to Cu/Zn ratio in the CuZnS layer. Here it is very clear that variation of efficiency is very much linear in case of Cu concentration. When copper concentration in the absorber increases, there will be diffusion of Cu to Indium sulphide layer forming $CuInS_2$ which enhances current density of the device. That means when more $CuInS_2$ forms between CuZnS and In_2S_3, more carriers are generated; gradually current density and efficiency of device increases. Fill factor is also a reason for enhancement in efficiency. When copper concentration increases in

absorber layer, some Cu atoms will be diffused to adjacent layer and remaining elements at the edge of absorber layer(edge which is in contact with ITO) enhances shunt resistance of cell. This reduction in series resistance contributes to the enhancement in fill factor.

5.4 Conclusion

CuZnS films having different concentrations of Cu and Zn were deposited and characterized. Devices using these CuZnS films were fabricated and they showed good junction with light activity. Structural analysis using XRD and Raman proved the formation of CuS depends on Zn or without the presence of Zn there will not be any crystalline CuS phase formation in CZS(at temperature 350^{o}C). Hall measurement says that there is minimum for carrier concentration at around 0.75 of Zn concentration. Similarly for mobility too there is a minimum. XPS analysis of cells show clear evidence of Cu diffusion and formation of new phases like copper Indium sulphide. Presence of Zn blocks the entry of In to CZS layer which is very clear in XPS analysis of Zinc rich cell. Copper concentration enhances performance parameters of cells and Cu rich cells always show good junction behavior and light activity. Zn poor cells show good fill factor along with current densities and show good solar cell behaviors.

References

[1] S H Mohamed. Photocatalytic, optical and electrical properties of copper-doped zinc sulfide thin films. *Journal of Physics D: Applied Physics*, 43:035406, 2010.

[2] Mustafa Oztaş, Metin Bedir, A Necmeddin Yazici, E Vural Kafadar, and Huseyin Toktams. Characterization of copper-doped sprayed zns thin films. *Physica B: Condensed Matter*, 381:40–46, 2006.

[3] Cheng He Ruan, Chung-Cheng Huang, Yow-Jon Lin, Guan-Ru He, Hsing Cheng Chang, and Ya Hui Chen. Electrical properties of cuxznysns4 films with different cu/zn ratios. *Thin solid films*, 550: 525–529, 2014.

[4] Qijie Guo, Grayson M Ford, Wei-Chang Yang, Bryce C Walker, Eric A Stach, Hugh W Hillhouse, and Rakesh Agrawal. Fabrication of 7.2% efficient cztsse solar cells using czts nanocrystals. *Journal of the American Chemical Society*, 132:17384–17386, 2010.

[5] M Messaoudi, M S Aida, N Attaf, T Bezzi, Jamal Bougdira, and G Medjahdi. Deposition of tin(ii)sulfide thin films by ultrasonic spray pyrolysis: Evidence of sulfur exo-diffusion. *Materials Science in Semiconductor Processing*, 17:38–42, 2014.

[6] Kiran Diwate, Kakasaheb Mohite, Manish Shinde, Sachin Rondiya, Amit Pawbake, Abhijit Date, Habib Pathan, and Sandesh Jadkar. Synthesis and characterization of chemical spray pyrolysed czts thin films for solar cell applications. *Energy Procedia*, 110:180–187, 2017.

[7] Claudia Malerba, Francesco Biccari, Cristy Leonor Azanza Ricardo, Matteo Valentini, Rosa Chierchia, Melanie Muller, Antonino San-

toni, Emilia Esposito, Pietro Mangiapane, Paolo Scardi, et al. Czts stoichiometry effects on the band gap energy. *Journal of alloys and compounds*, 582:528–534, 2014.

[8] V G Rajeshmon, C Sudha Kartha, K P Vijayakumar, C Sanjeeviraja, T Abe, and Y Kashiwaba. Role of precursor solution in controlling the opto-electronic properties of spray pyrolysed cu2znsns4 thin films. *Solar Energy*, 85:249–255, 2011.

[9] G S Harish and P Sreedhara Reddy. Synthesis and characterization of ce, cu co–doped zns nanoparticles. *Physica B: Condensed Matter*, 473:48–53, 2015.

[10] V G Rajeshmon, N Poornima, C Sudha Kartha, and K P Vijayakumar. Modification of the optoelectronic properties of sprayed in2s3 thin films by indium diffusion for application as buffer layer in czts based solar cell. *Journal of Alloys and Compounds*, 553:239–244, 2013.

[11] M V Santhosh, D R Deepu, C Sudha Kartha, K Rajeev Kumar, and K P Vijayakumar. All sprayed ito-free cuins2/in2s3 solar cells. *Solar Energy*, 108:508–514, 2014.

[12] M V Santhosh, D R Deepu, R Geethu, K Rajeev Kumar, C Sudha Kartha, and K P Vijayakumar. Spray pyrolysed microporous tio2 thin films by optimisation of substrate temperature for âĂŸall sprayedâĂŹsolar cells. *Semiconductor Science and Technology*, 29: 115026, 2014.

[13] Hidenori Noguchi, Agus Setiyadi, Hiromasa Tanamura, Takao Nagatomo, and Osamu Omoto. Characterization of vacuum-evaporated

tin sulfide film for solar cell materials. *Solar Energy Materials and Solar Cells*, 35:325–331, 1994.

[14] Angel Susan Cherian, T Abe, Y Kashiwaba, C Sudha Kartha, and K P Vijayakumar. Cuins2/in2s3 cells using a cost-effective technique: significance of precursor ratios on cell parameters. *Energy Procedia*, 15:283–290, 2012.

[15] Titipun Thongtem, Anukorn Phuruangrat, and Somchai Thongtem. Synthesis and analysis of cus with different morphologies using cyclic microwave irradiation. *Journal of Materials Science*, 42:9316–9323, 2007.

[16] Pu-Jun Jin, Zheng-Quan Yao, Mao Lin Zhang, Yu Hu Li, and Hui Ping Xing. A pigment (cus) identified by micro-raman spectroscopy on a chinese funerary lacquer ware of west han dynasty. *Journal of Raman Spectroscopy*, 41:222–225, 2010.

[17] Mehdi Adelifard, Hosein Eshghi, and Mohammad Mehdi Bagheri Mohagheghi. Synthesis and characterization of nanostructural cus–zns binary compound thin films prepared by spray pyrolysis. *Optics Communications*, 285:4400–4404, 2012.

[18] Y B He, A Polity, I Osterreicher, D Pfisterer, R Gregor, B K Meyer, and M Hardt. Hall effect and surface characterization of cu2s and cus films deposited by rf reactive sputtering. *Physica B: Condensed Matter*, 308:1069–1073, 2001.

[19] M Ali Yildirim and Ate. Annealing and light effect on structural, optical and electrical properties of cus, cuzns and zns thin films grown by the silar method.

[20] Haitao Zhu, Jixin Wang, and Daxiong Wu. Fast synthesis, formation mechanism, and control of shell thickness of cus hollow spheres. *Inorganic chemistry*, 48:7099–7104, 2009.

[21] S Gorai, D Ganguli, and S Chaudhuri. Synthesis of 1d cu2s with tailored morphology via single and mixed ionic surfactant templates. *Materials chemistry and physics*, 88:383–387, 2004.

[22] Woo-Young Kim, Balasaheb M Palve, Habib M Pathan, and Oh Shim Joo. Spray pyrolytic deposition of polycrystalline cu2s thin films. *Materials Chemistry and Physics*, 131:525–528, 2011.

[23] E Guneri and A Kariper. Optical properties of amorphous cus thin films deposited chemically at different ph values. *Journal of Alloys and Compounds*, 516:20–26, 2012.

[24] Cristina Nascu, Ileana Pop, Violeta Ionescu, E Indrea, and I Bratu. Spray pyrolysis deposition of cus thin films. *Materials letters*, 32: 73–77, 1997.

[25] L A Isac, A Duta, A Kriza, I A Enesca, and M Nanu. The growth of cus thin films by spray pyrolysis. In *journal of physics: Conference Series*, volume 61, page 477. IOP Publishing, 2007.

[26] Sanjay Kumar Swami, Anuj Kumar, and Viresh Dutta. Deposition of kesterite cu2znsns4 (czts) thin films by spin coating technique for solar cell application. *Energy Procedia*, 33:198–202, 2013.

[27] M Patel, I Mukhopadhyay, and A Ray. Structural, optical and electrical properties of spray-deposited czts thin films under a non-equilibrium growth condition. *Journal of Physics D: Applied Physics*, 45:445103, 2012.

[28] M V Santhosh. Improvement on the performance of spray deposited cuins2 in2s3 solar cell using extremely thin absorber layer with mixed phase of cuins2 and cu2s. 2015.

Chapter 6

Summary and Future scopes

6.1 Summary of the present work

Eventhough solar cell markets still stick on Si for high energy production, solar cell generation now entered into fourth generation which consists of bio-light sensitive materials. World tries to keep Si and other high efficient thin film materials aside due to problems related to their disposal, high cost and toxicity factors. Involvement of Organic solar cells, DSSC and perovskite solar cells in energy production can possibly result in eco-friendly energy harvesting side in 21^{st} century. Here we recognize importance of CuZnS(CZS) material as good absorber layer in solar cells. Deriving different solar cell materials from CIGS lead to the invention of CZTS and CZS. CZS is a material which has two different band gaps, various conductivity ranges and capable of showing different conductivity types(n or p) at different concentrations of its constituent elements.

In this work CuZnS thin films deposited using CBD technique and CSP technique were characterized, and devices were fabricated. Double band gap nature is the most prominent feature of CZS. Material exists as alloy or mixture of different phases of CuS and ZnS. Generally CuS phases are seen crystalline in nature while ZnS phase is amorphous. XPS analysis clearly showed that CZS deposited at different Cu concentrations have different compositions. The peculiarity of CZS is the possibility of tuning of the properties of the material. We could easily tune optical, electrical as well as structural properties of the material by varying the compositions of Cu, Zn or S in the material.

As of CZS is concerned, CBD deposited samples have less adhesion comparing to CSP deposited samples. We have fabricated devices using CZS with different buffer layers like CdS, ZnS and InS. CZS-InS combinations gave better device parameters than other buffer layer combinations. Devices fabricated with CSP show good junction parameters comparing to CBD deposited samples. Devices with CSP technique(devices with CSP deposited samples) show good improvement in Cu rich conditions i.e. Copper rich devices show good junction parameters. Among devices fabricated with CZS, we see an improvement in short circuit current with respect to increase in Cu concentration and open circuit voltage is not that affected with Cu concentration in CZS. Like Cu concentration, decrease in Zn concentration improves fill factor as well as short circuit current of the devices.

6.2 Future scopes

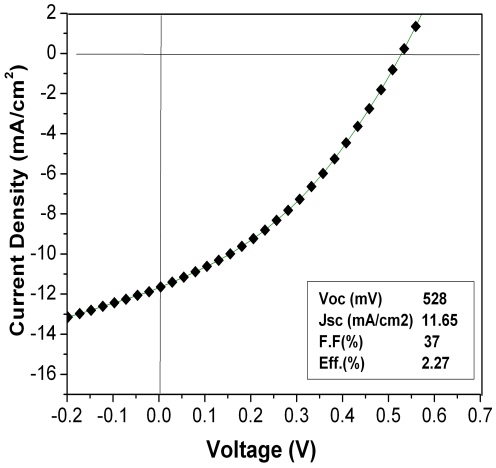

Figure 6.1: J-V characteristics of device fabricated using CuZnS having high Cu/Zn ratio

The "best cell" we mentioned in chapter 5 i.e. cell B4 was very rich(Cu/Zn=4) in Cu. On a curiosity we have fabricated another device having Cu/Zn=8(concentration of Zn is again reduced) and we found that short circuit and open circuit voltage are improved sacrificing fill factor. Device has efficiency of 2.27% and so far this is the maximum efficiency reporting regarding CuZnS cell(Fig.6.1). More studies are to be done on CuZnS devices in future, particularly variations on buffer layer compositions. CuZnS can be deposited using sulphates, nitrates and acetate salts for and we exactly do not know how the material properties will be varying with precursor variation.

We fabricated CZS devices on FTO also. Here FTO was deposited

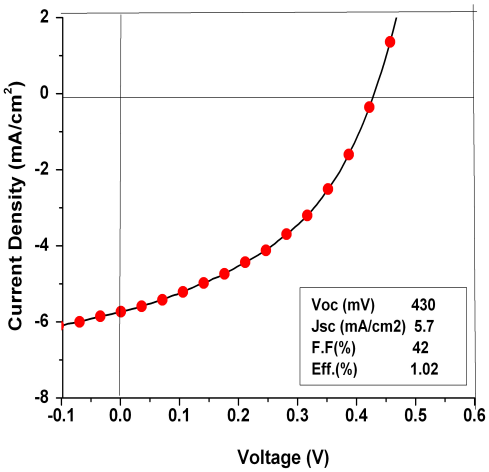

Figure 6.2: J-V characteristics of device fabricated using CuZnS on sprayed FTO substrate

using CSP technique and in short the whole device was fabricated using CSP technique. This device can be considered as fully sprayed solar cell. In Fig.6.2 the J-V characteristics of FTO cell is shown and seeing the cell parameters, we got an indication that device is promising. Even in case of devices fabricated on ITO coated substrates, we had obtained good junction characteristics for Cu poor absorbers(device parameters are similar to what we obtained using FTO substrates, which was reported in Applied Physics Letters). In the device Cu/Zn ratio is 0.4 where Cu is very low in concentration. We faced some technical issues regarding the deposition of Cu rich CZS on sprayed FTO, which can be rectified in future. Anyway we could see that "complete solar cell" fabrication is possible with spray pyrolysis technique. The establishment of all sprayed solar cells can easily make solar markets economically reachable for com-

mon people. Large area solar cells can be fabricated using spray pyrolysis technique. So far we used silver electrodes as top electrodes. Incorporation of different transparent conduction materials in CuZnS cells may improve the performance, where we can pass light through upper side also.

The material CuZnS is very new in photovoltaics. Deposition and device fabrication are to be extended to other fabrication techniques also. Double band gap nature and conductivity type tuning are promising for tandem solar cells and thin film transistors. High transmittance of CZS at lower Cu concentration favors transparent conducting material fabrication using CZS. Another interesting thing is that CZS can be utilized in perovskite solar cells and DSSC as good collecting electrodes due to the fact that material behaves like good conducting transparent p type material at low Cu concentration.

List of Tables

List of Figures